Involvement of Kinesin-related Smy1 and Rho GAP Gym1 in Regulating Vesicle Transport by Myosin V

A Dissertation

Presented to the Faculty of the Graduate School

of Cornell University

in Partial Fulfillment of the Requirements for the Degree of

Doctor of Philosophy

by

Kyaw Myo Lwin

May 2017

Kinesin-related Smy1 and A Novel Rho GAP, Gym1 in vesicle trafficking

Kyaw Myo Lwin, Ph.D.

Cornell University 2017

Every nucleated cell has a defined morphology to cater to the needs of its unique function. To generate polarity during growth, budding yeast *Saccharomyces cerevisiae* transports all necessary organelles into the bud. This transport requires the essential myosin V motor, Myo2. Using different cargo receptors, Myo2 transports secretory vesicles, mitochondria, vacuoles and other cargoes. A conditional mutant *myo2-66* in particular fails to transport secretory vesicles. Initially discovered as a multicopy suppressor of *myo2-66*, Smy1 suggested the involvement of a kinesin motor for transport of secretory vesicles. However, because suppression does not need either kinesin motor activity or an interaction with microtubules, the function of Smy1 remained elusive.

Here I show that kinesin-related Smy1 stabilizes the association between Myo2 and the secretory vesicle receptor, the Rab GTPase Sec4. Smy1 function is specific for secretory vesicle transport. Characterization of Smy1 individual domains indicates that full length Smy1 is required since the head domain is important for vesicle association and the tail domain for Myo2 binding. Furthermore, I used a *GAL1* cDNA library to suppress a conditional *myo2 smy1* mutant as a way to identify additional components that may function in secretory vesicle transport. One novel component we identified has a RhoGAP domain in its C-terminus, so I named it *GYM1* (***G***AP with ***Y***east ***M***yo2). I found that Gym1 is polarized to the bud and its localization is dependent on Myo2. Further, biochemical assays showed that Gym1specifically stimulates the GTPase activity of Rho3 and mutation of its critical arginine at residue 546 abolishes this activity. Genetic analysis also showed that the ability of Gym1 to suppress the *myo2 smy1* mutant requires the GAP activity towards Rho3. In mammalian cells, TC10 Rho proteins are also reported to mediate vesicle transport. This new finding of Rho3 and its associated GAP, Gym1 in budding yeast suggests that there is an interplay between Rho and Rab GTPases in secretory vesicle transport.

Biographical Sketch

Kyaw Myo Lwin (or Long Hui Chen) was born in January 24, 1983 in Yangon, Myanmar (Burma) to Tan Hyan Teong+ and Liao Zhi. Lwin as he goes by last Burmese name, grew up with one older sister and one younger brother. Lwin's grandparents migrated from "Hui'an" county in Fujian province, China, and they named "Hui" in their grandchildren middle name.

In Myanmar, every year, all 10th grade students all over the country sit for the national matriculation examination to be eligible to enroll at the universities of their choice. The examination lasts for 5 days and includes 9 subjects: Myanmar, English, Mathematics, Physics, Chemistry, Biology, Geography, History and Economics. Every year, ten students with the highest scores were chosen and given national medals, famously known as "**The Whole Burma Top Ten**" in the entire country. About 300,000 students sat for the national exam in 2000. Lwin stood one of the top ten students in the country and was awarded a merit scholarship to study medicine at the University of Medicine (1), Yangon, Myanmar.

In medical school, Lwin achieved the highest score in the past history of Physiology and Anatomy departments. Unsatisfied with the rigidity of the medical course, Lwin however dropped out of the medical school after 3 years and went abroad to study Biomedical Sciences at the University of Bradford, UK campus in Singapore. In 2008, Lwin graduated with 1st Class Honor and was awarded an outstanding student achievement.

After graduation, intrigued by biomedical research, Lwin joined the gastric cancer lab led by Dr. Kon Oi Lian at the National Cancer Center Singapore (NCCS). After two and half years' research on chromosomal translocations in gastric cancers, Lwin and his colleagues presented their findings at the American Association for Cancer Research (AACR) at Orlando, Florida, US.

In August 2011, Lwin came to the US for his doctoral training in Genetics and Development program at Cornell University. Under the guidance of Dr. Anthony Bretscher, Lwin discovered a novel gene in budding yeast that regulates vesicle trafficking and named *GYM1*.

In spare time, Lwin enjoys reading and writing. Lwin is good at playing snooker, ping pong, and badminton.

+The surname “Chen” is also spelled as “Tan” in Fujianese dialect.

Acknowledgement

To be absolutely honest, I skip acknowledgement when I read books. As a reader, this habit is not borne out of disrespect, but rather my interest does not lie in that part of the book. To write my dissertation without acknowledgement however would do disservice to those who have been integral part of my PhD journey and especially to this very dissertation book itself. Therefore, as a writer I foresee that this acknowledgement might not matter to others, but it does to me and to my scientific adventure itself.

First and foremost, I would like to thank my dissertation advisor, Dr. Bretscher, otherwise known as Tony. Tony has many qualities that make him an exceptional mentor, both intellectually and personally. Choosing his lab as my doctoral training was the best decision I ever made for my first step into a PhD journey. Without his understanding and patience, I would not be where I am now today. It was in 2011 – While giving a rotation talk, as cheery as he was, Tony ventured, "*Anyone knows what the Rab proteins are?*" My rookie answer "*Small molecular weight GTPase protein*" turned his head, had his finger pointing at me, and Tony exclaimed "*YES!!*" That was back in 2011 and I am now writing GTPase protein in my dissertation. My special thanks also go to Dr. Chris Fromme and Dr. Tim Huffaker. Their insightful discussions and rapt attention to my science has kept my research in the right direction.

I'd also like to thank those in the lab whom I'm fortunate to come across in my path: Dr. Felipé Santiago, Donghao Li, and Dr. Kirk Donovan who have been crucial to my knowledge in yeast genetics and foundation. It would also be an empty gesture without saying special thanks to Dr. Li Xu and Myungjoo (MJ) Shin for their insightful discussion on yeast and life events. I am also grateful to those who had to bear the brunt of my yeast discussion in group-meetings: Drs. - Ram, Damien, Jess and Cecilé. Last but not least, I also thank Dave McDermitt for his diligence and memory. Among the myriad of lab reagents and stocks, Dave can instantly

retrieve some stocks from 20 years ago. Their presence in the lab has indeed made the lab environment enjoyable to do science.

My story in Ithaca would not be complete without mention of Myat Tun Lin, Xian Qu, and Tao Sun. Hiking, playing ping pong and pool has kept my sanity in check. I'd also like to thank someone who brightened my stay in the US. I will end my already long acknowledgement with deep gratitude towards my parents whose wisdom has helped me along the way and my outlook on life. Anyone whose name I might have missed here due to space, I'd like to say "Thank you very much" for your support and understanding.

This dissertation will not materialize without the NIH R01 funding.

Table of Contents

Appendix : Investigating Smy1 individual domains and Characterization of Smy1 binding site on Myo2 tail

List of Figures

List of Tables

List of Abbreviations

AD	*GAL4* Activation Domain
ADP	Adenosine diphosphate
ARP	Actin related protein
ATP	Adenosine triphosphate
BD	*GAL4* Binding Domain
CBD	Cargo Binding Domain of Myo2 tail
CC	coiled-coil domain of either Myo2 or Smy1
cctail	Myo2 coiled-coil domain and its cargo binding tail/domain
CDC	Cell Division Cycle
DAD	Diaphanous Autoregulatory Domain
DID	Diaphanous Inhibitory Domain
DRF	Diaphanous related family
ER	Endoplasmic Reticulum
FH	Formin Homology
GAP	GTPase Activating Domain
GEF	Guanine nucleotide Exchange Factor
GTP	Guanosine Triphosphate
GDP	Guanosine Diphosphate
KLD	Kinesin-like motor Domain of Smy1
MBD	Myosin Binding Domain of Smy1
ORF	Open Reading Frame
P_i	inorganic Phosphate
RBD	RhoGTPase Binding Domain of Bni1 and Bnr1
TGN	trans-Golgi Network
TMD	Transmembrane domain

Chapter I

Introduction to the historical emergence of budding yeast as a model organism

Budding yeast, *Saccharomyces cerevisiae*, came a long way to become a model organism for scientific research in laboratory. Yeast has been used traditionally in brewing beers by fermenting sugars, and raising bread dough by releasing carbon dioxide, hence as the name implies – baker's yeast (Greig and Leu, 2009). Yeast is naturally found in vineyards and people have used crushed grapes in a variety of food processing (Mortimer, 2000). It was not until the late 1800s that Carlsberg laboratory employee Emil Christian Hansen isolated single colonies from a starter culture; from that time on, scientific experiments on yeast have ensued (Mortimer and Johnston, 1986). By using modern microscopy, baker's yeast was found to undergo a budding process during cell division and it became known as budding yeast, in contrast to fission yeast, *Schizosaccharomyces pombe*.

The budding yeast strain, S288C, that is used most widely, was first constructed in 1950 (Mortimer and Johnston, 1986). Many more strains were eventually created by genetic modifications. In 1996, with the effort of the international scientists' community, budding yeast set the milestone for the first-ever complete eukaryotic genome (Goffeau et al., 1996). Budding yeast has 16 chromosomes and 6604 protein-encoding genes or ORFs (Open Reading Frames) as of September, 2016 (http://www.yeastgenome.org/genomesnapshot). Out of 6604 ORFs, 78% (5155) were verified and their functions have been characterized. The functions of the remaining ORFs have been identified as more and more scientists have investigated yeast genetics.

Due to its high similarity to the DNA sequence of humans and similar functional homology between mammalian and yeast cells, budding yeast has been a workhorse for many scientists for discovering, investigating and understanding the intricate mechanisms of cells (Botstein et al., 1997; Kataoka et al., 1985). Budding yeast has been used as a model organism

for investigating cell division, DNA damage and repair, chromosome organization, transcription regulation, stress response, membrane trafficking, vesicle transport and more (Dekker et al., 2002; Greig and Leu, 2009; Hartwell et al., 1970; Lydall and Weinert, 1995; Novick et al., 1980).

The pinnacle of significant discovery was made when Lee Hartwell elucidated steps in cell cycle regulation in budding yeast and that the regulation was almost the same as in humans (Hartwell et al., 1970). Because disruption of some *CDC* genes (Cell Division Cycle) leads to cancer in humans, Lee Hartwell was awarded Nobel Prize in 2001 for his discovery of cell cycle regulation. Another stepping stone in understanding structures of the components critical for DNA transcription was also made in budding yeast by Roger Kornberg who later received the Nobel Prize in 2006 (Kornberg, 1974). Budding yeast also contributed to understanding vesicle trafficking and for this work, Randy Schekman received the Nobel prize in 2013 (Novick et al., 1980; Novick and Schekman, 1979). As of this writing in 2016, budding yeast contributed another Nobel laureate, Yoshinori Ohsumi, who developed an understanding of the cellular mechanism for self-eating which is also known as autophagy (Takeshige et al., 1992; Tsukada and Ohsumi, 1993). As a model organism, budding yeast has served as the envy of scientists and it has contributed an immense amount to our knowledge of cell biology.

Budding yeast – an excellent model for cell polarity

Budding yeast has been an excellent model for studying molecular processes that include establishment of cell polarity, inheritance of parental mitochondria, vacuoles or lysosomes, mRNA migration, biogenesis of proteins in the endoplasmic reticulum (ER), endocytosis, exocytosis and membrane trafficking (Botstein et al., 1997). Much progress toward understanding the basic cellular processes have therefore come from studies of budding yeast.

Figure 1.1

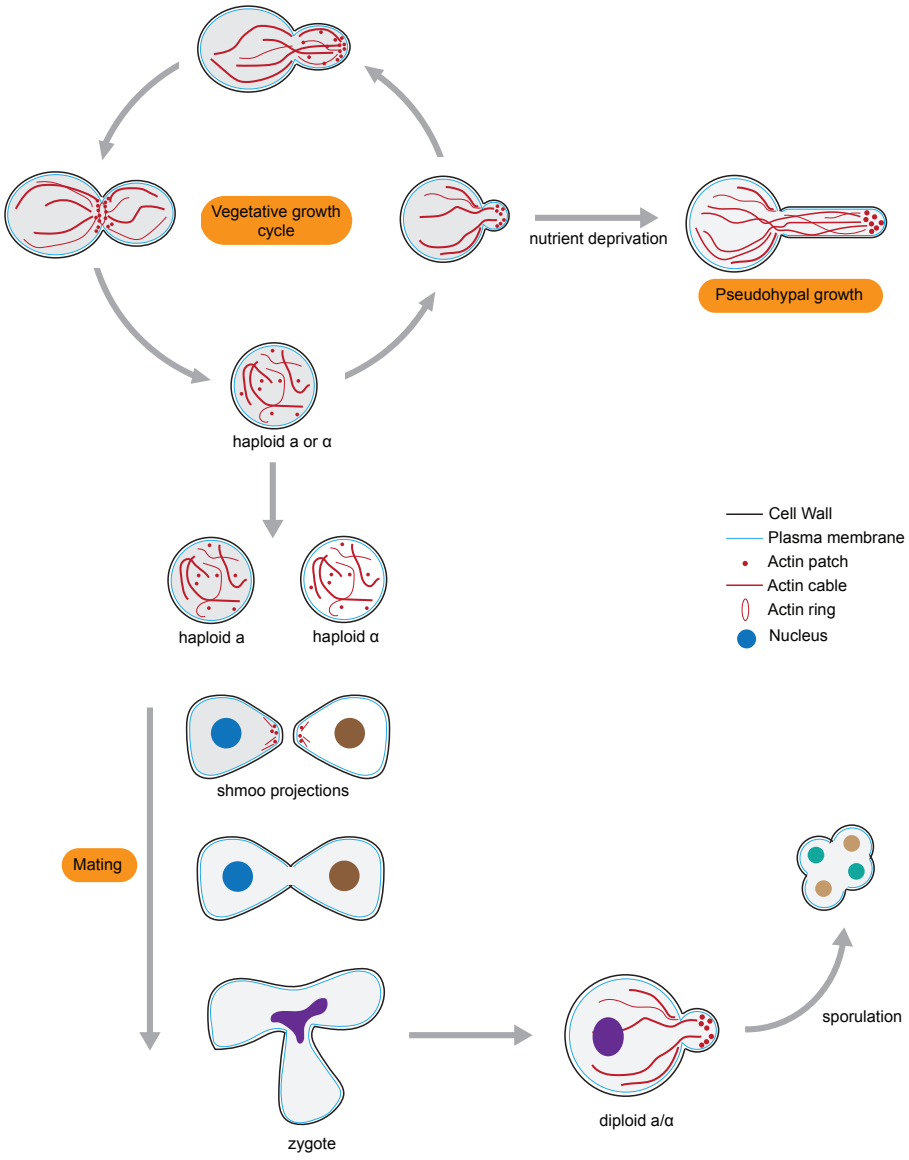

Figure 1.1. Life cycle of budding yeast in different conditions.
Vegatative growth cycle represents the growth cycle of either a haploid cell (mating type a or α) or a diploid cell (a/α). Cells undergo a budding process until a septin ring composed of actin filaments constricts the division between mother and daughter cells. Mating condition happens when two haploid cells with opposite mating types are grown together. Budding yeast under certain nutrient deprivation undergo pseudohyphal growth at the tip.

Budding yeast in nature is diploid. It undergoes meiosis under nutrient stress to form haploid spores in tetrads (Figure 1.1). Haploid cells can maintain either of two mating types (a or α). Budding yeast has three distinctive morphologies during its vegetative growth, mating and filamentous growth (Gimeno and Fink, 1994; Madden et al., 1992). Vegetative growth begins with an emergence of a small bud at the cell cortex and subsequently polarized growth ensues at the site of the bud. Cytokinesis, which is facilitated by contractile ring constriction at the bud neck, later ends the polarized growth, which generates two cells. On the other hand, during mating, haploid cells assume a pear-shaped morphology known as a "shmoo" formation, which facilitates the contact between two opposite mating cells. Budding yeast under certain types of nutrient deprivation also undergoes pseudohyphal growth at the tip (Figure 1.1).

The asymmetric growth of budding yeast therefore presents an excellent model to study mechanisms behind polarity establishment and a polarized growth (Pruyne and Bretscher, 2000). In the late 1900s, a number of labs discovered many mechanisms and proteins that govern the budding process in *Saccharomyces cerevisiae*. Using conditional mutants, Schekman and his colleagues showed that secretory vesicles accumulate at the site of bud formation in certain mutants, which led to the first discovery of a defined secretory pathway for establishing polarity in budding yeast (Novick et al., 1980; Novick and Schekman, 1979).

It was later found that yeast growth requires an essential myosin motor or Myo2 in budding yeast (Johnston et al., 1991). Adams and Pringle also showed that actin filaments, one of the cytoskeletons, were also polarized towards the site of growth and a cluster of actin patches were also found at the site of bud formation (Adams and Pringle, 1984). The first evidence, that Myo2 transports secretory vesicles along actin filaments, came from the analysis of the conditional actin-stabilizing mutant, *tpm1-2 tpm2Δ* (Pruyne et al., 1998). Further work from the Bretscher lab also showed that Myo2 tail was required for transporting secretory vesicles (Schott et al., 1999). Therefore polarity in budding yeast can be grouped into two main processes: (1) establishment of polarized actin filaments and (2) secretory vesicle transport and segregation of organelles by Myosin-V motors (Bretscher, 2003).

Polarized actin cytoskeletons

Among the myriad of proteins involved in the budding process, actin, an essential protein, assembles into three distinct structures during growth: (1) actin cables (2) cortical actin patches and (3) an actin ring at the bud neck, which are essential for polarized exocytosis, endocytosis, and cytokinesis, respectively (Figure 1.1) (Adams and Pringle, 1984; Gallwitz and Seidel, 1980; Gallwitz and Sures, 1980; Lippincott and Li, 1998; Moseley and Goode, 2006). Actin (*ACT1*) and tubulins (*TUB1*, *TUB2*, and *TUB3*) make up the major cytoskeletal elements, and yet it was unclear initially whether both actin filaments and microtubules were required for bud formation. It was not until 1988, when Huffaker *et al.*, used cold-sensitive tubulin *tub2* mutants, to show that microtubules are not required for secretory vesicle transport: instead, they are involved in nuclear migration (Huffaker et al., 1988). Using the microtubule depolymerizing agent, nocodazole, the Pringle lab also showed that microtubules were only required for nuclear migration and orientation (Jacobs et al., 1988).

Not only has the importance of actin cables been characterized but a number of actin-binding proteins were also identified. Sac6 (Fimbrin) was identified to be an actin-bundling protein (Adams et al., 1989). The actin stabilizing protein, tropomyosin Tpm1/2, was also discovered in the Bretscher lab (Liu and Bretscher, 1989). Capping protein (Cap2), Profilin (Pfy1), and Cofilin (Cof1) were later identified and characterized to regulate actin cables (Amatruda et al., 1990; Haarer et al., 1990; Moon et al., 1993). Actin binding protein (Abp1) was also found in cortical actin patches (Drubin et al., 1988).

During the early 2000s, the molecular mechanisms behind the formation of actin cables and cortical patches were unraveled. Initially discovered as a RhoGTPase interacting protein, Bni1, which is localized at the bud, was found to be involved in bipolar budding (Zahner et al., 1996). Bni1 is a member of a diaphanous related formins (DRF). DRF proteins have conserved FH domains (Formin Homology) that are implicated in cell polarity and actin organization.

Figure 1.2

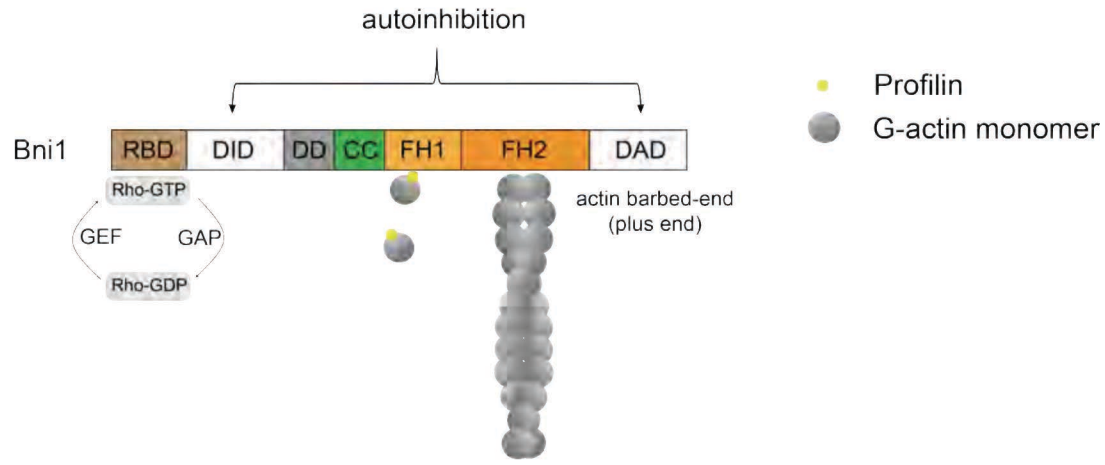

Figure 1.2. Actin polymerization by formin (Bni1).
Conceptual illustration of actin organizations (filaments and patches) in budding yeast.

Bni1 has a RhoGTPase binding domain (RBD) at its N-terminus and FH1 and FH2 domains near its C-terminus. The FH1 domain of Bni1 recruits profilin, which binds actin monomer, and the FH2 domain nucleates actin assembly (Figure 1.2) (Evangelista et al., 2002; Pruyne et al., 2002; Sagot et al., 2002). A mutation in the FH2 domain, therefore, results in loss of the Bni1 function. Budding yeast has two formin homologues: Bni1 and Bnr1; these assemble actin cables at the apical bud and at the bud neck, respectively (Pruyne et al., 2004).

Similar to actin nucleation for cable formation, several proteins were also identified to be involved in the formation of actin patches. The Arp2/3 complex, which is composed of 7 subunits containing the major ***A***ctin-***R***elated ***P***roteins (Arp2 and Arp3), is crucial for cortical actin patch assembly and endocytosis (Goley and Welch, 2006; Kaksonen et al., 2003). Nucleation promoting factors (NPF) were later found to be necessary for actin assembly by the Arp2/3 complex, which rendered a new actin filament that branches 70˚ from the existing one. The majority of NPFs have a WH domain (Wiskott-Aldrich syndrome protein or WASP homology) that binds G-actin. Budding yeast has one WASP homologue: Las17 or Bee1 (Figure 1.2) (Li, 1997; Madania et al., 1999).

Actin can assemble into either cables or patches during budding. To distinguish which structure is important for polarized growth, the Bretscher lab generated a conditional tropomyosin mutant, which is a protein that only localizes to the actin cables. They showed that polarized actin cables, rather than actin patches, were essential for transporting secretory vesicles by the myosin motor towards the site of bud emergence (Pruyne et al., 1998).

RhoGTPase Cdc42 – Master regulator of cell polarity

The small GTPase Rho proteins are involved in organization of the actin cytoskeleton and in establishment of the polarity. Yeast Cdc42 plays a central role in establishing polarity both in humans and in yeast. Because they have 85% sequence similarity, human Cdc42 can complement the yeast *cdc42* mutant (Johnson and Pringle, 1990; Munemitsu et al., 1990). Cdc42 is necessary for bud site selection and it is associated with a scaffolding complex, which is generally composed of Bem1, Cdc42, Cdc24, and Cla4 (Bose et al., 2001). Cdc24 is the guanine nucleotide exchange factor (GEF) for Cdc42, that activates Cdc42 to the GTP bound state. Cla4, a Cdc42 effector and a p21-activated kinase (PAK) family member, activates Cdc24 GEF by phosphorylation (Gulli et al., 2000). Activated Cdc24 further activates Cdc42-GTP which in turn binds to the scaffolding platform – Bem1, Cdc24, Cla4 – resulting in a positive feedback loop for Cdc42 activation.

Cdc42 activates formin to initiate actin assembly at the cell cortex. Formins stay in the autoinhibitory state when their N-terminal DID (Diaphanous Inhibitory Domain) interacts with C-terminal DAD (Diaphanous Autoregulatory Domain) (Figure 1.2) (Goode and Eck, 2007). Binding of the RhoGTPase at the formin RhoGTPase binding domain (RBD) presumably opens up the profilin binding FH1 domain and facilitates the assembly of actin monomers at the FH2 domain. Budding yeast has six Rho GTPases (Rho1, Rho2, Rho3, Rho4, Rho5 and Cdc42). Cdc42, Rho1, and Rho3 physically interact with Bni1 and are purported to be prime activators of Bni1 activity in the bud. The polarisome complex, which is composed of Bni1, Spa2, Pea2 and Bud6, is involved subsequently in the formation of polarized actin cables

(Bi and Park, 2012). Cdc42 is proposed to undergo actin-based Myo2 motor transport towards the bud, which generates a positive feedback cycle of Cdc42-GTP clustering at the tip by subsequently recruiting more formin for actin assembly at the site of bud emergence (Bi and Park, 2012; Wedlich-Soldner et al., 2003). However, this model remains controversial with a new finding that Cdc42 polarizes in the bud with an actin-independent manner (Woods et al., 2016).

Myosin V motor : motor activity

Myosins are a large family of actin-based motors. The myosin superfamily was first classified based on motor head domains. Later classification based on myosin tails also similarly corresponded to head domain classes (Thompson and Langford, 2002). Each class of myosin has distinct functions. Budding yeast has five myosin genes, two of which encode class V myosins (*MYO2* and *MYO4*). Myo2 is responsible for delivery of secretory vesicles and segregation of organelles, whereas Myo4 transports Ash1 mRNA actively into the bud for determination of mating type (Haarer et al., 1994; Johnston et al., 1991; Schott et al., 1999). Myo1p (class II) is involved in actin ring constriction during cytokinesis at the bud neck (Bi, 2001; Lippincott and Li, 1998). Endocytosis and cell wall biogenesis require Myo3 and Myo5 (class I) (Bi, 2001; Goodson et al., 1996; Goodson and Spudich, 1995).

One of the functions of Myo2 was first uncovered by studying the temperature-sensitive (*ts*) *myo2-66* mutant (Johnston et al., 1991). Later work showed that Myo2 transports secretory vesicles to the bud tip without interfering with protein biosynthesis. The *myo2-66* mutant has a profound effect on cell wall synthesis, which is evidenced by chitin delocalization, a major component in the cell wall. The mutant also showed a loss of vacuole inheritance (Hill et al., 1996). Those earlier observations on the *myo2* mutant indicated that Myo2 was involved in intracellular transport. Similarly, mammals have three isoforms of Class V Myosin (MyoVa, Vb, Vc); each are expressed differentially in different tissues. MyoVa is highly expressed in the brain, testis, and skin, and MyoVb and MyoVc are expressed primarily in epithelial cells

(Prekeris and Terrian, 1997; Reck-Peterson et al., 2000; Rodriguez and Cheney, 2002; Swiatecka-Urban et al., 2007). Studying mammalian MyoV and yeast Myo2 has resulted in an understanding of the molecular function of the myosin V motor. Myosin Vs have three distinct domains: (1) the motor head domain (2) the α-helical "neck" domain or the lever arm, and (3) the globular tail domain or cargo binding domain.

The motor head domain

MyoV undergoes substantial conformational changes in its motor head domain during actin-based transport. Unlike conventional muscle myosin II, which only performs a single stroke with an actin filament during muscle contraction, myoV undergoes pre-stroke and post-stroke conformational changes, which can be seen in X-ray crystal structures and EM images (Coureux et al., 2004; Walker et al., 2000). A first clear picture of how myosin V motor adopts different head conformations became available when the Houdusse lab showed the X-ray crystal structure of the myosin V motor either in the presence or absence of nucleotides (Coureux et al., 2004; Coureux et al., 2003).

The myosin motor head consists of a nucleotide-binding pocket, an actin-binding interface, and several deep clefts (Rayment, 1996; Trybus, 2008). The MyoV head domain contains an upper 50kDa domain and a lower 50kDa domain that are connected by an internal loop, the structure of which forms a cleft. The cleft exists in the middle of the actin-binding interface that is contributed by both upper and lower 50kDa domains (Figure 1.3). In the absence of nucleotide, a core 7 beta-pleated sheet restructures the conformation of the MyoV head in such a way that a cleft assumes a closed position, which brings the actin-binding interface together and facilitates a strong binding of the MyoV motor head to actin.

Figure 1.3

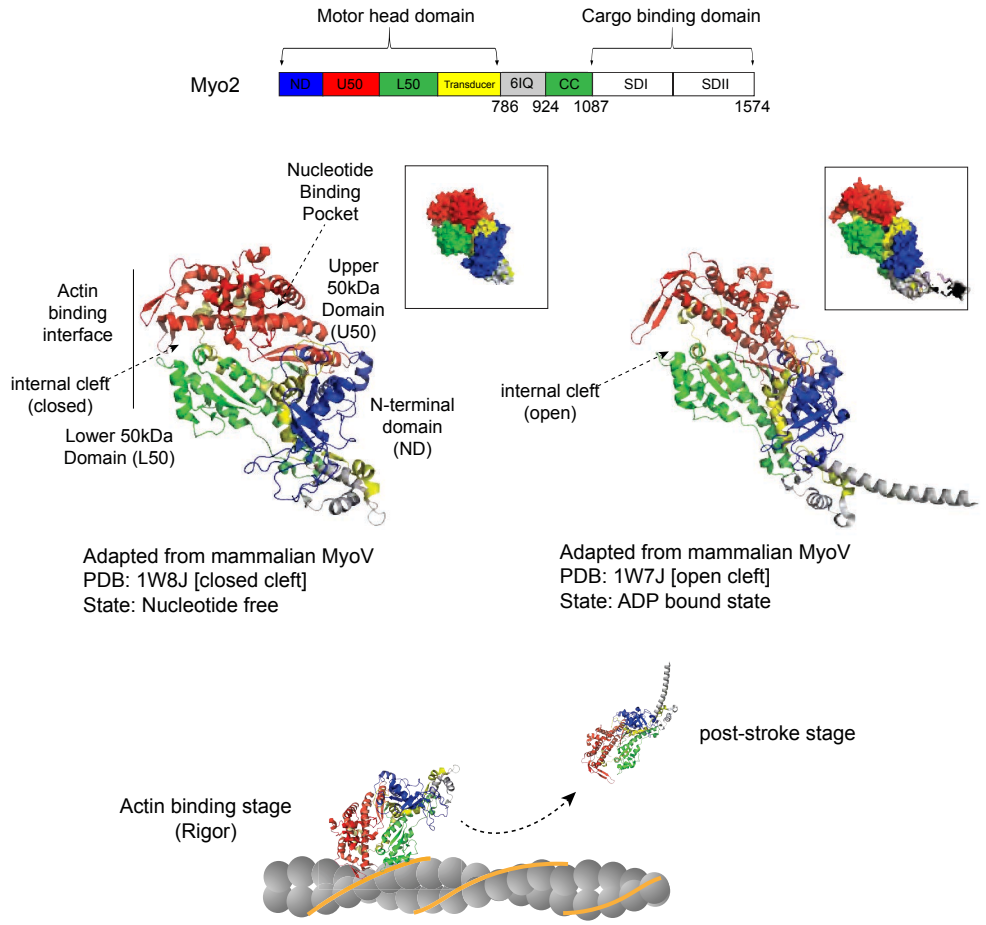

Figure 1.3. Myosin V motor head conformational change upon nucleotide binding and actin-binding (rigor state). **ND** = N-terminal domain; **U50** = upper 50kDa domain; **L50** = lower 50kDa domain; **Transducer** = converter to relay powerstroke through the lever arm; **6IQ** = IQ motifs repeat; **CC** = coiled-coil domain; **SDI** = sub-domain I; **SDII** = sub-domain II

The motor head undergoes several stages, "no nucleotide → ATP → ADP + Pi → ADP → no nucleotide", with different affinities toward binding actin. Underlined stages indicate the weak actin binding conditions (De La Cruz et al., 1999; Hammer and Sellers, 2012). The binding of ATP weakens the actin-myosin interaction. The rate-limiting step in the MyoV kinetic cycle is the lease of ADP, which suggests that MyoV has a high duty ratio (i.e., actin bound stage) (De La Cruz et al., 1999).

MyoV movement was initially considered to follow either a hand-over-hand or an inchworm model. The hand-over-hand model suggests that the trailing head swings after ATP hydrolysis, which brings the trailing head forward (74nm) to become a leading head. An inchworm model proposes that both heads move by 37nm simultaneously without the swinging process. The hand-over-hand model was established when EM images and single fluorophore imaging confirmed the model (Walker et al., 2000; Yildiz et al., 2003). Using the mouse MyoVa heavy chain and taking a snapshot of MyoVa movement on actin filaments by electron microscopy, Walker *et al.* showed that both heads of myosin V bind to actin filaments separated by 13 actin subunits (Walker et al., 2000). By labeling a single calmodulin with their optical technique call FIONA [fluorescence imaging with one-nanometer accuracy], Yildiz *et al.,* also observed that there was a 74nm fluorophore displacement with MyoV movement (Yildiz et al., 2003). Although the leading head was bound to actin in the ADP bound stage, the trailing head underwent ATP hydrolysis that generated a power stroke and turned the trailing head ahead of the leading head. The new leading head diffused and bound the 13th actin subunit in the ADP bound stage and the MyoV kinetic cycle continued (Vale, 2003).

Because MyoV spends most of its kinetic cycle at the actin bound stage, it is considered a processive motor protein (De La Cruz et al., 1999). The processivity of yeast Myo2 became controversial when Reck-Peterson et al., showed that Myo2 did not co-sediment with actin in the presence of ATP, unlike MyoVa from a chick brain (Reck-Peterson et al., 2001). The Mooseker lab therefore suggested that at least 5 Myo2 motors are required for the processive run on actin cables. In line with this, the Trybus group also claimed that kinesin-related Smy1

drove the Myo2 processivity by acting as a passenger (Hodges et al., 2009). In a similar fashion, the Trybus group later claimed that Myo2 processivity was also enhanced by tropomyosins on actin filaments (Hodges et al., 2012). In the Bretscher lab, Donovan found that about 10 Myo2 motors were associated with moving secretory vesicles (Donovan and Bretscher, 2012). Whether or not a single yeast Myo2 motor *in vivo* is capable of a processive run on actin cables without any activator such as Smy1 remains to be tested.

The lever arm

The myosin lever arm has IQ motifs – a consensus sequence of IQx*xx*RG*xxx*R with a stretch of an additional 23-25 amino acid residues in between each IQ motif, where x represents any amino acid. A tandem repeat of IQ motifs can be found in heavy chains of many myosins. IQ motifs are among the calmodulin and myosin light chain binding targets (Trybus, 2008). Followed by the longest α-helical lever arm (24nm), the myosin V motor head exerts mechanical force that is produced by ATP hydrolysis through the lever arm. The MyoV lever arm, which contains six IQ motifs, each of which binds light chains of calmodulin or members of the calmodulin family, is three times longer than muscle myosin and eight times longer than its motor counterpart, kinesin. The long lever arm allows myosin to take a bigger step for every ATP hydrolyzed (37nm) (Vale, 2003). Intramolecular tension between the lever arms due to ADP dissociation from the actomyosin-ADP complex generates the power stroke that allows the myosin to move in a discrete step of 37nm in a single event (Forgacs et al., 2008). In line with this, the Bretscher and Sellers labs also found that lengthening both yeast Myo2 and mammalian MyoV to 8IQ also increased the speed of MyoV (Sakamoto et al., 2005; Schott et al., 2002).

S. cerevisiae has two IQ motif-binding proteins; calmodulin (Cmd1) and the essential myosin light chain (Mlc1) (Stevens and Davis, 1998). Cmd1 was the first of the myosin light chain family that was discovered in budding yeast (Cyert, 2001). Both myosin light chains have lobe structures at their NH_2 and COOH termini. Both N- and C-lobes of Cmd1 bind the IQ1 motif, which buries an amphiphilic α-helical consensus sequence. Unlike mammalian -

Figure 1.4

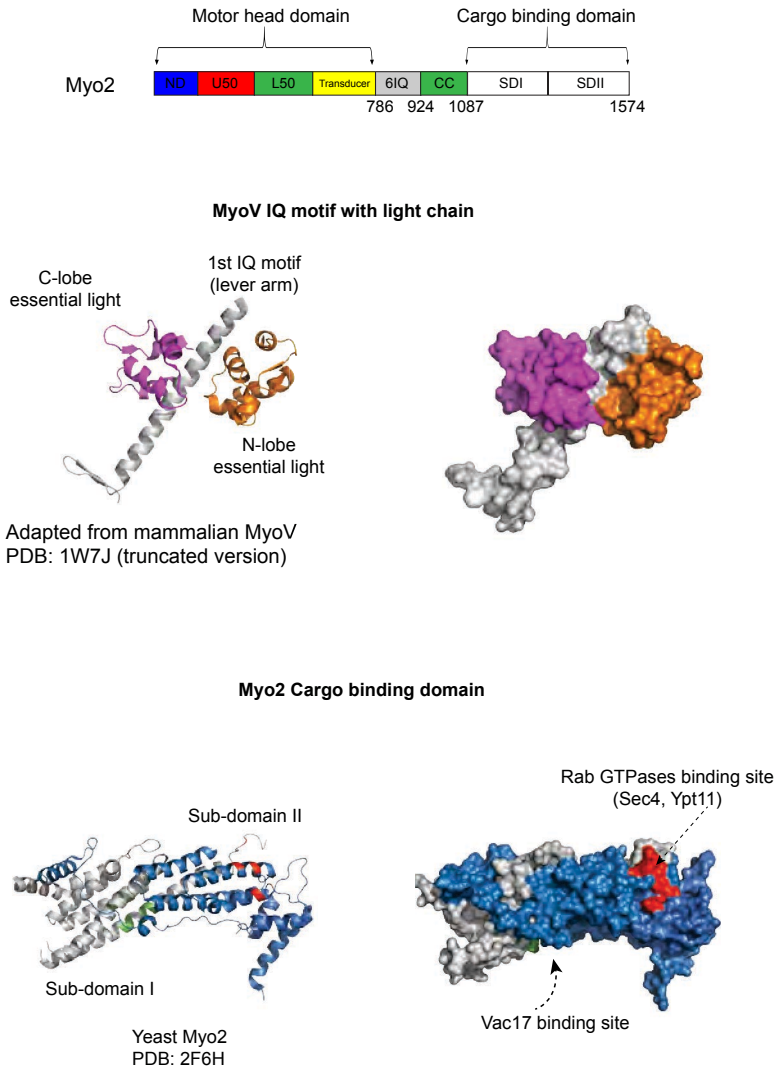

Figure 1.4. Myosin V IQ motif bound with myosin light chain and Myo2 cargo binding domain.
Both N-lobe and C-lobe of the essential light chain bind the lever arm and regulate the kinetic cycle of the myosin motor. Myo2 cargo binding domain has two sub-domains: SD(I) in gray and SD(II) blue colors. Rab GTPases binding site is colored in red.

calmodulin, CaM, yeast Cmd1 functions in a Ca^{2+} independent manner, which is shown by the *cmd1* mutant that fails to bind calcium (Brockerhoff and Davis, 1992). Mlc1 binds IQ2 with both of its N- and C-lobes (Figure 1.4). Only the Mlc1 C-lobe binds IQ4 but the N-lobe is still open and is proposed to bind other proteins (Terrak et al., 2003). Although IQ motifs are highly conserved, variation in a non-consensus sequence is proposed to regulate the myosin light chain binding affinity and, subsequently, the MyoV motor function. In mammalian MyoV, it has been established that availability of calcium regulates the kinetic cycle of the myosin motor (Lu et al., 2006). A low calcium level activates the closed-form of MyoV through CaM binding although a high level of calcium stops MyoV motility (Krementsov et al., 2004; Lu et al., 2006). The IQ motif in MyoVa can also bind syntaxin-1A (t-SNARE), which displaces CaM and supposedly regulates the exocytosis process (Watanabe et al., 2005).

The globular tail domain (coiled-coil and cargo binding domain)

The tail domain has a coiled-coil motif for homodimerization and the most class-specific cargo-binding globular tail domain, also known as cargo binding domain (CBD) which binds diverse cargos by specific adaptor proteins (Eves et al., 2012; Schott et al., 1999). The coiled-coil domain is composed of seven amino acid motifs in tandem or in heptad repeats. The hydrophobicity of the 1st and 4th residues facilitates the internal dimerization of the coiled coils (Kumar-Singh et al., 1991). The heptad repeats vary from myosin class to class. The longest repeat can be seen in muscle myosin II and the shortest repeat, which has virtually no coiled-coil, in myosin VI. MyoV has an intermediate length of ~ 60 heptad repeats with a PEST site after 20 repeats (Trybus, 2008). The PEST site represents an amino acid sequence that is rich in Proline (P), Glutamic acid (E), Serine (S), and Threonine (T) and the sequence is found in rapidly degraded proteins (Rogers et al., 1986). The site can be cleaved by calpain enzyme *in vitro* (Nascimento et al., 1996). The MyoV motor dimer after PEST site cleavage is referred to as MyoV-HMM (heavy meromyosin). The function of PEST site *in vivo* is not understood clearly. Although vertebrate MyoVa, Vb and yeast Myo4 contain PEST sites, vertebrate MyoVc and yeast Myo2 do not possess PEST sites in their coiled-coil domains (Reck-Peterson et al., 2000).

The coiled-coil domain is also known to interact with Rho3 GTPase, which is also involved in exocytosis (Adamo et al., 1999; Robinson et al., 1999).

The cargo-binding domain (CBD) in yeast Myo2 has been crystallized. *In vitro* proteolysis shows that Myo2 CBD has two major subdomains, each of which is composed of five α-helices (Pashkova et al., 2006). Subdomain I is primarily responsible for vacuolar inheritance, subdomain II for secretory vesicle transport, and each domain is joined by a long helix (Figure 1.4) (Catlett and Weisman, 1998; Pashkova et al., 2006). The CBD is involved in cargo transport, and by observing the human MyoV, the CBD is also implicated in the inhibited state of Myo2 by head to tail interaction (Li et al., 2008). Each cargo has their respective receptors or adaptors to bind the CBD. The vacuole receptor-binding site on subdomain I is offset by 180˚ from the secretory vesicle binding site on subdomain II. Although each subdomain has their respective cargo recognition, both domains are mutually required for Myo2 function, which indicates that the globular structure of the Myo2 tail is required for its functional conformation. Similarly, mammalian MyoV also has a similar arrangement of globular tail domain (Wei et al., 2013).

There have been several findings on phosphorylation regulation of myosin V motor. Using mass spectrometry phosphopeptide mapping on MyoV from *Xenopus* eggs, Karcher et al., determined that phosphorylation at the 1650 serine residue in the CBD results in dissociation of MyoV from its melanosome organelles. The phosphorylation at site S1650 corresponds to calcium/calmodulin-dependent protein kinase II (CaMKII): inhibition of the kinase prevents the release of MyoV from its organelle (Karcher et al., 2001). The Bretscher lab also showed that residues (1131-1176aa) at the subdomain I were highly phosphorylated and important for inhibition of cell growth, as shown by overexpression lethality of the Myo2 CBD alone (1131-1574aa). The residue T1131 was predicted to be a substrate of cAMP-dependent protein kinase A (PKA) (Legesse-Miller et al., 2006). The Weisman lab also found that Ptc1, a type 2C protein phosphatase, was necessary for association of Myo2 CBD with its receptors such as Vac17, Inp2, and Mmr1 for vacuole, peroxisome and mitochondria transport, respectively. Deletion of

Ptc1 resulted in defective vacuole inheritance (Jin et al., 2009). These observations suggest that Myo2 association and disassociation with its cargo is also regulated by dephosphorylation and phosphorylation events, respectively.

Recently, the Weisman lab has shown that mitochondria and vacuole organelle receptors Mmr1 and Vac17 have overlapping binding sites on Myo2 CBD (described later). The competition between Mmr1 and Vac17 presumably mediates the volume of each organelle that is inherited in daughter cells (Eves et al., 2012). Regulation of the inheritance of diverse organelles into the bud by their respective receptors is beginning to emerge. The functional importance of class V myosin CBD in polarized growth and organelle segregation has made the myosin tail a good candidate to study its specific cargo recognition in detail (Eves et al., 2012; Wei et al., 2013).

Myosin V motor : cargo selectivity through receptor availability

With its tail domain, Myo2p transports a variety of cargos to the bud tip: **post-Golgi secretory vesicles** (Govindan et al., 1995; Schott et al., 1999), **trans-Golgi network** (Arai et al., 2008; Rossanese et al., 2001), **mitochondria** (Altmann et al., 2008; Itoh et al., 2002), **vacuoles** (Catlett and Weisman, 1998; Hill et al., 1996; Ishikawa et al., 2003; Tang et al., 2003), **peroxisomes** (Hoepfner et al., 2001), and **microtubules** (Beach et al., 2000; Hwang et al., 2003; Yin et al., 2000). The mammalian homolog MyoV is also involved in cargo transport, such as membrane vesicles, mRNA, and melanosomes (Reck-Peterson et al., 2000).

Insight into "The receptor or adaptor model" of Myo2 comes from how the Myo2 cargo-binding domain (CBD) is able to select diverse cargos with cargo-specific, receptor proteins (Hammer and Sellers, 2012; Bretscher, 2003). Structural analysis and genetic mutations of Myo2 CBD has allowed mapping of several binding sites for receptor proteins (Eves et al., 2012; Wei et al., 2013). Several receptors have been identified; Rab GTPase Sec4 in mediating post-Golgi secretory vesicles transport (Santiago-Tirado et al., 2011), the Vac17p receptor that

interacts with Vac8p on vacuole membrane (Tang et al., 2003; Wang et al., 1998), the Inp2p receptor in peroxisomes (Fagarasanu et al., 2006), the Mmr1p in segregating mitochondria (Itoh et al., 2004) and the Kar9p-Bim1p in recruiting microtubules (Hwang et al., 2003; Yin et al., 2000). I will describe in detail three cargos that are transported by Myo2.

Vacuolar inheritance

Vacuoles are essential storage organelles involved in cell homeostasis, pH regulation, ions storage, and protein degradation (Klionsky et al., 1990). Similar organelles can be found in mammals known as lysosomes. Vacuoles are generated by membranes from the secretory and endocytic pathways. Vacuolar proteins such as carboxypeptidase Y and proteinase A (Klionsky et al., 1990) are sorted at the Golgi complex by Vps proteins (vacuolar protein sorting or initially known as vacuolar protein targeting, Vpt) (Banta et al., 1988; Robinson et al., 1988). The idea of vacuolar inheritance began with the observation that vacuoles in the bud were connected to their maternal vacuoles by long tubular tracks along actin filaments, which suggested that they were segregated actively into the bud (Hill et al., 1996; Weisman and Wickner, 1988). Vacuole inheritance is not essential for yeast growth due to the ability of cells to synthesize vacuoles "de novo" in the bud. This phenomenon allows scientists to classify mutants based on vacuole phenotype rather than overall growth phenotype. Three classes of vacuole mutants have been identified (Wang et al., 1996). In Class I, multilobed vacuoles were found in *vac8, vac9* and *vac10* mutants. In Class II, rounded nodules on vacuole membranes were found in *vac2, vac5, vac6, vac11,* and *vac12*. Enlarged scission defect vacuoles were found in Class III *vac7* and *fab1* mutants.

Receptor-mediated vacuole transport by Myo2 became clear in 1998 when the Weisman lab generated the *myo2-2* (G1248D) mutant that specifically failed to transport vacuoles into the bud (Catlett and Weisman, 1998). They also identified a potential vacuolar receptor Vac8, a mutant of which was also defective in vacuole inheritance (Wang et al., 1998). Vac8 is myristoylated and palmitoylated at its N-terminus and such modification is important for its localization at the vacuolar membrane. Because Vac8 lacks a transmembrane domain (TMD),

the interaction between Vac8 and the vacuole is solely due to lipid-membrane interaction. However due to lack of direct physical interaction between Myo2 and Vac8, it has been suggested that another receptor exists between the Myo2 cargo binding domain and the Vac8 protein (Wang et al., 1998).

A full picture of vacuolar active transport by Myo2 became clear when Ishikawa et al. identified the vacuole receptor Vac17 (Ishikawa et al., 2003). Using the *myo2-2* mutant as a host that supposedly has a weak interaction between *myo2* CBD and Vac8, Weisman and colleagues hypothesized that overexpression of the potential bridging receptor will suppress *myo2-2* mutant. As a suppressor of *myo2*-2, Vac17 physically interacts with the Myo2 tail and deletion of the Myo2 binding site on Vac17 (109-190aa) abrogated vacuole inheritance (Ishikawa et al., 2003). Vac17 also interacts with vacuole membrane protein Vac8, and this receptor complex Myo2-Vac17-Vac8 is responsible for vacuole inheritance. Vacuole transport is regulated by availability of the Vac17 receptor and removal of the PEST sequence on Vac17 lengthens its stability and vacuoles were aberrantly transported back to the bud neck (Tang et al., 2003).

Vacuole inheritance is also dependent on the cell cycle. Since Vac17 was a critical receptor for vacuole transport, the abundance of Vac17 through the cell cycle might predict the regulation of vacuole inheritance (Tang et al., 2003). Expression of Vac17 was found to fluctuate as the cell growth continued. Vac17 expression peaked during the G1/S phase in newly formed buds, and it declined gradually during the M phase in cytokinesis. How Vac17 is regulated is interesting. Peng and Weisman claimed that cyclin-dependent kinase (Cdk1) controlled Vac17 function by phosphorylation. Phosphorylation of Vac17 was parallel with cell cycle dependent movement of the vacuole into the bud. Mutation of the Vac17 phosphorylation site resulted in partial defects in vacuole inheritance (Peng and Weisman, 2008). Later, it was also found that phosphorylation of Vac17 recruited DmaI and E3 ligase, which were required for targeting the Vac17 for proteasomal degradation and for releasing Myo2 from its vacuole cargo (Yau et al., 2014).

Mitochondrial inheritance

Mitochondria are required for aerobic respiration and they possess their own set of mitochondrial DNA. Unlike vacuoles, mitochondria are branched, tubular networks that spread throughout the cell, and their inheritance in the bud is an active process. The first clue that mitochondria were transported by actin tracks was found by Drubin and colleagues who showed that mitochondrial organization and segregation were defective in actin mutants. In wild-type cells, mitochondria were seen as a string-like, tubular structure along actin filaments whereas 50% of the mitochondria were seen clumped together in *act1-108* and *act1-133* mutants. The mutants had mutations that were critical for myosin binding, which indicated that actin-myosin interaction was required for proper organization of mitochondria (Drubin et al., 1993).

The first observation that mitochondria displayed ATP-dependent motility on actin filaments was made in the Liza Pon lab. Having isolated yeast mitochondria, the Pon lab experimented with a modified sliding filament assay on immobilized mitochondria. With a low level of ATP (10μM), they observed unidirectional motility of mitochondria, although with a higher level of ATP or none at all, mitochondria showed no motility (Simon et al., 1995). This finding was consistent with the idea that actin-based Myo2 motors undergo an ATP dependent kinetic cycle on actin filaments. However, further experiments on the *myo2* mutant showed no defect in mitochondrial motility. That was puzzling in the beginning. The year 1995 was full of excitement, and many discoveries were made on actin-based Myo2 motor movement. Due to limited knowledge of the Myo2 motor at the time, we came to realize why the Pon lab did not detect a mitochondrial defect in the *myo2* mutant in the first place. A lot of information on the Myo2 motor became available in later years.

The *myo2* mutant that the Pon lab used was *myo2-66,* which has a defective secretory vesicle transport, rather than mitochondria segregation. The mitochondrial receptors that were discovered in later years bind at the Myo2 cargo-binding domain (CBD). The *myo2-66* allele, however, lies in the motor head domain. This became clear when the Matsui lab identified a

receptor for mitochondria inheritance. Using powerful yeast two-hybrid library screening, Itoh et al. discovered that the Myo2 tail interacted with the Rab like GTPase Ypt11. The Myo2 tail also coimmunoprecipitiated with Ypt11. Overexpression of Ypt11 brought more mitochondria into the bud, which suggested that Myo2 was an active transporter for mitochondria by the Ypt11 receptor protein (Itoh et al., 2002). However, deletion of *ypt11* causes a partial defect in mitochondria inheritance, but no effect on mitochondrial motility and morphology (Boldogh et al., 2004; Itoh et al., 2002). The Matsui lab further created *myo2* mutants: *myo2-338* and *myo2-573,* which were synthetically lethal with *ypt11Δ* and defective in mitochondria distribution.

Another mitochondrial receptor, Mmr1, was discovered when the Matsui lab explored overexpression suppression screening on the *myo2-573* mutant (Itoh et al., 2004). Although deletion of *mmr1* or *ypt11* had no significant effect on mitochondria distribution, the double mutant *mmr1Δ ypt11Δ* was inviable (Itoh et al., 2004). The Bretscher lab also showed that in the absence of *ypt11*, Mmr1 receptor became essential and was required for active transport of mitochondria (Chernyakov et al., 2013). This finding showed that budding yeast has two redundant receptors for mitochondria segregation. Eves et al. also identified receptor-binding sites on Myo2 CBD. The Ypt11 receptor binds Myo2 subdomain II on CBD, and the binding site overlaps with the receptor Sec4 for the secretory vesicle (Eves et al., 2012).

Secretory vesicles

Post-Golgi secretory vesicles constitute a major membranous organelle that is transported by Myo2 motors in polarized growth (Bretscher, 2003). Composed of a variety of proteins, phospholipids, and enzymes, secretory vesicles are targeted towards their destinations. Synthesized and originated from the endoplasmic reticulum (ER), several proteins in vesicles undergo posttranslational modifications in the Golgi complex, and resume their secretory pathway towards the plasma membrane (PM) where they deposit proteins and membranes (Barlowe and Miller, 2013). In addition, failure of Myo2p to segregate organelles such as the trans-Golgi network, endoplasmic reticulum, vacuoles, mitochondria, and peroxisomes to the growing bud is different, phenotypically and fundamentally, from that of

Myo2p to deliver secretory vesicles. Myo2 mutants, that fail to transport secretory vesicles, cause polarized growth arrest, undergo isotropic growth, and ultimately result in cell death (Govindan et al., 1995; Schott et al., 1999). Because my research is on secretory vesicle transport, I will describe the secretory pathway briefly below.

Polarized distribution of secretory vesicles

The overall outline of secretion came alive when George Palade first showed the sequential steps in the secretory pathway. Pancreatic acinar cells are well known for their exocrine function (i.e., secreting digestive enzymes). With the amino acid radiolabeling technique, and varying time-pulsed autoradiographs that were coupled with thin-sliced, pancreatice cells from guinea pigs, several vesicles were seen to emerge from rough endoplasmic reticulum and end at the periphery of zymogen granules at the Golgi complex (Jamieson and Palade, 1967a; Jamieson and Palade, 1967b; Jamieson and Palade, 1968). This was the first demonstration of the existence of the secretory pathway in the form of small vesicles. Palade was awarded the Nobel Prize in 1974.

Fifteen years later, Peter Novick and Randy Schekman further fine-tuned our knowledge of the secretion process in a more defined pathway. Using genetically tractable and biochemically testable budding yeast, they created the first ever conditional mutant, *sec1-1,* that accumulated secretory proteins such as invertase and acid phosphatase in small vesicles at the restrictive temperature of 37˚C (Novick and Schekman, 1979). Out of 188 mutants that they screened, they found 23 complementation groups that could be categorized into early (pre-Golgi) or late secretory pathways (post-Golgi) (Novick et al., 1981; Novick et al., 1980). Those genes became known as building blocks for sequential steps in the secretory pathway and Randy Schekman was later awarded the Nobel Prize in 2013.

Early secretory pathway

A number of secretory proteins such as Sec12, Sec13, Sec18, and Sec23 are involved in the early secretory steps (Novick et al., 1981). Blockage in the early steps results in ER proliferation and no vesicles will be formed. Synthesis of a small vesicle, or COPII vesicle begins at the ER. The COPII vesicle has two layers of coats and is composed of five cytosolic proteins: Sar1, Sec23, Sec24, Sec13, and Sec31. *In vitro* reconstitution of COPII vesicles further deepened our understanding of how these proteins worked mechanistically (Barlowe et al., 1994; Salama et al., 1993).

ER resident protein Sec12 is a GEF for Sar1, thereby activating Sar1 to the GTP-bound form. Activated Sar1 reveals its amino amphipathic helix that inserts into the ER membrane. Localized Sar1 recruits inner COPII coats comprised of heterodimer Sec23/24 and a small curvature is formed at the ER site as a result. Sec23 is a Sar1 RabGTPase-activating protein (GAP), and primes the intrinsic GTPase activity of Sar1. With the arrival of the outer coat heterotetramer Sec13/31, the hydrolytic activity increases tenfold and COPII vesicle buds off from the ER (Fromme and Schekman, 2005). The ordered assembly of vesicle formation is highly conserved in other systems, and they are localized at certain ER sites known as ER exit site (ERES) in mammalian cells (Jensen and Schekman, 2011).

COPII vesicles represent anterograde movement from ER to Golgi but COPI vesicles mediate retrograde movement from Golgi to ER (Spang and Schekman, 1998). The budded COPII vesicles diffuse and fuse at the cisternae Golgi with the help of a dozen proteins. The first member of the RabGTPases, Ypt1, together with Uso1, a protein that contains an extended coiled-coil domain, guides the COPII vesicles (60-70nm) towards the cis-Golgi site (Nakajima et al., 1991; Segev et al., 1988). The TRAPPI complex (Transport protein particle I) comprised of six subunits (Bet3, Bet5, Trs20, Trs23, Trs31, and Trs33) facilitates the tethering of the COPII vesicles at the Golgi membranes by binding of the Bet 3 to COPII Sec23 subunit (Cai et al., 2007).

Fusion of the COPII vesicle at its target cis-Golgi membrane is completed by the SNARE complex (**s**oluble **N**-ethylmaleimide-sensitive factor **a**ttachment protein **re**ceptors). The SNARE complex has 3 proteins: (1) Synaptobrevin or v-SNARE, (2) Syntaxin or t-SNARE and (3) SNAP-25 or t-SNARE (Weber et al., 1998). The complex has a four-helix bundle: one helix from the v-SNARE, one from the syntaxin and two from the SNAP-25. Structural analysis indicated that a "zero" ionic layer exists in the helix bundle that zippers together, which drives fusion of the vesicle with the target membrane. The ionic layer comes from one arginine "R" residue on v-SNARE (hence R-SNARE) and three glutatmine "Q" residues from t-SNARE (Q-SNARE) (Fasshauer et al., 1998; Sutton et al., 1998). With COPII vesicle fusion in budding yeast, Bet1 serves as a v-SNARE, but Sed5, Bos1 and Sec22 serve as t-SNAREs (Parlati et al., 2000). Yeast has at least 24 members of the SNARE family (Burri and Lithgow, 2004). However, cells have evolved to function efficiently with compartment-specific SNARE pairs as in Golgi, vacuole, and endosomal fusion (Furukawa and Mima, 2014; McNew et al., 2000).

Late secretory pathway parallels the Rab cascade

The first insight, that Myo2 motor is essential in late secretory stage and it transports secretory vesicles came from the investigation of conditional *myo2-66* mutant and actin-stabilizing mutant *tpm1/2* (Johnston et al., 1991; Pruyne et al., 1998). In the Bretscher lab, Daniel Schott also observed that mutations in Myo2 CBD, e.g, *myo2-12*, resulted in a phenotype similar to that of the *myo2-66* in which vesicles accumulated and resulted in isotropic growth. This suggested that Myo2 CBD was a potential target for association of vesicles (Schott et al., 1999). Another crucial finding by Schott was that reducing the length of the Myo2 lever arm (6IQ → 0IQ) significantly decreased the Myo2 mobility from 3μm/s to 0.2μm/s, which was coupled with a similar decrease in secretory vesicle movement that was observed by GFP-Sec4 (Schott et al., 2002). These data suggested that the actin-based Myo2 motor was primarily responsible for vectorial transport of secretory vesicles.

Rab GTPases are master regulators of membrane trafficking (Hutagalung and Novick, 2011). Ypt31/32 are TGN (Trans-Golgi Network)-localized Rab GTPases. Ypt32 recruits Sec2

which is a Sec4 GEF (Ortiz et al., 2002). Sec2 activates cytosolic Sec4 into a GTP-bound form. Activated Sec4 is then localized to the exocytic vesicle from the TGN by its prenyl group at its C-terminus (Calero et al., 2003). Both Ypt32 and Sec4 in the GTP state bind the Myo2 tail, thereby activating the inhibited form of Myo2 (Donovan and Bretscher, 2012; Jin et al., 2011; Lipatova et al., 2008). The crucial importance of the Rab cascade in association with the Myo2 tail with vesicles was observed clearly in *ypt31Δ/ypt32ts* when the initial Rab Ypt32 function at the TGN was blocked at the restrictive temperature of 37˚C (Lipatova et al., 2008).

The next puzzle would be establishing the GEF for Ypt31/32. A potential GEF candidate was the TRAPPII complex (Morozova et al., 2006). However, controversy abounded as several papers presented different findings from different labs. The TRAPPII complex consists of 9 subunits: Trs120, Trs130, and Trs65 in addition to the six subunits of TRAPPI (Bet3, Bet5, Trs20, Trs23, Trs31, and Trs33). The four subunits of the TRAPPI complex (Bet3, Bet5, Trs23 and Trs31) make up a core domain that acts as a Ypt1 GEF, which is involved in the ER-Golgi pathway described earlier (Kim et al., 2016). The Segev lab claimed that by having three new subunits, the TRAPPII complex exerted its GEF activity on Ypt31/32 at the TGN and that facilitated the formation of exocytic vesicle (Morozova et al., 2006). The Susan Ferro-Novick group, however, observed that the TRAPPII complex still activated Ypt1 although it had no GEF activity on Ypt31/32 pairs. The conflicting finding was further extended when Pinar et al. paper showed that the TRAPPII complex activates RabE, Ypt31 ortholog, in *Aspergillus nidulans* (Pinar et al., 2015). It became definitive when the Fromme lab showed that TRAPPII complex activates Ypt31/32 and plays an important role in this late secretory step (Thomas and Fromme, 2016).

In parallel with the Rab cascade, membrane composition of the Golgi plays a critical role. Phospholipid PI4P (phosphatidylinositol 4-phosphate), which is catalyzed by Pik1 (PI 4-kinase), is enriched in the Golgi membrane (Flanagan et al., 1993; Walch-Solimena and Novick, 1999). As post-Golgi vesicles mature en route to the plasma membrane, PI4P is converted to $PI4,5P_2$ by PM-localized Mss4 (PI4P 5-kinase) (Homma et al., 1998). Therefore changes in the

level of PI4P may regulate secretory vesicle transport. Indeed Santiago-Tirado et al., showed that increasing the level of PI4P by overexpressing Pik1 suppressed the conditional *myo2* mutant, *myo2-12*. A chimera with the PH domain that recognizes PI4P fused to Myo2 tail, can suppress *myo2-12*, which suggested that binding PI4P can supplement a defect in the Myo2 binding Sec4 (Santiago-Tirado et al., 2011).

Exocytic process

As post-Golgi vesicles mature in the late secretory stage, activated Sec4 recruits its effector Sec15, displacing Ypt31/32 (Medkova et al., 2006; Ortiz et al., 2002). Subsequently Sec15, one of the exocyst subunits, primes the vesicle to tether and dock at the PM for fusion competence. During the span of 7 years, the Novick lab contributed to a clearer picture of the exocyst complex. The majority of the first 23 *SEC* complementation groups represent the exocyst components (Novick et al., 1980). Beginning with Sec8 and Sec15, the Novick lab found that vesicles were accumulated in the mutants and that they appeared to be downstream of Sec4 (Bowser et al., 1992). Subsequently, with a genetic approach, co-immunoprecipitation, and peptide microsequencing, further work by the Novick lab demonstrated that the exocyst is a hetero-octomeric complex that contains Sec3, Sec5, Sec6, Sec8, Sec10, Sec15, Exo70, and Exo84 (Guo et al., 1999; TerBush et al., 1996; TerBush and Novick, 1995).

The Myo2 tail interacts with Sec15 and Exo70, indicating that the vesicle-transporting Myo2 motors dock at the PM by physically interacting with the exocyst (Jin et al., 2011). Conditional mutant *sec15-1* leads to a polarized accumulation of secretory vesicles in the bud, indicating that the exocyst complex plays an important role in vesicles fusion at the plasma membrane (Salminen and Novick, 1989; Walch-Solimena et al., 1997). It is still an open question whether all 8 subunits of the exocyst complex come together or if they are assembled at the site of vesicle fusion in the bud. Using the fluorescence recovery after photobleaching method (FRAP), the Novick lab found that six subunits (Sec5p, Sec6p, Sec8p, Sec10p, Sec15p, and Exo84p) showed the similar mobility as the secretory vesicle marked by GFP-Sec4 (half-life = ~ 12s). The other two subunits Sec3 and Exo70 exhibited a slower mode of recovery.

Using the actin-depolymerizing agent, Latrunculin A, all six subunits lost their polarity but Sec3 and Exo70 retain the polarity in the bud (Boyd et al., 2004). This finding indicated that certain subunits of the exocyst complex localized at the plasma membrane and the other subunits were recruited as the vesicles matured. Recently the Mary Munson group showed that the exocyst complex was comprised of two stable four-subunits modules, which were packed together as long rods (Heider et al., 2016). Sec15 and Exo70 occupied the outermost position in one module but the other module consisted of Sec3 in its outermost position, which suggested that each module had different functions regarding the exocytic mechanism. That is Sec15 and Exo70 will react primarily to the cytosolic side of the incoming vesicles and the other module facing the PM will cooperate with the PM components. In addition Sec3 directly interacted with Rho1 in its GTP-bound form and Sec3 polarity was lost in the *rho1-5* mutant (Guo et al., 2001). How those Rho GTPases cooperate with the exocyst, vesicle tethering, and fusion events at the plasma membrane would be an interesting area of research into the secretory pathway.

The secretory vesicle finally reaches its destination, the plasma membrane. The fusion of the vesicle membrane and the acceptor membrane (PM) is finally completed by the SNARE complex. As described earlier, v- and t-SNAREs help zipper vesicle and acceptor membranes together. In the case of vesicle fusion at the PM, Snc1 or Snc2 (v-SNARE) from the vesicle and Sso1 or Sso2 (Syntaxin homolog) and Sec9 (SNAP-25 homolog) at the PM pair up to form the SNARE complex and fusion occurs (Aalto et al., 1993; Brennwald et al., 1994; Protopopov et al., 1993). Regarding the timeline of the events, Bretscher and Donovan showed that Sec4 RabGTPase, master regulator of vesicle trafficking, needed to be deactivated by its GAP, Msb3/4 (Donovan and Bretscher, 2012). The Myo2 motor was then released 4 seconds before the final fusion of the vesicle into the membrane (Donovan and Bretscher, 2015).

Kinesin motors in brief

Because kinesin-like Smy1 is the focal point of my dissertation, how Smy1 became a scientists' mystery protein over the last 20 years will be answered by explaining the importance of the kinesin motor protein in organelle transport. Discovery of the kinesin motor itself was interesting and a rewarding experience for scientists. The first ATP-dependent motor protein discovered was skeletal muscle myosin II (Bailey, 1942). While looking for motors in the giant axon of squid, Ron Vale and colleagues stumbled upon a novel motor in axons that they named kinesin (the Greek *kinein* meaning, to move) (Vale et al., 1985).

The founding member of the kinesin superfamily proteins (KIFs) is a heterotetrameric motor composed of two identical kinesin heavy chains (KHCs) and two kinesin light chains (KLCs) (Gennerich and Vale, 2009). Walking on microtubules in a hand-over-hand manner, kinesins in general are plus-end directed motors and dyneins, which is another class of microtubule-based motors, are minus-end directed motors. The number of kinesin superfamily proteins in mammals has 45 members and 15 families, which have been created based on the homology of their domains: Kinesin-1 to Kinesin-14B (Hirokawa et al., 2009; Lawrence et al., 2004). In neurons, kinesins move distally towards the synapses and transport synaptic vesicle precursors. In non-neuronal cells, kinesins are directed from the microtubule organizing center to the periphery of the cells. Kinesin motors play several roles in mitochondria, lysosomes, endosomes, late-Golgi, and vesicle transport (Hirokawa, 1998; Hirokawa et al., 2009). How kinesin motors transport several organelles in molecular detail compared to myosin motors is poorly understood. Budding yeast has 6 kinesin motor proteins: Cin8p, Kar3p, Kip1p, Kip2p, Kip3p, Smy1p, and one cytoplasmic dynein motor: Dyn1p (aka Dhc1p) (Hildebrandt and Hoyt, 2000). Of the six kinesins motors, only four motors (Cin8p, Kip1p, Kip3p, and Kar3p) are involved in kinetochore assembly, spindle orientation, chromosome segregation, and mitosis (Tytell and Sorger, 2006).

Initially discovered as a suppressor of the conditional *myo2* mutant *myo2-66,* Smy1 (Suppressor of Myo2) was proposed as a potential candidate for another microtubule-based kinesin-related motor protein (Lillie and Brown, 1992). Smy1p has three distinct domains: a kinesin-like motor domain, a predicted coiled-coil domain and a C-terminal myosin-binding domain (Beningo et al., 2000). Despite the sequence similarity with motor domains of the kinesin superfamily, Smy1p does not require microtubules for its function, and deletion of *SMY1* (*smy1Δ*) does not affect membrane trafficking and growth overall (Lillie and Brown, 1998). Characterization of Smy1p function, therefore, suggests an intriguing yet challenging investigation. Disruption of microtubules or mutating the potential ATPase residues in the Smy1 motor domain does not disrupt Smy1 localization and its suppression activity.

The first proposal of Smy1 function came to light when the Trybus group claimed that Smy1 enhances the processivity of Myo2 by acting as an electrostatic tether to the actin cables (Hodges et al., 2009). Although the model is attractive, they did not mention why *smy1Δ* has no overall effect on Myo2 processivity *in vivo*. Their model showed how Myo2p-ΔGT (lacking a globular tail domain) was still processive *in vitro* due to the abundance of Smy1 that acted as an electrostatic tether to the actin cables. However this model fails to explain why overexpressed Smy1 can not suppress the temperature-sensitive phenotype of the *myo2-14* mutant that was created in our lab, which has two mutations at the CBD and amber mutation at 1536aa (stop codon) (Schott et al., 1999). Interestingly, the function of Smy1p was revisited in 2011 when the Bruce Goode lab showed that Smy1p was a passenger protein on Myo2p and that it acted as a formin Bnr1p damper, thereby suppressing the extensive formation of actin filaments that originated at the bud neck (Chesarone-Cataldo et al., 2011). Unfortunately, both of these models fail to explain why overexpression of Smy1 suppresses the *ts* phenotype of *myo2-66* and other conditional *myo2* tail mutants (Schott et al., 1999), which left the the exact function of Smy1p even more elusive. Therefore my dissertation aims to describe a potential role of Smy1 in the vesicle transport pathway.

Implications of defective Myo2 dependent secretory pathway

Because a vast number of functional proteins are conserved evolutionarily, many of the molecules that are involved in membrane trafficking such as the ER and the Golgi apparatus, intra-Golgi trafficking, and trans-Golgi to plasma membrane, have their homologs in mammalian cells (Schwartz et al., 2007). Intuitively, any disruption in vesicle trafficking results in yeast death. Parallel with this phenomenon, interference in mammalian vesicle trafficking also causes secretion-related diseases (Ton et al., 2002). The dilute mouse mutant has a mutation of the myosin-V, giving rise to a pale coat color and death due to neurological disorders three weeks after birth (Mercer et al., 1991), which indicated the importance of transport of melanosomes and smooth endoplasmic reticulum (SER) in the skin and neurons, respectively (Evans et al., 1997; Takagishi et al., 1996). In humans, MyoVa has been implicated in synaptic vesicle transport, myelination, potentiation in the nervous system, and insulin secretion (Correia et al., 2008; Prekeris and Terrian, 1997; Sloane and Vartanian, 2007; Varadi et al., 2005).

The receptor model of yeast Myo2p in cargo recognition and transport can also be applied to mammalian cells. Humans have 38 myosin genes, including three class V myosin genes (MyoVa, Vb and Vc) (Berg et al., 2001). MyoVa, the mammalian homolog of yeast Myo2p, is involved in pigment transport. Rab27a on melanosomes is recruited by melanophilin (Slac2-a adaptor protein) to MyoVa motors for local transport (Fukuda et al., 2002; Sckolnick et al., 2013; Strom et al., 2002). A defect in any of the components results in the Griscelli syndrome, which is characterized by hypopigmentation and neurodegeneration (Ménasché et al., 2002; Pastural et al., 1997). Taking advantages of the similarity of membrane trafficking from yeast to humans, some researchers have proposed a new platform to express mammalian secretory proteins in yeast ectopically to characterize the proteins involved in neurodegenerative diseases (Ocampo and Barrientos, 2011).

Focus of the dissertation

With the revolution of so many scientific discoveries and applications over the past half century, researchers have turned the 20th century into the molecular biology era. Beginning from a crude knowledge of vesicle trafficking in yeast, many labs have made significant contributions to understanding the process of vesicle trafficking in molecular detail. Many proteins have been identified with respect to their roles in the secretory vesicle pathway. My dissertation will highlight molecular functions of the proteins that play important roles in regulating vesicle transport.

Smy1 was initially believed to be a microtubule-based kinesin motor protein. Further studies showed otherwise. Since then, the function of Smy1 has been claimed to be either a Myo2 processivity agent, or an actin filament regulator. The functions of Smy1 seem to have many roles and yet those observations do not explain why Smy1 suppresses the *myo2-66* mutant that has a secretory defect. The main function of Smy1 remains elusive. The focus of my thesis was to investigate the molecular function of Smy1 suppression on *myo2-66* in detail which subsequently led to a discovery of a new RhoGAP protein, *GYM1* (name given in this thesis) that also plays an important role in vesicle trafficking. Because RabGTPases are major membrane trafficking proteins, the involvement of Gym1 in the secretory pathway will be the first RhoGAP protein that bridges the gap between Rab and RhoGTPases in the yeast secretory pathway. The regulatory process imposed by proteins such as kinesin-related Smy1 and RhoGAP Gym1 in Myo2 delivery cycle will be applicable to other secretory systems.

References

Aalto, M.K., H. Ronne, and S. Keränen. 1993. Yeast syntaxins Sso1p and Sso2p belong to a family of related membrane proteins that function in vesicular transport. *The EMBO journal*. 12:4095-4104.

Adamo, J.E., G. Rossi, and P. Brennwald. 1999. The Rho GTPase Rho3 has a direct role in exocytosis that is distinct from its role in actin polarity. *Molecular biology of the cell*. 10:4121-4133.

Adams, A.E., D. Botstein, and D.G. Drubin. 1989. A yeast actin-binding protein is encoded by SAC6, a gene found by suppression of an actin mutation. *Science*. 243:231-233.

Adams, A.E., and J.R. Pringle. 1984. Relationship of actin and tubulin distribution to bud growth in wild-type and morphogenetic-mutant Saccharomyces cerevisiae. *J Cell Biol*. 98:934-945.

Altmann, K., M. Frank, D. Neumann, S. Jakobs, and B. Westermann. 2008. The class V myosin motor protein, Myo2, plays a major role in mitochondrial motility in Saccharomyces cerevisiae. *The Journal of cell biology*. 181:119-130.

Amatruda, J.F., J.F. Cannon, K. Tatchell, C. Hug, and J.A. Cooper. 1990. Disruption of the actin cytoskeleton in yeast capping protein mutants. *Nature*. 344:352-354.

Arai, S., Y. Noda, S. Kainuma, I. Wada, and K. Yoda. 2008. Ypt11 functions in bud-directed transport of the Golgi by linking Myo2 to the coatomer subunit Ret2. *Current biology : CB*. 18:987-991.

Bailey, K. 1942. Myosin and adenosinetriphosphatase. *The Biochemical journal*. 36:121-139.

Banta, L.M., J.S. Robinson, D.J. Klionsky, and S.D. Emr. 1988. Organelle assembly in yeast: characterization of yeast mutants defective in vacuolar biogenesis and protein sorting. *J Cell Biol*. 107:1369-1383.

Barlowe, C., L. Orci, T. Yeung, M. Hosobuchi, S. Hamamoto, N. Salama, M.F. Rexach, M. Ravazzola, M. Amherdt, and R. Schekman. 1994. COPII: a membrane coat formed by Sec proteins that drive vesicle budding from the endoplasmic reticulum. *Cell*. 77:895-907.

Barlowe, C.K., and E.A. Miller. 2013. Secretory protein biogenesis and traffic in the early secretory pathway. *Genetics*. 193:383-410.

Beach, D.L., J. Thibodeaux, P. Maddox, E. Yeh, and K. Bloom. 2000. The role of the proteins Kar9 and Myo2 in orienting the mitotic spindle of budding yeast. *Current biology : CB*. 10:1497-1506.

Beningo, K.A., S.H. Lillie, and S.S. Brown. 2000. The yeast kinesin-related protein Smy1p exerts its effects on the class V myosin Myo2p via a physical interaction. *Molecular biology of the cell*. 11:691-702.

Berg, J.S., B.C. Powell, and R.E. Cheney. 2001. A millennial myosin census. *Mol Biol Cell*. 12:780-794.

Bi, E. 2001. Cytokinesis in budding yeast: the relationship between actomyosin ring function and septum formation. *Cell structure and function*. 26:529-537.

Bi, E., and H.O. Park. 2012. Cell polarization and cytokinesis in budding yeast. *Genetics*. 191:347-387.

Boldogh, I.R., S.L. Ramcharan, H.-C. Yang, and L.A. Pon. 2004. A type V myosin (Myo2p) and a Rab-like G-protein (Ypt11p) are required for retention of newly inherited mitochondria in yeast cells during cell division. *Molecular biology of the cell*. 15:3994-4002.

Bose, I., J.E. Irazoqui, J.J. Moskow, E.S. Bardes, T.R. Zyla, and D.J. Lew. 2001. Assembly of scaffold-mediated complexes containing Cdc42p, the exchange factor Cdc24p, and the effector Cla4p required for cell cycle-regulated phosphorylation of Cdc24p. *J Biol Chem*. 276:7176-7186.

Botstein, D., S.A. Chervitz, and J.M. Cherry. 1997. Yeast as a model organism. *Science (New York, N.Y.)*. 277:1259-1260.

Bowser, R., H. Muller, B. Govindan, and P. Novick. 1992. Sec8p and Sec15p are components of a plasma membrane-associated 19.5S particle that may function downstream of Sec4p to control exocytosis. *J Cell Biol*. 118:1041-1056.

Boyd, C., T. Hughes, M. Pypaert, and P. Novick. 2004. Vesicles carry most exocyst subunits to exocytic sites marked by the remaining two subunits, Sec3p and Exo70p. *The Journal of cell biology*. 167:889-901.

Brennwald, P., B. Kearns, K. Champion, S. Keränen, V. Bankaitis, and P. Novick. 1994. Sec9 is a SNAP-25-like component of a yeast SNARE complex that may be the effector of Sec4 function in exocytosis. *Cell*. 79:245-258.

Bretscher, A. 2003. Polarized growth and organelle segregation in yeast: the tracks, motors, and receptors. *J Cell Biol*. 160:811-816.

Brockerhoff, S.E., and T.N. Davis. 1992. Calmodulin concentrates at regions of cell growth in Saccharomyces cerevisiae. *J Cell Biol*. 118:619-629.

Burri, L., and T. Lithgow. 2004. A complete set of SNAREs in yeast. *Traffic*. 5:45-52.

Cai, H., S. Yu, S. Menon, Y. Cai, D. Lazarova, C. Fu, K. Reinisch, J.C. Hay, and S. Ferro-Novick. 2007. TRAPPI tethers COPII vesicles by binding the coat subunit Sec23. *Nature*. 445:941-944.

Calero, M., C.Z. Chen, W. Zhu, N. Winand, K.A. Havas, P.M. Gilbert, C.G. Burd, and R.N. Collins. 2003. Dual prenylation is required for Rab protein localization and function. *Mol Biol Cell*. 14:1852-1867.

Catlett, N.L., and L.S. Weisman. 1998. The terminal tail region of a yeast myosin-V mediates its attachment to vacuole membranes and sites of polarized growth. *Proceedings of the National Academy of Sciences of the United States of America*. 95:14799-14804.

Chernyakov, I., F. Santiago-Tirado, and A. Bretscher. 2013. Active segregation of yeast mitochondria by Myo2 is essential and mediated by Mmr1 and Ypt11. *Curr Biol*. 23:1818-1824.

Chesarone-Cataldo, M., C. Guérin, J.H. Yu, R. Wedlich-Soldner, L. Blanchoin, and B.L. Goode. 2011. The myosin passenger protein Smy1 controls actin cable structure and dynamics by acting as a formin damper. *Developmental cell*. 21:217-230.

Correia, S.S., S. Bassani, T.C. Brown, M.F. Lise, D.S. Backos, A. El-Husseini, M. Passafaro, and J.A. Esteban. 2008. Motor protein-dependent transport of AMPA receptors into spines during long-term potentiation. *Nat Neurosci*. 11:457-466.

Coureux, P.D., H.L. Sweeney, and A. Houdusse. 2004. Three myosin V structures delineate essential features of chemo-mechanical transduction. *EMBO J*. 23:4527-4537.

Coureux, P.D., A.L. Wells, J. Menetrey, C.M. Yengo, C.A. Morris, H.L. Sweeney, and A. Houdusse. 2003. A structural state of the myosin V motor without bound nucleotide. *Nature*. 425:419-423.

Cyert, M.S. 2001. Genetic analysis of calmodulin and its targets in Saccharomyces cerevisiae. *Annu Rev Genet*. 35:647-672.

De La Cruz, E.M., A.L. Wells, S.S. Rosenfeld, E.M. Ostap, and H.L. Sweeney. 1999. The kinetic mechanism of myosin V. *Proc Natl Acad Sci U S A*. 96:13726-13731.

Dekker, J., K. Rippe, M. Dekker, and N. Kleckner. 2002. Capturing chromosome conformation. *Science*. 295:1306-1311.

Donovan, K.W., and A. Bretscher. 2012. Myosin-V is activated by binding secretory cargo and released in coordination with Rab/exocyst function. *Dev Cell*. 23:769-781.

Donovan, K.W., and A. Bretscher. 2015. Tracking individual secretory vesicles during exocytosis reveals an ordered and regulated process. *J Cell Biol*. 210:181-189.

Drubin, D.G., H.D. Jones, and K.F. Wertman. 1993. Actin structure and function: roles in mitochondrial organization and morphogenesis in budding yeast and identification of the phalloidin-binding site. *Mol Biol Cell*. 4:1277-1294.

Drubin, D.G., K.G. Miller, and D. Botstein. 1988. Yeast actin-binding proteins: evidence for a role in morphogenesis. *J Cell Biol*. 107:2551-2561.

Evangelista, M., D. Pruyne, D.C. Amberg, C. Boone, and A. Bretscher. 2002. Formins direct Arp2/3-independent actin filament assembly to polarize cell growth in yeast. *Nature cell biology*. 4:260-269.

Evans, L.L., J. Hammer, and P.C. Bridgman. 1997. Subcellular localization of myosin V in nerve growth cones and outgrowth from dilute-lethal neurons. *J Cell Sci*. 110 (Pt 4):439-449.

Eves, P.T., Y. Jin, M. Brunner, and L.S. Weisman. 2012. Overlap of cargo binding sites on myosin V coordinates the inheritance of diverse cargoes. *The Journal of cell biology*. 198:69-85.

Fagarasanu, A., M. Fagarasanu, G.A. Eitzen, J.D. Aitchison, and R.A. Rachubinski. 2006. The peroxisomal membrane protein Inp2p is the peroxisome-specific receptor for the myosin V motor Myo2p of Saccharomyces cerevisiae. *Developmental cell*. 10:587-600.

Fasshauer, D., R.B. Sutton, A.T. Brunger, and R. Jahn. 1998. Conserved structural features of the synaptic fusion complex: SNARE proteins reclassified as Q- and R-SNAREs. *Proc Natl Acad Sci U S A*. 95:15781-15786.

Flanagan, C.A., E.A. Schnieders, A.W. Emerick, R. Kunisawa, A. Admon, and J. Thorner. 1993. Phosphatidylinositol 4-kinase: gene structure and requirement for yeast cell viability. *Science*. 262:1444-1448.

Forgacs, E., S. Cartwright, T. Sakamoto, J.R. Sellers, J.E. Corrie, M.R. Webb, and H.D. White. 2008. Kinetics of ADP dissociation from the trail and lead heads of actomyosin V following the power stroke. *J Biol Chem*. 283:766-773.

Fromme, J.C., and R. Schekman. 2005. COPII-coated vesicles: flexible enough for large cargo? *Curr Opin Cell Biol*. 17:345-352.

Fukuda, M., T.S. Kuroda, and K. Mikoshiba. 2002. Slac2-a/melanophilin, the missing link between Rab27 and myosin Va: implications of a tripartite protein complex for melanosome transport. *The Journal of biological chemistry*. 277:12432-12436.

Furukawa, N., and J. Mima. 2014. Multiple and distinct strategies of yeast SNAREs to confer the specificity of membrane fusion. *Sci Rep*. 4:4277.

Gallwitz, D., and R. Seidel. 1980. Molecular cloning of the actin gene from yeast Saccharomyces cerevisiae. *Nucleic Acids Res*. 8:1043-1059.

Gallwitz, D., and I. Sures. 1980. Structure of a split yeast gene: complete nucleotide sequence of the actin gene in Saccharomyces cerevisiae. *Proc Natl Acad Sci U S A*. 77:2546-2550.

Gennerich, A., and R.D. Vale. 2009. Walking the walk: how kinesin and dynein coordinate their steps. *Curr Opin Cell Biol*. 21:59-67.

Gimeno, C.J., and G.R. Fink. 1994. Induction of pseudohyphal growth by overexpression of PHD1, a Saccharomyces cerevisiae gene related to transcriptional regulators of fungal development. *Mol Cell Biol*. 14:2100-2112.

Goffeau, A., B.G. Barrell, H. Bussey, R.W. Davis, B. Dujon, H. Feldmann, F. Galibert, J.D. Hoheisel, C. Jacq, M. Johnston, E.J. Louis, H.W. Mewes, Y. Murakami, P. Philippsen, H. Tettelin, and S.G. Oliver. 1996. Life with 6000 genes. *Science*. 274:546, 563-547.

Goley, E.D., and M.D. Welch. 2006. The ARP2/3 complex: an actin nucleator comes of age. *Nature reviews. Molecular cell biology*. 7:713-726.

Goode, B.L., and M.J. Eck. 2007. Mechanism and function of formins in the control of actin assembly. *Annu Rev Biochem*. 76:593-627.

Goodson, H.V., B.L. Anderson, H.M. Warrick, L.A. Pon, and J.A. Spudich. 1996. Synthetic lethality screen identifies a novel yeast myosin I gene (MYO5): myosin I proteins are required for polarization of the actin cytoskeleton. *The Journal of cell biology*. 133:1277-1291.

Goodson, H.V., and J.A. Spudich. 1995. Identification and molecular characterization of a yeast myosin I. *Cell motility and the cytoskeleton*. 30:73-84.

Govindan, B., R. Bowser, and P. Novick. 1995. The role of Myo2, a yeast class V myosin, in vesicular transport. *The Journal of cell biology*. 128:1055-1068.

Greig, D., and J.Y. Leu. 2009. Natural history of budding yeast. *Curr Biol*. 19:R886-890.

Gulli, M.P., M. Jaquenoud, Y. Shimada, G. Niederhauser, P. Wiget, and M. Peter. 2000. Phosphorylation of the Cdc42 exchange factor Cdc24 by the PAK-like kinase Cla4 may regulate polarized growth in yeast. *Mol Cell*. 6:1155-1167.

Guo, W., D. Roth, C. Walch-Solimena, and P. Novick. 1999. The exocyst is an effector for Sec4p, targeting secretory vesicles to sites of exocytosis. *The EMBO journal*. 18:1071-1080.

Guo, W., F. Tamanoi, and P. Novick. 2001. Spatial regulation of the exocyst complex by Rho1 GTPase. *Nature cell biology*. 3:353-360.

Haarer, B.K., S.H. Lillie, A.E. Adams, V. Magdolen, W. Bandlow, and S.S. Brown. 1990. Purification of profilin from Saccharomyces cerevisiae and analysis of profilin-deficient cells. *J Cell Biol*. 110:105-114.

Haarer, B.K., A. Petzold, S.H. Lillie, and S.S. Brown. 1994. Identification of MYO4, a second class V myosin gene in yeast. *Journal of cell science*. 107 (Pt 4):1055-1064.

Hammer, J.A., 3rd, and J.R. Sellers. 2012. Walking to work: roles for class V myosins as cargo transporters. *Nature reviews. Molecular cell biology*. 13:13-26.

Hartwell, L.H., J. Culotti, and B. Reid. 1970. Genetic control of the cell-division cycle in yeast. I. Detection of mutants. *Proc Natl Acad Sci U S A*. 66:352-359.

Heider, M.R., M. Gu, C.M. Duffy, A.M. Mirza, L.L. Marcotte, A.C. Walls, N. Farrall, Z. Hakhverdyan, M.C. Field, M.P. Rout, A. Frost, and M. Munson. 2016. Subunit connectivity, assembly determinants and architecture of the yeast exocyst complex. *Nat Struct Mol Biol*. 23:59-66.

Hildebrandt, E.R., and M.A. Hoyt. 2000. Mitotic motors in Saccharomyces cerevisiae. *Biochimica et biophysica acta*. 1496:99-116.

Hill, K.L., N.L. Catlett, and L.S. Weisman. 1996. Actin and myosin function in directed vacuole movement during cell division in Saccharomyces cerevisiae. *The Journal of cell biology*. 135:1535-1549.

Hirokawa, N. 1998. Kinesin and dynein superfamily proteins and the mechanism of organelle transport. *Science*. 279:519-526.

Hirokawa, N., Y. Noda, Y. Tanaka, and S. Niwa. 2009. Kinesin superfamily motor proteins and intracellular transport. *Nature reviews. Molecular cell biology*. 10:682-696.

Hodges, A.R., C.S. Bookwalter, E.B. Krementsova, and K.M. Trybus. 2009. A nonprocessive class V myosin drives cargo processively when a kinesin- related protein is a passenger. *Current biology : CB*. 19:2121-2125.

Hodges, A.R., E.B. Krementsova, C.S. Bookwalter, P.M. Fagnant, T.E. Sladewski, and K.M. Trybus. 2012. Tropomyosin is essential for processive movement of a class V myosin from budding yeast. *Curr Biol*. 22:1410-1416.

Hoepfner, D., M. van den Berg, P. Philippsen, H.F. Tabak, and E.H. Hettema. 2001. A role for Vps1p, actin, and the Myo2p motor in peroxisome abundance and inheritance in Saccharomyces cerevisiae. *The Journal of cell biology*. 155:979-990.

Homma, K., S. Terui, M. Minemura, H. Qadota, Y. Anraku, Y. Kanaho, and Y. Ohya. 1998. Phosphatidylinositol-4-phosphate 5-kinase localized on the plasma membrane is essential for yeast cell morphogenesis. *J Biol Chem*. 273:15779-15786.

Huffaker, T.C., J.H. Thomas, and D. Botstein. 1988. Diverse effects of beta-tubulin mutations on microtubule formation and function. *J Cell Biol*. 106:1997-2010.

Hutagalung, A.H., and P.J. Novick. 2011. Role of Rab GTPases in membrane traffic and cell physiology. *Physiol Rev*. 91:119-149.

Hwang, E., J. Kusch, Y. Barral, and T.C. Huffaker. 2003. Spindle orientation in Saccharomyces cerevisiae depends on the transport of microtubule ends along polarized actin cables. *The Journal of cell biology*. 161:483-488.

Ishikawa, K., N.L. Catlett, J.L. Novak, F. Tang, J.J. Nau, and L.S. Weisman. 2003. Identification of an organelle-specific myosin V receptor. *The Journal of cell biology*. 160:887-897.

Itoh, T., A. Toh-E, and Y. Matsui. 2004. Mmr1p is a mitochondrial factor for Myo2p-dependent inheritance of mitochondria in the budding yeast. *The EMBO journal*. 23:2520-2530.

Itoh, T., A. Watabe, A. Toh-E, and Y. Matsui. 2002. Complex formation with Ypt11p, a rab-type small GTPase, is essential to facilitate the function of Myo2p, a class V myosin, in mitochondrial distribution in Saccharomyces cerevisiae. *Molecular and cellular biology*. 22:7744-7757.

Jacobs, C.W., A.E. Adams, P.J. Szaniszlo, and J.R. Pringle. 1988. Functions of microtubules in the Saccharomyces cerevisiae cell cycle. *J Cell Biol*. 107:1409-1426.

Jamieson, J.D., and G.E. Palade. 1967a. Intracellular transport of secretory proteins in the pancreatic exocrine cell. I. Role of the peripheral elements of the Golgi complex. *J Cell Biol*. 34:577-596.

Jamieson, J.D., and G.E. Palade. 1967b. Intracellular transport of secretory proteins in the pancreatic exocrine cell. II. Transport to condensing vacuoles and zymogen granules. *J Cell Biol*. 34:597-615.

Jamieson, J.D., and G.E. Palade. 1968. Intracellular transport of secretory proteins in the pancreatic exocrine cell. 3. Dissociation of intracellular transport from protein synthesis. *J Cell Biol*. 39:580-588.

Jensen, D., and R. Schekman. 2011. COPII-mediated vesicle formation at a glance. *J Cell Sci*. 124:1-4.

Jin, Y., A. Sultana, P. Gandhi, E. Franklin, S. Hamamoto, A.R. Khan, M. Munson, R. Schekman, and L.S. Weisman. 2011. Myosin V transports secretory vesicles via a Rab GTPase cascade and interaction with the exocyst complex. *Dev Cell*. 21:1156-1170.

Jin, Y., P. Taylor Eves, F. Tang, and L.S. Weisman. 2009. PTC1 is required for vacuole inheritance and promotes the association of the myosin-V vacuole-specific receptor complex. *Mol Biol Cell*. 20:1312-1323.

Johnson, D.I., and J.R. Pringle. 1990. Molecular characterization of CDC42, a Saccharomyces cerevisiae gene involved in the development of cell polarity. *J Cell Biol*. 111:143-152.

Johnston, G.C., J.A. Prendergast, and R.A. Singer. 1991. The Saccharomyces cerevisiae MYO2 gene encodes an essential myosin for vectorial transport of vesicles. *The Journal of cell biology*. 113:539-551.

Kaksonen, M., Y. Sun, and D.G. Drubin. 2003. A pathway for association of receptors, adaptors, and actin during endocytic internalization. *Cell*. 115:475-487.

Karcher, R.L., J.T. Roland, F. Zappacosta, M.J. Huddleston, R.S. Annan, S.A. Carr, and V.I. Gelfand. 2001. Cell cycle regulation of myosin-V by calcium/calmodulin-dependent protein kinase II. *Science*. 293:1317-1320.

Kataoka, T., S. Powers, S. Cameron, O. Fasano, M. Goldfarb, J. Broach, and M. Wigler. 1985. Functional homology of mammalian and yeast RAS genes. *Cell*. 40:19-26.

Kim, J.J., Z. Lipatova, and N. Segev. 2016. TRAPP Complexes in Secretion and Autophagy. *Front Cell Dev Biol*. 4:20.

Klionsky, D.J., P.K. Herman, and S.D. Emr. 1990. The fungal vacuole: composition, function, and biogenesis. *Microbiol Rev*. 54:266-292.

Kornberg, R.D. 1974. Chromatin structure: a repeating unit of histones and DNA. *Science*. 184:868-871.

Krementsov, D.N., E.B. Krementsova, and K.M. Trybus. 2004. Myosin V: regulation by calcium, calmodulin, and the tail domain. *J Cell Biol*. 164:877-886.

Kumar-Singh, R., S.A. Jordan, G.J. Farrar, and P. Humphries. 1991. Poly (T/A) polymorphism at the human retinal degeneration slow (RDS) locus. *Nucleic Acids Res*. 19:5800.

Lawrence, C.J., R.K. Dawe, K.R. Christie, D.W. Cleveland, S.C. Dawson, S.A. Endow, L.S. Goldstein, H.V. Goodson, N. Hirokawa, J. Howard, R.L. Malmberg, J.R. McIntosh, H. Miki, T.J. Mitchison, Y. Okada, A.S. Reddy, W.M. Saxton, M. Schliwa, J.M. Scholey, R.D. Vale, C.E. Walczak, and L. Wordeman. 2004. A standardized kinesin nomenclature. *J Cell Biol*. 167:19-22.

Legesse-Miller, A., S. Zhang, F.H. Santiago-Tirado, C.K. Van Pelt, and A. Bretscher. 2006. Regulated phosphorylation of budding yeast's essential myosin V heavy chain, Myo2p. *Mol Biol Cell*. 17:1812-1821.

Li, R. 1997. Bee1, a yeast protein with homology to Wiscott-Aldrich syndrome protein, is critical for the assembly of cortical actin cytoskeleton. *J Cell Biol*. 136:649-658.

Li, X.D., H.S. Jung, Q. Wang, R. Ikebe, R. Craig, and M. Ikebe. 2008. The globular tail domain puts on the brake to stop the ATPase cycle of myosin Va. *Proc Natl Acad Sci U S A*. 105:1140-1145.

Lillie, S.H., and S.S. Brown. 1992. Suppression of a myosin defect by a kinesin-related gene. *Nature*. 356:358-361.

Lillie, S.H., and S.S. Brown. 1998. Smy1p, a kinesin-related protein that does not require microtubules. *The Journal of cell biology*. 140:873-883.

Lipatova, Z., A.A. Tokarev, Y. Jin, J. Mulholland, L.S. Weisman, and N. Segev. 2008. Direct interaction between a myosin V motor and the Rab GTPases Ypt31/32 is required for polarized secretion. *Mol Biol Cell*. 19:4177-4187.

Lippincott, J., and R. Li. 1998. Sequential assembly of myosin II, an IQGAP-like protein, and filamentous actin to a ring structure involved in budding yeast cytokinesis. *The Journal of cell biology*. 140:355-366.

Liu, H.P., and A. Bretscher. 1989. Disruption of the single tropomyosin gene in yeast results in the disappearance of actin cables from the cytoskeleton. *Cell*. 57:233-242.

Lu, H., E.B. Krementsova, and K.M. Trybus. 2006. Regulation of myosin V processivity by calcium at the single molecule level. *J Biol Chem*. 281:31987-31994.

Lydall, D., and T. Weinert. 1995. Yeast checkpoint genes in DNA damage processing: implications for repair and arrest. *Science*. 270:1488-1491.

Madania, A., P. Dumoulin, S. Grava, H. Kitamoto, C. Scharer-Brodbeck, A. Soulard, V. Moreau, and B. Winsor. 1999. The Saccharomyces cerevisiae homologue of human Wiskott-Aldrich syndrome protein Las17p interacts with the Arp2/3 complex. *Mol Biol Cell*. 10:3521-3538.

Madden, K., C. Costigan, and M. Snyder. 1992. Cell polarity and morphogenesis in Saccharomyces cerevisiae. *Trends Cell Biol*. 2:22-29.

McNew, J.A., F. Parlati, R. Fukuda, R.J. Johnston, K. Paz, F. Paumet, T.H. Sollner, and J.E. Rothman. 2000. Compartmental specificity of cellular membrane fusion encoded in SNARE proteins. *Nature*. 407:153-159.

Medkova, M., Y.E. France, J. Coleman, and P. Novick. 2006. The rab exchange factor Sec2p reversibly associates with the exocyst. *Mol Biol Cell*. 17:2757-2769.

Ménasché, G., A. Fischer, and G. de Saint Basile. 2002. Griscelli syndrome types 1 and 2. *American journal of human genetics*. 71:1237-1238; author reply 1238.

Mercer, J.A., P.K. Seperack, M.C. Strobel, N.G. Copeland, and N.A. Jenkins. 1991. Novel myosin heavy chain encoded by murine dilute coat colour locus. *Nature*. 349:709-713.

Moon, A.L., P.A. Janmey, K.A. Louie, and D.G. Drubin. 1993. Cofilin is an essential component of the yeast cortical cytoskeleton. *J Cell Biol*. 120:421-435.

Morozova, N., Y. Liang, A.A. Tokarev, S.H. Chen, R. Cox, J. Andrejic, Z. Lipatova, V.A. Sciorra, S.D. Emr, and N. Segev. 2006. TRAPPII subunits are required for the specificity switch of a Ypt-Rab GEF. *Nature cell biology*. 8:1263-1269.

Mortimer, R.K. 2000. Evolution and variation of the yeast (Saccharomyces) genome. *Genome Res*. 10:403-409.

Mortimer, R.K., and J.R. Johnston. 1986. Genealogy of principal strains of the yeast genetic stock center. *Genetics*. 113:35-43.

Moseley, J.B., and B.L. Goode. 2006. The yeast actin cytoskeleton: from cellular function to biochemical mechanism. *Microbiol Mol Biol Rev*. 70:605-645.

Munemitsu, S., M.A. Innis, R. Clark, F. McCormick, A. Ullrich, and P. Polakis. 1990. Molecular cloning and expression of a G25K cDNA, the human homolog of the yeast cell cycle gene CDC42. *Mol Cell Biol*. 10:5977-5982.

Nakajima, H., A. Hirata, Y. Ogawa, T. Yonehara, K. Yoda, and M. Yamasaki. 1991. A cytoskeleton-related gene, uso1, is required for intracellular protein transport in Saccharomyces cerevisiae. *J Cell Biol*. 113:245-260.

Nascimento, A.A., R.E. Cheney, S.B. Tauhata, R.E. Larson, and M.S. Mooseker. 1996. Enzymatic characterization and functional domain mapping of brain myosin-V. *J Biol Chem*. 271:17561-17569.

Novick, P., S. Ferro, and R. Schekman. 1981. Order of events in the yeast secretory pathway. *Cell*. 25:461-469.

Novick, P., C. Field, and R. Schekman. 1980. Identification of 23 complementation groups required for post-translational events in the yeast secretory pathway. *Cell*. 21:205-215.

Novick, P., and R. Schekman. 1979. Secretion and cell-surface growth are blocked in a temperature-sensitive mutant of Saccharomyces cerevisiae. *Proc Natl Acad Sci U S A*. 76:1858-1862.

Ocampo, A., and A. Barrientos. 2011. Developing yeast models of human neurodegenerative disorders. *Methods in molecular biology*. 793:113-127.

Ortiz, D., M. Medkova, C. Walch-Solimena, and P. Novick. 2002. Ypt32 recruits the Sec4p guanine nucleotide exchange factor, Sec2p, to secretory vesicles; evidence for a Rab cascade in yeast. *J Cell Biol*. 157:1005-1015.

Parlati, F., J.A. McNew, R. Fukuda, R. Miller, T.H. Sollner, and J.E. Rothman. 2000. Topological restriction of SNARE-dependent membrane fusion. *Nature*. 407:194-198.

Pashkova, N., Y. Jin, S. Ramaswamy, and L.S. Weisman. 2006. Structural basis for myosin V discrimination between distinct cargoes. *EMBO J*. 25:693-700.

Pastural, E., F.J. Barrat, R. Dufourcq-Lagelouse, S. Certain, O. Sanal, N. Jabado, R. Seger, C. Griscelli, A. Fischer, and G. de Saint Basile. 1997. Griscelli disease maps to chromosome 15q21 and is associated with mutations in the myosin-Va gene. *Nat Genet*. 16:289-292.

Peng, Y., and L.S. Weisman. 2008. The cyclin-dependent kinase Cdk1 directly regulates vacuole inheritance. *Dev Cell*. 15:478-485.

Pinar, M., H.N. Arst, Jr., A. Pantazopoulou, V.G. Tagua, V. de los Rios, J. Rodriguez-Salarichs, J.F. Diaz, and M.A. Penalva. 2015. TRAPPII regulates exocytic Golgi exit by mediating nucleotide exchange on the Ypt31 ortholog RabERAB11. *Proc Natl Acad Sci U S A*. 112:4346-4351.

Prekeris, R., and D.M. Terrian. 1997. Brain myosin V is a synaptic vesicle-associated motor protein: evidence for a Ca2+-dependent interaction with the synaptobrevin-synaptophysin complex. *J Cell Biol*. 137:1589-1601.

Protopopov, V., B. Govindan, P. Novick, and J.E. Gerst. 1993. Homologs of the synaptobrevin/VAMP family of synaptic vesicle proteins function on the late secretory pathway in S. cerevisiae. *Cell*. 74:855-861.

Pruyne, D., and A. Bretscher. 2000. Polarization of cell growth in yeast. I. Establishment and maintenance of polarity states. *Journal of cell science*. 113 (Pt 3):365-375.

Pruyne, D., M. Evangelista, C. Yang, E. Bi, S. Zigmond, A. Bretscher, and C. Boone. 2002. Role of formins in actin assembly: nucleation and barbed-end association. *Science (New York, N.Y.)*. 297:612-615.

Pruyne, D., L. Gao, E. Bi, and A. Bretscher. 2004. Stable and dynamic axes of polarity use distinct formin isoforms in budding yeast. *Mol Biol Cell*. 15:4971-4989.

Pruyne, D.W., D.H. Schott, and A. Bretscher. 1998. Tropomyosin-containing actin cables direct the Myo2p-dependent polarized delivery of secretory vesicles in budding yeast. *J Cell Biol*. 143:1931-1945.

Rayment, I. 1996. The structural basis of the myosin ATPase activity. *J Biol Chem*. 271:15850-15853.

Reck-Peterson, S.L., D.W. Provance, Jr., M.S. Mooseker, and J.A. Mercer. 2000. Class V myosins. *Biochimica et biophysica acta*. 1496:36-51.

Reck-Peterson, S.L., M.J. Tyska, P.J. Novick, and M.S. Mooseker. 2001. The yeast class V myosins, Myo2p and Myo4p, are nonprocessive actin-based motors. *J Cell Biol*. 153:1121-1126.

Robinson, J.S., D.J. Klionsky, L.M. Banta, and S.D. Emr. 1988. Protein sorting in Saccharomyces cerevisiae: isolation of mutants defective in the delivery and processing of multiple vacuolar hydrolases. *Mol Cell Biol*. 8:4936-4948.

Robinson, N.G., L. Guo, J. Imai, E.A. Toh, Y. Matsui, and F. Tamanoi. 1999. Rho3 of Saccharomyces cerevisiae, which regulates the actin cytoskeleton and exocytosis, is a GTPase which interacts with Myo2 and Exo70. *Mol Cell Biol*. 19:3580-3587.

Rodriguez, O.C., and R.E. Cheney. 2002. Human myosin-Vc is a novel class V myosin expressed in epithelial cells. *J Cell Sci*. 115:991-1004.

Rogers, S., R. Wells, and M. Rechsteiner. 1986. Amino acid sequences common to rapidly degraded proteins: the PEST hypothesis. *Science*. 234:364-368.

Rossanese, O.W., C.A. Reinke, B.J. Bevis, A.T. Hammond, I.B. Sears, J. O'Connor, and B.S. Glick. 2001. A role for actin, Cdc1p, and Myo2p in the inheritance of late Golgi elements in Saccharomyces cerevisiae. *The Journal of cell biology*. 153:47-62.

Sagot, I., A.A. Rodal, J. Moseley, B.L. Goode, and D. Pellman. 2002. An actin nucleation mechanism mediated by Bni1 and profilin. *Nature cell biology*. 4:626-631.

Sakamoto, T., A. Yildez, P.R. Selvin, and J.R. Sellers. 2005. Step-size is determined by neck length in myosin V. *Biochemistry*. 44:16203-16210.

Salama, N.R., T. Yeung, and R.W. Schekman. 1993. The Sec13p complex and reconstitution of vesicle budding from the ER with purified cytosolic proteins. *EMBO J*. 12:4073-4082.

Salminen, A., and P.J. Novick. 1989. The Sec15 protein responds to the function of the GTP binding protein, Sec4, to control vesicular traffic in yeast. *J Cell Biol*. 109:1023-1036.

Santiago-Tirado, F.H., A. Legesse-Miller, D. Schott, and A. Bretscher. 2011. PI4P and Rab inputs collaborate in myosin-V-dependent transport of secretory compartments in yeast. *Developmental cell*. 20:47-59.

Schott, D., J. Ho, D. Pruyne, and A. Bretscher. 1999. The COOH-terminal domain of Myo2p, a yeast myosin V, has a direct role in secretory vesicle targeting. *The Journal of cell biology*. 147:791-808.

Schott, D.H., R.N. Collins, and A. Bretscher. 2002. Secretory vesicle transport velocity in living cells depends on the myosin-V lever arm length. *The Journal of cell biology*. 156:35-39.

Schwartz, S.L., C. Cao, O. Pylypenko, A. Rak, and A. Wandinger-Ness. 2007. Rab GTPases at a glance. *J Cell Sci*. 120:3905-3910.

Sckolnick, M., E.B. Krementsova, D.M. Warshaw, and K.M. Trybus. 2013. More Than Just a Cargo Adapter: Melanophilin Prolongs and Slows Processive Runs of Myosin Va. *J Biol Chem*.

Segev, N., J. Mulholland, and D. Botstein. 1988. The yeast GTP-binding YPT1 protein and a mammalian counterpart are associated with the secretion machinery. *Cell*. 52:915-924.

Simon, V.R., T.C. Swayne, and L.A. Pon. 1995. Actin-dependent mitochondrial motility in mitotic yeast and cell-free systems: identification of a motor activity on the mitochondrial surface. *J Cell Biol*. 130:345-354.

Sloane, J.A., and T.K. Vartanian. 2007. Myosin Va controls oligodendrocyte morphogenesis and myelination. *J Neurosci*. 27:11366-11375.

Spang, A., and R. Schekman. 1998. Reconstitution of retrograde transport from the Golgi to the ER in vitro. *J Cell Biol*. 143:589-599.

Stevens, R.C., and T.N. Davis. 1998. Mlc1p is a light chain for the unconventional myosin Myo2p in Saccharomyces cerevisiae. *J Cell Biol*. 142:711-722.

Strom, M., A.N. Hume, A.K. Tarafder, E. Barkagianni, and M.C. Seabra. 2002. A family of Rab27-binding proteins. Melanophilin links Rab27a and myosin Va function in melanosome transport. *The Journal of biological chemistry*. 277:25423-25430.

Sutton, R.B., D. Fasshauer, R. Jahn, and A.T. Brunger. 1998. Crystal structure of a SNARE complex involved in synaptic exocytosis at 2.4 A resolution. *Nature*. 395:347-353.

Swiatecka-Urban, A., L. Talebian, E. Kanno, S. Moreau-Marquis, B. Coutermarsh, K. Hansen, K.H. Karlson, R. Barnaby, R.E. Cheney, G.M. Langford, M. Fukuda, and B.A. Stanton. 2007. Myosin Vb is required for trafficking of the cystic fibrosis transmembrane conductance regulator in Rab11a-specific apical recycling endosomes in polarized human airway epithelial cells. *J Biol Chem*. 282:23725-23736.

Takagishi, Y., S. Oda, S. Hayasaka, K. Dekker-Ohno, T. Shikata, M. Inouye, and H. Yamamura. 1996. The dilute-lethal (dl) gene attacks a Ca2+ store in the dendritic spine of Purkinje cells in mice. *Neurosci Lett*. 215:169-172.

Takeshige, K., M. Baba, S. Tsuboi, T. Noda, and Y. Ohsumi. 1992. Autophagy in yeast demonstrated with proteinase-deficient mutants and conditions for its induction. *J Cell Biol*. 119:301-311.

Tang, F., E.J. Kauffman, J.L. Novak, J.J. Nau, N.L. Catlett, and L.S. Weisman. 2003. Regulated degradation of a class V myosin receptor directs movement of the yeast vacuole. *Nature*. 422:87-92.

TerBush, D.R., T. Maurice, D. Roth, and P. Novick. 1996. The Exocyst is a multiprotein complex required for exocytosis in Saccharomyces cerevisiae. *EMBO J*. 15:6483-6494.

TerBush, D.R., and P. Novick. 1995. Sec6, Sec8, and Sec15 are components of a multisubunit complex which localizes to small bud tips in Saccharomyces cerevisiae. *J Cell Biol*. 130:299-312.

Terrak, M., G. Wu, W.F. Stafford, R.C. Lu, and R. Dominguez. 2003. Two distinct myosin light chain structures are induced by specific variations within the bound IQ motifs-functional implications. *EMBO J*. 22:362-371.

Thomas, L.L., and J.C. Fromme. 2016. GTPase cross talk regulates TRAPPII activation of Rab11 homologues during vesicle biogenesis. *J Cell Biol*. 215:499-513.

Thompson, R.F., and G.M. Langford. 2002. Myosin superfamily evolutionary history. *Anat Rec*. 268:276-289.

Ton, V.K., D. Mandal, C. Vahadji, and R. Rao. 2002. Functional expression in yeast of the human secretory pathway Ca(2+), Mn(2+)-ATPase defective in Hailey-Hailey disease. *J Biol Chem*. 277:6422-6427.

Trybus, K.M. 2008. Myosin V from head to tail. *Cell Mol Life Sci*. 65:1378-1389.

Tsukada, M., and Y. Ohsumi. 1993. Isolation and characterization of autophagy-defective mutants of Saccharomyces cerevisiae. *FEBS Lett*. 333:169-174.

Tytell, J.D., and P.K. Sorger. 2006. Analysis of kinesin motor function at budding yeast kinetochores. *J Cell Biol*. 172:861-874.

Vale, R.D. 2003. Myosin V motor proteins: marching stepwise towards a mechanism. *J Cell Biol*. 163:445-450.

Vale, R.D., T.S. Reese, and M.P. Sheetz. 1985. Identification of a novel force-generating protein, kinesin, involved in microtubule-based motility. *Cell*. 42:39-50.

Varadi, A., T. Tsuboi, and G.A. Rutter. 2005. Myosin Va transports dense core secretory vesicles in pancreatic MIN6 beta-cells. *Mol Biol Cell*. 16:2670-2680.

Walch-Solimena, C., R.N. Collins, and P.J. Novick. 1997. Sec2p mediates nucleotide exchange on Sec4p and is involved in polarized delivery of post-Golgi vesicles. *The Journal of cell biology*. 137:1495-1509.

Walch-Solimena, C., and P. Novick. 1999. The yeast phosphatidylinositol-4-OH kinase pik1 regulates secretion at the Golgi. *Nature cell biology*. 1:523-525.

Walker, M.L., S.A. Burgess, J.R. Sellers, F. Wang, J.A. Hammer, 3rd, J. Trinick, and P.J. Knight. 2000. Two-headed binding of a processive myosin to F-actin. *Nature*. 405:804-807.

Wang, Y.X., N.L. Catlett, and L.S. Weisman. 1998. Vac8p, a vacuolar protein with armadillo repeats, functions in both vacuole inheritance and protein targeting from the cytoplasm to vacuole. *J Cell Biol*. 140:1063-1074.

Wang, Y.X., H. Zhao, T.M. Harding, D.S. Gomes de Mesquita, C.L. Woldringh, D.J. Klionsky, A.L. Munn, and L.S. Weisman. 1996. Multiple classes of yeast mutants are defective in vacuole partitioning yet target vacuole proteins correctly. *Mol Biol Cell*. 7:1375-1389.

Watanabe, M., K. Nomura, A. Ohyama, R. Ishikawa, Y. Komiya, K. Hosaka, E. Yamauchi, H. Taniguchi, N. Sasakawa, K. Kumakura, T. Ushiki, O. Sato, M. Ikebe, and M. Igarashi. 2005. Myosin-Va regulates exocytosis through the submicromolar Ca2+-dependent binding of syntaxin-1A. *Mol Biol Cell*. 16:4519-4530.

Weber, T., B.V. Zemelman, J.A. McNew, B. Westermann, M. Gmachl, F. Parlati, T.H. Sollner, and J.E. Rothman. 1998. SNAREpins: minimal machinery for membrane fusion. *Cell*. 92:759-772.

Wedlich-Soldner, R., S. Altschuler, L. Wu, and R. Li. 2003. Spontaneous cell polarization through actomyosin-based delivery of the Cdc42 GTPase. *Science*. 299:1231-1235.

Wei, Z., X. Liu, C. Yu, and M. Zhang. 2013. Structural basis of cargo recognitions for class V myosins. *Proc Natl Acad Sci U S A*. 110:11314-11319.

Weisman, L.S., and W. Wickner. 1988. Intervacuole exchange in the yeast zygote: a new pathway in organelle communication. *Science*. 241:589-591.

Woods, B., H. Lai, C.F. Wu, T.R. Zyla, N.S. Savage, and D.J. Lew. 2016. Parallel Actin-Independent Recycling Pathways Polarize Cdc42 in Budding Yeast. *Curr Biol*. 26:2114-2126.

Yau, R.G., Y. Peng, R.R. Valiathan, S.R. Birkeland, T.E. Wilson, and L.S. Weisman. 2014. Release from myosin V via regulated recruitment of an E3 ubiquitin ligase controls organelle localization. *Dev Cell*. 28:520-533.

Yildiz, A., J.N. Forkey, S.A. McKinney, T. Ha, Y.E. Goldman, and P.R. Selvin. 2003. Myosin V walks hand-over-hand: single fluorophore imaging with 1.5-nm localization. *Science*. 300:2061-2065.

Yin, H., D. Pruyne, T.C. Huffaker, and A. Bretscher. 2000. Myosin V orientates the mitotic spindle in yeast. *Nature*. 406:1013-1015.

Zahner, J.E., H.A. Harkins, and J.R. Pringle. 1996. Genetic analysis of the bipolar pattern of bud site selection in the yeast Saccharomyces cerevisiae. *Mol Cell Biol*. 16:1857-1870.

Chapter II

Kinesin-related Smy1 enhances the Rab-dependent association of myosin-V with secretory cargo

Overview

As previously described in Chapter I, the Myo2 motor transports a number of cargos via its specific receptors. Initially discovered as a suppressor of the conditional myosin mutant *myo2-66*, Smy1 presents a potential player in the Myo2 dependent cargo transport pathway. Due to its sequence similarity to the kinesin motor domain, Smy1 was initially thought to be involved in cargo transport. Yeast two-hybrid experiment showed that Smy1 interacts with Myo2 cargo-binding domain (Beningo et al., 2000). Smy1p was also found to colocalize with Myo2p in the bud by immunofluorescence and also found to colocalize with secretory vesicles (Hodges et al., 2009; Lillie and Brown, 1994). Our lab and other groups have shown that *smy1Δ* is synthetically lethal with *myo2-66*, other conditional *myo2* tail mutants, and late secretory mutants such as *sec2-56*, *sec4-8* (Lillie and Brown, 1998)[see table II from the paper]. All of these findings suggested that Smy1 is most likely to be involved in the Myo2p dependent transport of secretory vesicles. In addition, since *smy1Δ* does not show synthetic genetic effects with exocyst complex mutants such as *sec5-24*, *sec15-1*, and the SNARE protein, *sec9-4*, Smy1p function is likely restricted to the late secretory vesicle transport rather than in exocytosis (Lillie and Brown, 1998; Schott et al., 1999). [Kirk Donovan unpublished data on vesicle tracking together with Smy1 also suggests that possibility, i.e., Smy1 have no effect on the timeline of vesicle fusion.]

Smy1 function however becomes more diverse as other labs have found different phenotypes from *smy1* mutant. Trybus group claimed that Smy1 increases Myo2 processivity on actin filaments. By acting as an electrostatic tether between Myo2 and actin, Smy1 facilitates Myo2 processive run on actin filaments (Hodges et al., 2009). The Goode lab also found that

Smy1 is actually a formin damper at the bud-neck. Deleting *smy1* causes more kinks in actin filaments (Chesarone-Cataldo et al., 2011). With a diverse array of Smy1 function, it was still unclear how overexpression of Smy1 can suppress temperature sensitive *myo2* mutants that fail to transport secretory vesicles. My research on Smy1 therefore tries to elucidate the function of Smy1 regarding Myo2 dependent vesicle trafficking. Much of this chapter has been reproduced from our publication in Molecular Biology of the Cell (MBoC) (Lwin et al., 2016).

Materials and Methods

Yeast strains and transformation

Yeast strains and plasmids used in this study are listed in Table 3 and 4. Standard media and techniques for yeast growing and transformation were used (Sherman, 1991). Briefly, for transformation, 5ml of log phase OD_{600} = ~ 0.8 cells were harvested and resuspended in a mixture of 36µl of 1 M LiAc, 240 µl of 50% PEG 3350 (w/v), 50µl of salmon sperm DNA 10mg/mL, 1µg of DNA constructs, and volume-adjustable 29 μl H_2O (Gietz and Woods, 2002). Cells were incubated at 42˚C for 45 minutes and transformants were selected on selective synthetic dropout media plates. Gene deletion and chromosomal GFP tagging were performed by standard PCR-mediated techniques (Longtine et al., 1998). Plasmids from yeast were isolated using the plasmid isolation kit (YeaStar Genomic DNA kit).

Screen for *myo2* sensitized alleles (*myo2^{sens}*)

The *myo2* mutant library cloned into pRS303 (Schott et al., 1999) was used. Briefly, the Myo2 tail (1119aa – 1574aa) was PCR-mutagenized with forward primer 5'MYO2: ClaI-GATAATGAAATCGATATTATGGAAGA and reverse primer 3'MYO2: BamHI-CGGGATCCATTATCATACTATACTATTGACAAATACTTC to make 5 independent DNA libraries (Schott et al., 1999). When cut with SpeI and transformed into yeast, the library plasmid replaces the EcoRI-ClaI region of *MYO2* with the mutagenized sequence. DNA from each library was transformed into the *smy1Δ*+pRS316-*SMY1* strain with selection on SD-ura-his plates at 26˚C. Approximately ~200 colonies/plate with 20 plates were replicated on SD-

his+5-FOA (5-Fluoroorotic acid) and incubated at 26˚C for 3 days to detect which *myo2* mutant alleles could not grow in the absence of the pRS316-*SMY1* plasmid. 33 candidates that did not grow on SD-his+5-FOA were chosen and re-confirmed. 17 *myo2*^{sens} mutants were confirmed and sequenced to identify their mutations.

Error-prone PCR of *SMY1* and plasmid mutant library construction

Error-prone PCR was performed as described (Cadwell and Joyce, 1992). The final concentration of 0.15mM $MnCl_2$ was used during 10 PCR cycles, giving a mutagenesis rate of about 0.67/1000nt. To construct a *smy1* mutant library, forward primer 5'SMY1: NotI-TGAATGTTTGAATAGTAATG located -300 nt upstream of the Smy1 translation start site (ATG), and reverse primer 3'SMY1: BamHI-TTTCAATTTTTCTCATTTTTC located 179 nt downstream of the Smy1 stop codon, were used to PCR amplify and mutagenize *SMY1*. An upstream fragment (-300 to -600 upstream of the start site) that will create the first crossover for homologous recombination was amplified using BamHI-ACATCAAGATTATAGCTGTC and XhoI-CAATCACAGTGTATTATCTC primers. This fragment was cloned into pRS304 (*TRP1*) backbone vector after cutting with BamHI and XhoI to generate pRS304-HR. The mutant *SMY1* library was cut with NotI and BamHI and ligated into the pRS304-HR vector to generate pRS304-HR-*SMY1* library. To collect sufficient mutant library, 10,000 colonies were grown on LB+Amp plates and amplified. Before transforming the mutant library into yeast cells, the pRS304-HR-*SMY1* plasmid was linearized with BamHI.

Screen for conditional *smy1* mutants

Transformation of the strains carrying the *myo2-41*, *myo2-43*, *myo2-51*, and *myo2-57* alleles (ABY3319, ABY3318, ABY3317, ABY3316) with the pRS304-HR-*SMY1* plasmid library with selection on SD-his -trp was used to generate new *SMY1* alleles. Approximately ~200 transformants/plate on 15 plates were grown at 26˚C for 3 days. Plates were then replicated on another SD-his-trp plate and incubated at 37˚C for 3 days to detect which *smy1* mutant alleles cannot grow at 37˚C. 21 *smy1*^{ts} alleles were recovered after retesting, and then sequenced.

Plasmid construction

The integrating plasmids pRS306 GFP-Sec4 (*URA3*) and pRS306 Myo2cctail-3GFP (*URA3*) used to tag Sec4 and Myo2 have been described (Donovan and Bretscher, 2012). To create pRS305 Smy1cctail-3mCherry for chromosomal integration, the C-terminal half of *SMY1* (1000-1968nt) was amplified and ligated into the pRS305 vector between XhoI and BamHI. 3mCherry was cloned between BamHI and NotI. For homologous recombination, the 3' region of *SMY1* between the NotI and SacI sites (427nt) was ligated into the vector. The vector was linearized by HindIII before transformation. For 3HA tagging at chromosomal *SMY1* gene, the 3mCherry from pRS305 Smy1cctail-3mCherry was replaced with 3HA. The functional construct was verified by western blotting using anti-HA antibody [16B12 (ab130275)]. For overexpression constructs, the *SMY1* ORF flanked by 1000 nt upstream and downstream was cloned into YEp351 between the XmaI and PstI sites. The functional construct was verified by western blotting with Smy1 antibody. For creating Myo2-4IQ in BY4741 background, the integrating plasmid pRS303 Myo2-4IQ was constructed as described (Schott et al., 2002). To create pRS303 myo2-4IQ-41, mutation of I1462T in Myo2 cargo binding region was introduced by PCR based site-directed mutagenesis.

Smy1 Antibody generation

SMY1 tagged with *SUMO* was expressed in Rosetta™ 2(DE3) pLysS competent. Bacterially expressed Smy1-SUMO was selected on a Ni^{2+} resin, and then the SUMO tag cleaved with Ulp1. The SUMO-cleaved Smy1p was gel purified and antibodies generated commercially (Pocono Rabbit Farm and Laboratory).

Microscopy

Micrographs were acquired on a CSU-X spinning disc confocal microscopy system (Intelligent Imaging Innovations) with a DMI 6000B microscope (Leica), 100x1.45 NA objective and a QuantEM EMCCD camera (Photometrics) or an HQII CCD camera (Photometrics) with 2x magnifying lens. All images shown are maximum projection of 7 confocal slices taken 0.28 μm apart, unless stated otherwise. Images were analyzed and processed with Slidebook 6.0

software (Intelligent Imaging Innovations). The images were further adjusted in Photoshop (Adobe) to give the clearest presentation of the results and assembled in Illustrator (Adobe). For live-cell imaging of yeast cells, cells were attached to a glass-bottomed dish coated with Concanavalin A (EY laboratories) and washed with respective cell medium. Imaging at high temperatures was performed in an environmental chamber (Okolab). Quantification of the number of fluorescent proteins on transporting secretory vesicles was done as described (Donovan and Bretscher, 2012). Staining cells with phalloidin has also been described (Donovan and Bretscher, 2012).

Yeast two-hybrid constructs and analysis

The coding sequence for Myo2cctail (2776-4725nt) was fused with the DNA activation domain in pGADT7 vector between NdeI and BamHI. The Smy1 myosin-binding domain (1308-1968nt) was fused with DNA binding domain in pGBKT7. The AH109 strain co-transformed with both plasmids was selected in media lacking leucine and tryptophan (SD-2DO: double dropout). Interaction was detected by growth on medium lacking leucine, tryptophan and histidine (SD-3DO: triple dropout).

Immunoblotting

Overnight cultures were harvested and resuspended in disruption buffer (20mM Tris-CL, pH 7.9, 10mM $MgCl_2$, 1mM EDTA, 5% glycerol, 1mM dithiothreitol, 0.3M ammonium sulfate, 1mM PMSF, and 1x Sigma yeast protease inhibitor cocktail) with 0.1g acid-washed glass beads (Sigma-Aldrich, St. Louis, MO, USA). Vigorous vortexing was done at 4˚C for 3 times with 1 minute each and 1 minute in between resting on ice. The crude lysates were centrifuged at 17,000 g in a table-top centrifuge in a cold room (4˚C) for 10 minutes and supernatant was collected. For temperature sensitive strains, cells were grown at 26˚C overnight, and adjusted to log phase OD_{600}=0.8 the next day. Cells were then shifted to 35˚C for 2 hours. Upon harvesting, cells were chilled on ice, washed twice with ice-cold water, frozen in dry ice and stored at -80°C. The concentrations of protein samples were measured using Bradford assay. The samples were resolved by SDS-PAGE, transferred to Immobilon-P membrane (Millipore),

then blocked for 1 hour in 5% milk in PBS-T (0.1% Tween). Membranes were incubated with primary antibodies for 1 hour: mouse monoclonal anti-GFP antibody (Santa Cruz Biotechnology, Santa Cruz, CA, USA), or rabbit polyclonal antibody against Myo2tail, Smy1, Sec4 (generated in the lab) and G6PDH. After washing, membranes were incubated with secondary antibodies: IRDye goat anti-mouse and donkey anti-rabbit antibodies. Membranes were analyzed using the Odyssey infrared imaging system (LI-COR Biosciences, Lincoln, NE, USA).

Coimmunoprecipitation

Total yeast protein extracts were prepared using the same protocols described above. 10µl of GFP-Trap® resin (ChromoTek) was used for 1mg of each cell lysate and agitated at 4˚C for 2 hours. Bound protein was eluted with 50µl hot (95°C) SDS-PAGE loading buffer. Eluted proteins were resolved on 7-15% split SDS gels.

Results

Smy1 polarity depends on its association with Myo2.

To explore whether Smy1 polarization is dependent on interaction with Myo2 (Beningo et al., 2000) or secretory vesicles (Hodges et al., 2009), we examined its localization in specific *myo2* mutants. We have described temperature-sensitive mutations in the tail domain of Myo2 that confer defects in transport of secretory vesicles or inheritance of mitochondria (Chernyakov et al., 2013; Schott et al., 1999). The conditional mutant, *myo2-14*, has a 35 amino acid truncation of the Myo2 tail that abolishes its two-hybrid interaction with Smy1 (Figure 2.1 A) and confers a conditional defect in mitochondrial inheritance (Chernyakov et al., 2013). Consistent with the two-hybrid data, *SMY1* overexpression has no suppressive effect on the conditional growth of *myo2-14*, but does suppress the conditional growth phenotype of *myo2-12* and other tail domain mutations that confer a conditional defect in transport of secretory vesicles (Schott et al., 1999). In *myo2-14* cells both Myo2 and the secretory vesicle marker Sec4 are polarized, yet Smy1 is not (Figures 2.1 B and C). Thus, to be polarized, Smy1 requires an interaction with Myo2, and is not associated with secretory vesicles independently of Myo2 as suggested (Hodges et al., 2009). In order to delineate the function of Smy1, we set out to generate mutations in *SMY1* that confer a conditional growth phenotype. Analysis of such conditional mutants should reveal a function for Smy1.

Isolation of conditional *myo2^{sens} smy1^{ts}* mutants

Earlier work has shown that cells lacking Smy1 grow well and Myo2 remains polarized (Lillie and Brown, 1992). The only reported phenotype of *smy1Δ* cells is the presence of thicker and more kinked actin cables (Chesarone-Cataldo et al., 2011; Eskin et al., 2016). We confirm that *smy1Δ* cells grow well and Myo2 is still polarized (Figure 2.2, A and B). Phalloidin staining of actin showed little change in actin structures in *smy1*Δ cells (Figure 2.2 B). As the effects of *smy1*Δ on actin cables is unrelated to the genetic relationships between -

Figure 2.1

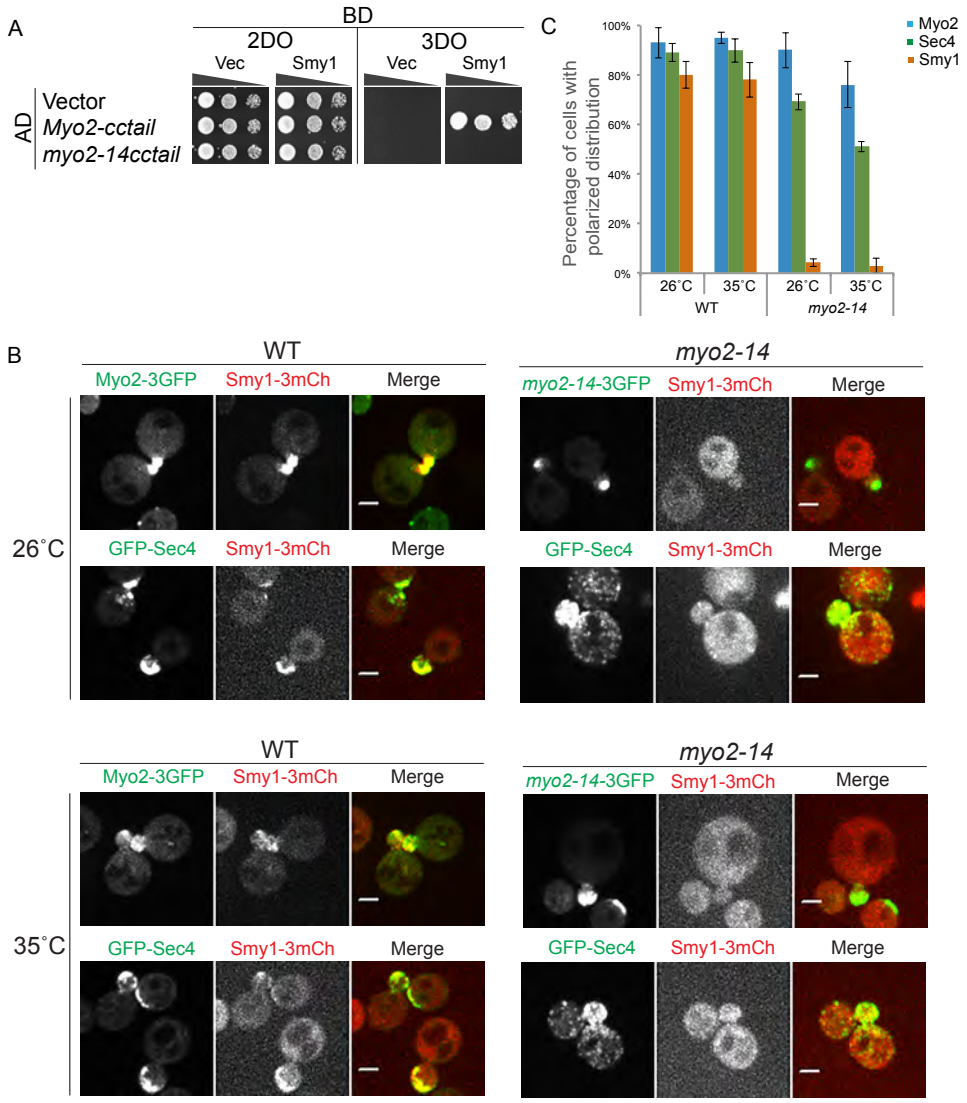

Figure 2.1. Smy1 polarity depends on its association with Myo2.
(A) Yeast two-hybrid interactions between Myo2-cctail (926-1575aa) fused to the activation domain (AD) and Smy1-MBD (Myosin Binding Domain; 562-656aa) fused to the binding domain (BD).
(B) Localization of Myo2, Smy1 and Sec4 in the indicated strains at 26˚C and after shifting to the restrictive temperature at 35˚C for 1hr; each gene was tagged with three copies of the indicated fluorescent protein. Scale bars, 2μm.
(C) Quantification of small budded cells (≤ 2μm) with polarized Myo2, Sec4 and Smy1 at 26˚C and after shifting to 35˚C for 1hr. Error bars indicate SD. (n=50).

Myo2 and Smy1 (Eskin et al., 2016), we have not explored the reason for this apparent discrepancy, although it is worth noting that the Eskin et al. study used the W303 genetic background, whereas our studies employ the S288C background.

Both the original *myo2-66* conditional head domain mutation as well as many of our conditional *myo2* tail mutations can be suppressed by *SMY1* over-expression, indicating a close functional relationship between Myo2 and Smy1 (Schott et al., 1999). Moreover, *myo2-66* shows synthetic lethality with *smy1Δ* (Lillie and Brown, 1992). Therefore we began our Smy1 journey with creating conditional *myo2 smy1* mutants so that we can study the molecular function of Smy1 in detail. A previous graduate student, Donghao Li, contributed his effort in creating the conditional *smy1* mutants which I detailed in Materials and Methods. By using the *myo2* mutant library created by Daniel Schott (Schott et al., 1999), Donghao first created the *myo2* mutants that were sensitive to *smy1Δ*, i.e., *myo2 smy1Δ* is inviable even at the permissive temperature at 26˚C (Figure 2.2 C and E). 17 such sensitized alleles (*myo2*^{sens}) were recovered and they have between one and four missense mutations (Table 1). Four of these (*myo2-41, myo2-47, myo2-51* each with a single missense mutation and *myo2-57* with three) were chosen to further generate conditional mutations in chromosomal *SMY1* (Figure 2.2 D). We generated 21 *myo2 smy1* mutants. I followed up with sequencing. Sequence analysis showed that these *smy1* ts alleles contain between one and four mutations (Table 2). Strikingly, almost all the mutations were found to lie in the head domain of Smy1 (Figure 2.2 F).

We selected the *myo2-41 smy1-15* conditional mutant for detailed study (Figure 2.2 G). The *myo2-41* mutation alone, or in combination with *smy1-15*, had no effect on the protein level of either Myo2, or its receptor Sec4, when shifted to 35°C for one hour (Figure 2.2 H), or on the actin cytoskeleton when cells were grown at 26˚C or shifted to 35˚C (Figure 2.2 I). All the strains grew normally at 26˚C and their division times were 90 ± 20 min at 26˚C (n=20 cells for each strain). At the restrictive temperature of 35°C, the single *myo2-41* and *smy1-15* mutants grew normally with division times of 80 ± 25 min (n=25 cells for each, mean ± SD).

Table 1, related to Figure 2.2. Mutations in the *myo2^{sens}* alleles

myo2^{sens}	Mutations
myo2-41	I1462T
myo2-42	N1416D Q1571H
myo2-43	L1446P
myo2-44	L1310Q I1475S
myo2-45	N1242T V1448A
myo2-46	L1446P
myo2-47	F1347S
myo2-48	K1295E M1369K I1453N Y1478F
myo2-49	L1446P S1519C
myo2-50	L1411P D1431V
myo2-51	K1444M
myo2-52	L1446R
myo2-53	D1186V N1416Y
myo2-54	I1346T I1491T K1541N
myo2-55	F1347Y
myo2-56	L1331F A1336S
myo2-57	W1367R Y1415S S1520G

Figure 2.2

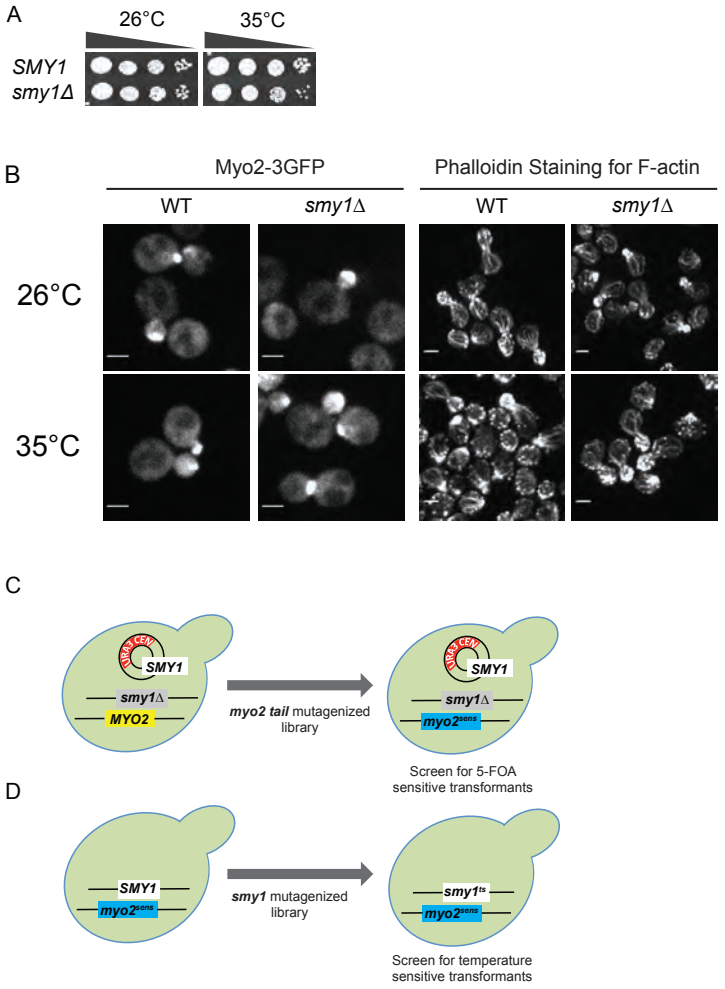

Figure 2.2. Generation of *myo2*^{sens} *smy1*^{ts} mutants
(A) Growth assay for WT and *smy1Δ* at 26˚C and 35˚C. Growth of 10-fold serial dilutions on YPD plates after 2 days.
(B) Myo2-3GFP and actin structures stained with phalloidin in the indicated mutants. Scale bars: 2μm.
(C) and (D) Schematic illustration of two step mutagenesis for generating the *myo2*^{sens} *smy1*^{ts} conditional mutants.

Figure 2.2 (Continued)

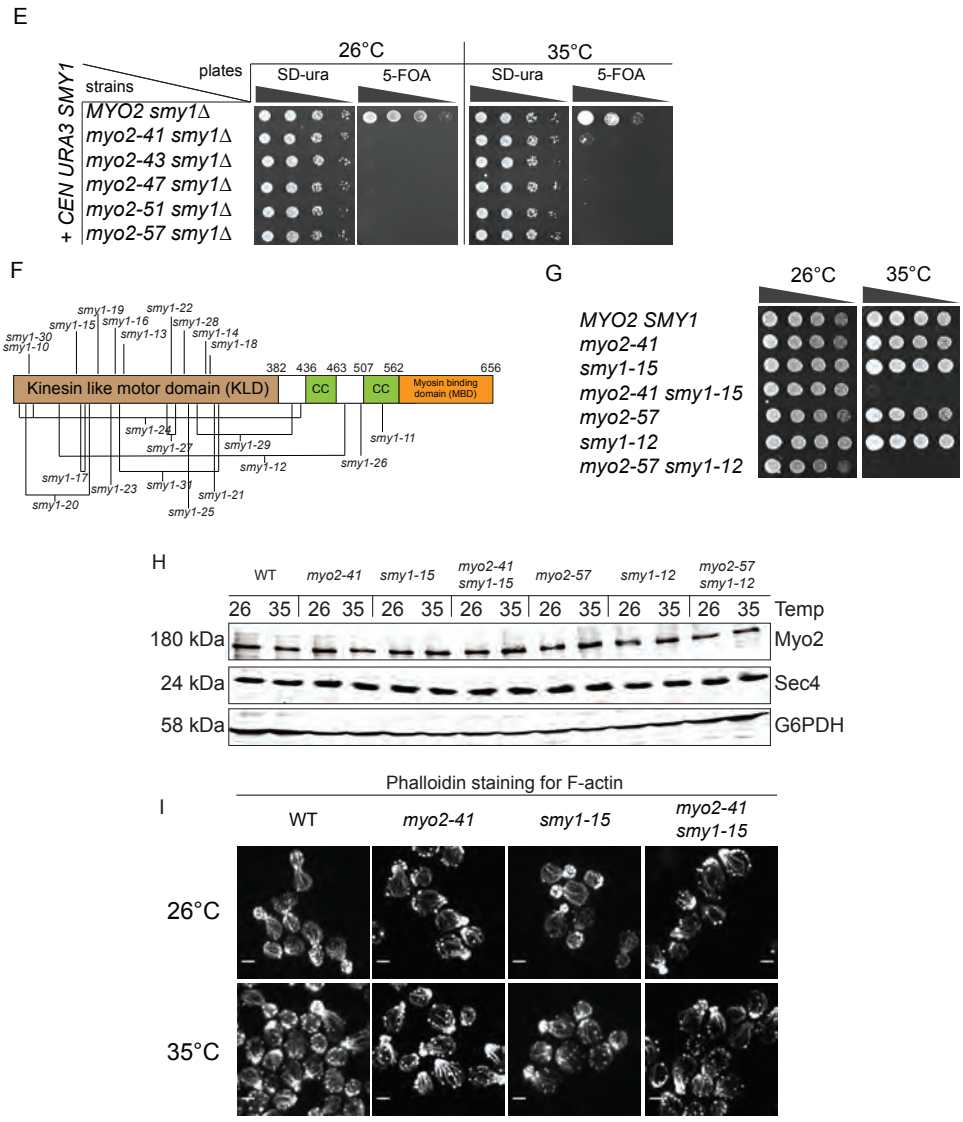

Figure 2.2 (Continued). Conditional *myo2 smy1* mutants.
(E) Synthetic lethality of *smy1Δ* with *myo2*^{sens} alleles. All strains carry the *CEN URA3 SMY1*. Growth of 10-fold diluted cells on SD-ura, 5-FOA plates and incubated at 26˚C and 35˚C for 2 days.
(F) Location of the mutations in the *smy1*^{ts} alleles.
(G) Growth of temperature sensitive strains: *myo2-41 smy1-15* and *myo2-57 smy1-12*.
(H) Temperature sensitivity of *smy1*^{ts} alleles is not due to Myo2 degradation and Sec4.
(I) Actin structures stained with phalloidin in the indicated mutants. Scale bars: 2μm.

Table 2, related to Figure 2.3. Mutations in conditional *smy1* alleles

smy1^{ts}	nucleotide change	amino acid change	recovered from *myo2*^{sens}
smy1-10	T170C	L57P	*myo2-41, myo2-51*
smy1-11	A1588G	N529D	*myo2-41*
smy1-12	T293G A1427G	I98R A476R	*myo2-41, myo2-47, myo2-57*
smy1-13	A515G	D172G	*myo2-41*
smy1-14	T866G	I289S	*myo2-41*
smy1-15	T337C	Y113H	*myo2-41*
smy1-16	G501A A1087G	M167I R363R	*myo2-41*
smy1-18	T875G	L292W	*myo2-41*
smy1-19	A381G C404T	S127S P135L	*myo2-41*
smy1-20	G85A A352G	E29K S118G	*myo2-41*
smy1-21	T892C	S298P	*myo2-41*
smy1-22	A700G	R234G	*myo2-41*
smy1-23	T190C T434C	L64L L145P	*myo2-41, myo2-47*
smy1-24	T76C G176A T1217C	C26R R59H I406T	*myo2-41, myo2-57*
smy1-25	T805C	F269L	*myo2-41*
smy1-26	A1062G C1161T T1498C C1761T	T354T D387D S500P I587I	*myo2-57*
smy1-27	T650C T713C	V217A V238A	*myo2-57*
smy1-28	A800G	E267G	*myo2-57*
smy1-29	A839G T1151C	D280G F384S	*myo2-57*
smy1-30	T170C T993G	L57P L331L	*myo2-47*
smy1-31	A508C C929T	T170P A310V	*myo2-47*

myo2-41 smy1-15 mutant confers a conditional defect in binding secretory vesicles

The sensitizing mutation in *myo2-41* (I1462T) lies on the surface of the Myo2 tail adjacent to the Rab binding site to which Sec4, Ypt31/32, and Ypt11 bind (Figure 2.3 A) (Eves et al., 2012). The mutation in *smy1-15* (Y113H) lies in the kinesin-like motor domain (Figure 2.3 B). To explore the localization of Myo2 and Smy1 in these cells, each was tagged with different fluorescent proteins, which did not affect the growth characteristics of the strains. The Myo2 motors are polarized to the site of growth in *MYO2*, *myo2-41,* and *smy1-15* cells at both 26˚C and after shifting to 35˚C (Figure 2.3, C and E). When the double mutant *myo2-41 smy1-15* was shifted to the restrictive temperature for one hour, the polarization of *myo2-41*-3GFP persisted whereas *smy1-15*-3mCherry became depolarized. This depolarization of Smy1-3mCherry was also seen after a short shift to the restrictive temperature (Figure 2.3 C). We next sought to determine the effect of the mutations on secretory vesicle delivery. Secretory vesicles marked with chromosomally tagged GFP-Sec4 were polarized in the single mutants, but in the double *myo2-41 smy1-15* mutant they were depolarized after a short shift to 35˚C (Figure 2.3, D and E). Thus, the conditional *smy1-15* mutation results in both a dissociation of Smy1 from Myo2 and a defect in secretory vesicle transport at the restrictive temperature.

To determine whether the different *myo2^{sens}* alleles might have yielded *smy1* alleles potentially affecting different functions, we combined *myo2-41* with 15 of the *smy1* alleles we had generated in different *myo2^{sens}* backgrounds. All 15 grew at the permissive temperature, and became inviable at the restrictive temperature (Figure 2.3 F), suggesting that all the *smy1* alleles are affecting the same function. To document this further, we also characterized the single and double mutants of *myo2-57 smy1-12* and found that the same uncoupling of both secretory vesicles and Smy1 from polarized Myo2 occurred at the restrictive temperature. Thus, the combined genetic and localization data reveal that a critical function of Smy1 in the *myo2^{sens}* strains is to link Myo2 to secretory vesicles.

Figure 2.3

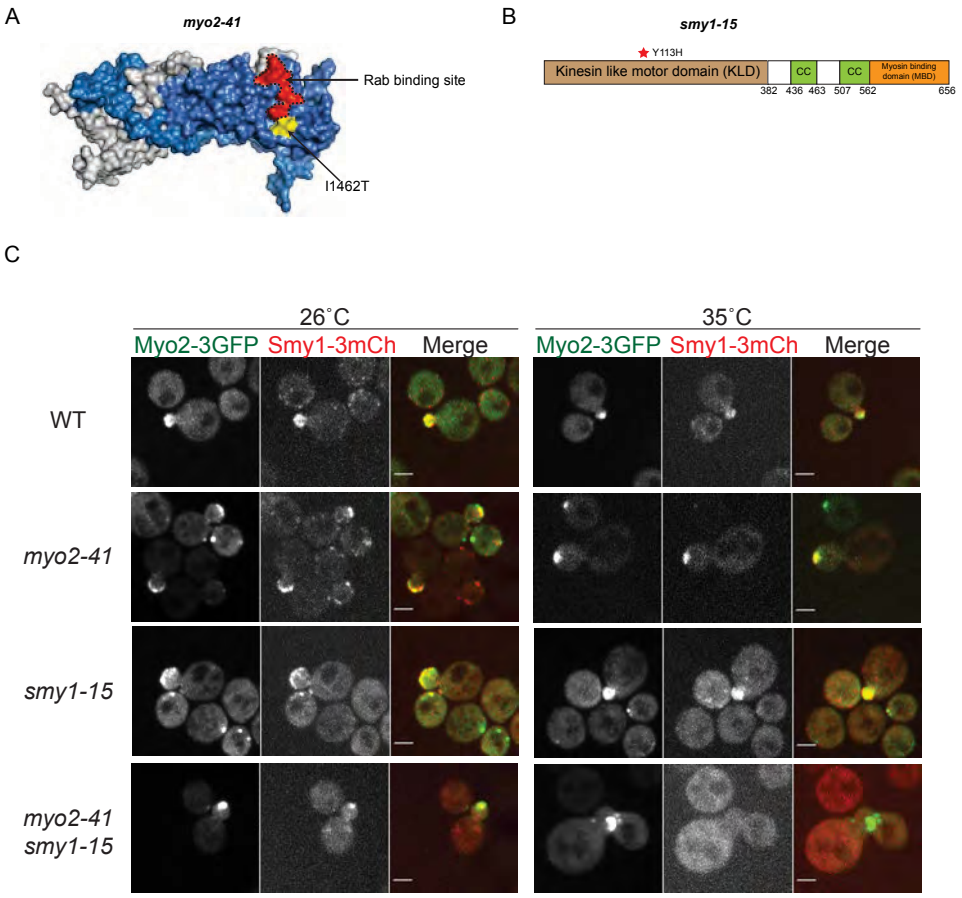

Figure 2.3. *myo2-41 smy1-15* mutant confers a conditional defect in binding secretory vesicles.
(A) Location of the mutation in *myo2-41* colored yellow on the structure of the Myo2 tail. Sub-domain I is in gray (1152–1309aa) and sub-domain II and linker is in blue (1310–1574aa). The mapped Rab binding site (Eves et al., 2012) is shown in red.
(B) Mutation in *smy1-15* allele (Y113H) is mapped to kinesin-like head domain (KLD).
(C) Localization of Myo2 and Smy1 in the indicated strains at 26°C or after shifting to 35°C for 1hr or 10 min for *myo2-41 smy1-15*. Scale bars, 2μm.

Figure 2.3 (Continued)

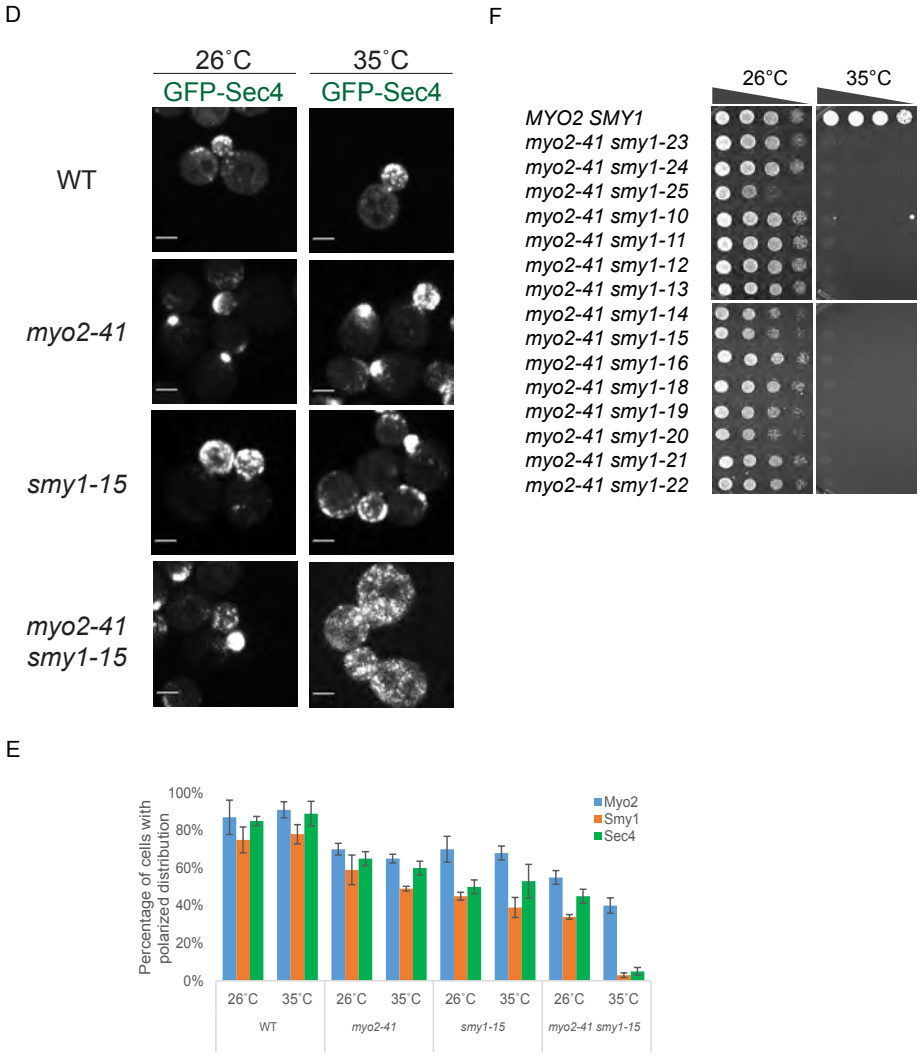

Figure 2.3 (continued). ***myo2-41 smy1-15*** **mutant confers a conditional defect in binding secretory vesicles.**
(D) Localization of Sec4 in the indicated strains at 26°C or after shifting to 35°C for 1hr or 10 min for myo2-41 smy1-15. Scale bars, 2μm.
(E) Quantification of small budded (≤ 2μm) cells with polarized Myo2, Sec4 and Smy1 at 26˚C and after shifting to 35˚C for 1hr. Mean values are from three independent experiments (n=50 each) and error bars indicate SD.
(F) Growth assay of *myo2-41* coupled with several smy1^{ts} alleles. 10 fold serially diluted cells spotted on YPD plates at 26˚C and 35˚C and incubated for 2 days.

The *myo2-41* allele compromises the ability of Myo2 to bind Sec4.

The sensitizing mutation in *myo2-41* lies adjacent to the Rab binding site (Figure 2.3 A). Yeast two-hybrid analysis showed that *myo2-41* is compromised in its ability to interact with Sec4 (Figure 2.4 A), thereby implying that Smy1 likely functions to enhance the interaction between Myo2 and Sec4 necessary for secretory vesicle transport. Consistent with this model, overexpression of *SEC4* from a multi-copy plasmid suppresses the *myo2-41 smy1-15* mutant and results in repolarization of GFP-Sec4 (Figure 2.4, B, C and D). Indeed, overexpression of *SEC4* suppresses all the *myo2-41 smy1*^{ts} mutants (Figure 2.4 E). However, over-expression of *SEC4* was unable to suppress the lethality of *myo2-41 smy1*Δ (Figure 2.4 F). Therefore, even when *SEC4* is over-expressed, Smy1-15 still provides an essential function in *myo2-41 smy1-15* cells at the permissive temperature.

Smy1 enhances the association between Sec4 and Myo2 and their association with secretory vesicles

The interaction between Sec4 and Myo2 is difficult to capture by coimmunoprecipitation, presumably because it is relatively transient and only exists during transport and tethering of secretory vesicles. Thus, in immunoprecipitates of Myo2-3GFP, only a trace of endogenous Sec4 can be detected (Figure 2.5 A). Since Smy1 and Sec4 bind Myo2 (Beningo et al., 2000; Santiago-Tirado et al., 2011), *SMY1* over-expression might enhance the Myo2/Sec4 interaction. Consistent with this model, when *SMY1* is overexpressed in an otherwise wild type cell, a significant amount of endogenous Sec4 is recovered in Myo2-3GFP immunoprecipitates (Figure 2.5 A), without affecting the levels of endogenous Myo2 or Sec4 (Figure 2.5, B and C). Moreover, Smy1 is also recovered with Myo2 and Sec4.

To explore whether Smy1 expression affects the number of Myo2 motors or Sec4 receptors associated with secretory vesicles, we quantitated the number of each in *SMY1*, *smy1*Δ and *SMY1* overexpressing cells.

Figure 2.4

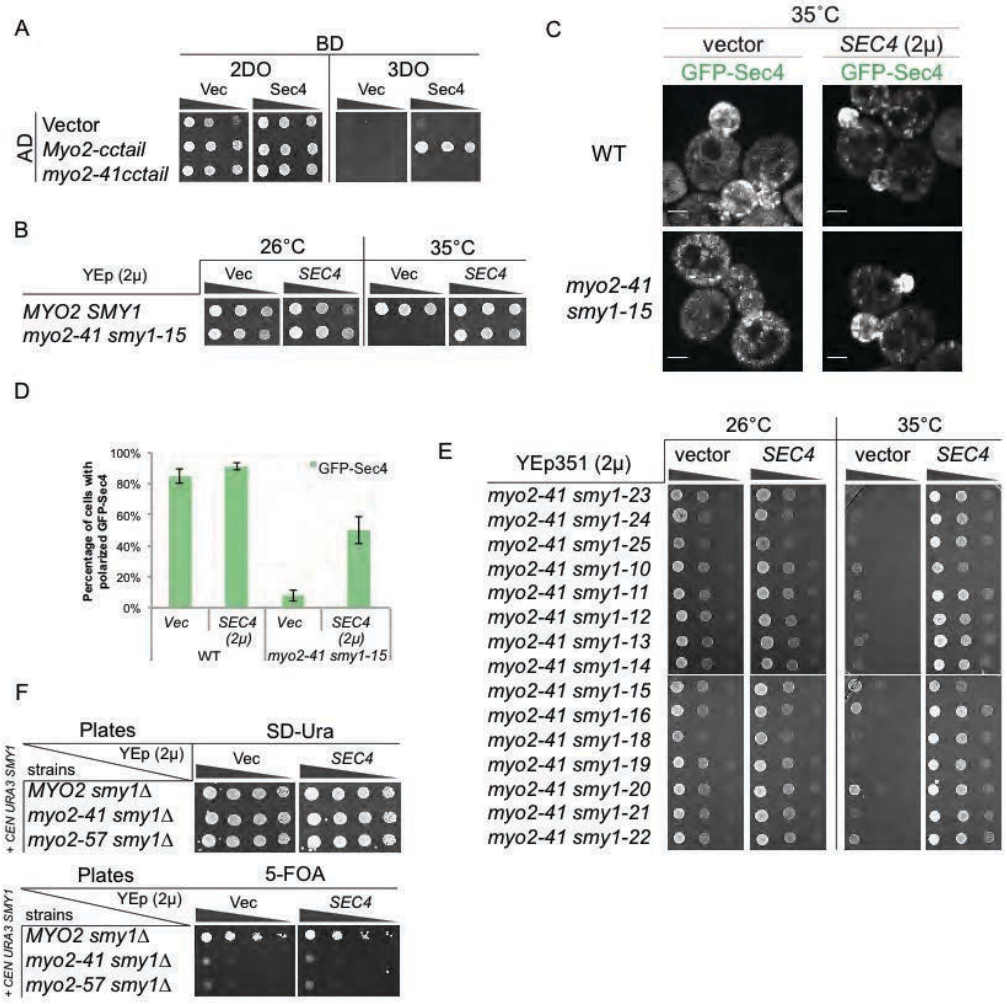

Figure 2.4. The *myo2-41* allele compromises the ability of Myo2 to bind Sec4.
(A) Yeast two-hybrid interactions between the wildtype- or *myo2-41*-cctail (926-1575aa) fused to the activation domain (AD) and Sec4ΔCC fused to the binding domain (BD).
(B) Overexpression of *SEC4* on a multicopy 2μ plasmid can suppress *myo2-41 smy1-15* mutant.
(C) Overexpression of *SEC4* restores the polarity of secretory vesicles in *myo2-41 smy1-15* at 35˚C. Scale bar: 2μm.
(D) Quantitation of the percentage of small budded cells with polarized GFP-Sec4 at 35˚C in WT and *myo2-41 smy1-15*. Mean values are from three independent experiments (n=50 each) and error bars indicate SD.
(E) Overexpression suppression of *SEC4* on *myo2-41 smy1*^{ts} mutants.
(F) Growth of *myo2-41 smy1*Δ or *myo2-57 smy1*Δ with a *URA3 CEN SMY1* plasmid and *SEC4* on a multicopy 2μ plasmid. Cells were spotted on SD-ura and 5-FOA plates with 10-fold serial dilutions.

To quantify the number of Myo2 molecules, we used as standard the 80 Cse4-3xGFP centromeric histone molecules per anaphase cluster (Lawrimore et al., 2011). As the speed of transport of actively transporting secretory vesicles is very fast in wild type cells and precludes estimating the numbers of these molecules on vesicles, we have previously quantitated the number of molecules on the slower moving secretory vesicles in cells where the Myo2 protein has been altered to have 4IQ motifs rather than the normal 6IQ motifs, which has no effect on growth rate (Schott et al., 2002). In these Myo2-4IQ cells, secretory vesicles being actively transported utilize about 40% of the total Myo2 in the cell with each vesicle having about 10 Myo2 motors (Donovan and Bretscher, 2012). Using the same strategy, we confirm that there are about 11 ± 4 (n=52) Myo2 motors on moving secretory vesicles in Myo2-4IQ cells, and this is not significantly altered in *smy1*Δ cells, 11 ± 5 (n=45) (Figure 2.5, D and E). However, in cells overexpressing *SMY1*, where the Smy1 level is enhanced about 20-fold due its presence on a 2μ plasmid, the number of motors per transporting secretory vesicle is increased about 1.5 fold, to 15 ± 4 (n=60), representing about 60% of all the motors in the cell (Figure 2.5 E). Also consistent with earlier results, we found that there are 50 ± 14 (n=50) and 47 ± 13 (n=50) Sec4 molecules per secretory vesicle in wild-type and *smy1Δ* cells, respectively. Overexpression of *SMY1* also enhances the number of GFP-Sec4 receptors per transporting secretory vesicle by about 1.5 fold to 75 ± 15 (n=50) (Figure 2.5, F and G). Thus, *SMY1* overexpression significantly enhances the number of Myo2 and Sec4 copies per secretory vesicle.

We also estimated the number of Smy1 molecules per secretory vesicle. Since Smy1 has a potential coiled-coil region between its head and tail, we first explored whether it has the ability to dimerize in vivo. Plasmids driving the expression of either Smy1-3GFP (Smy1-FL) or just the head (Smy1-KLD-3GFP, 1-382aa), or the head and coiled-coil region of Smy1 (Smy1-KLD+CC-3GFP, 1-562aa) were introduced into a strain expressing Smy1-3HA from its endogenous promoter. Smy1-3HA was immunoprecipitated, and both Smy1-3GFP and Smy1-KLD+CC-3GFP, but not Smy1-KLD-3GFP, were found to coimmunoprecipitate with it (Figure 2.5 H).

Figure 2.5

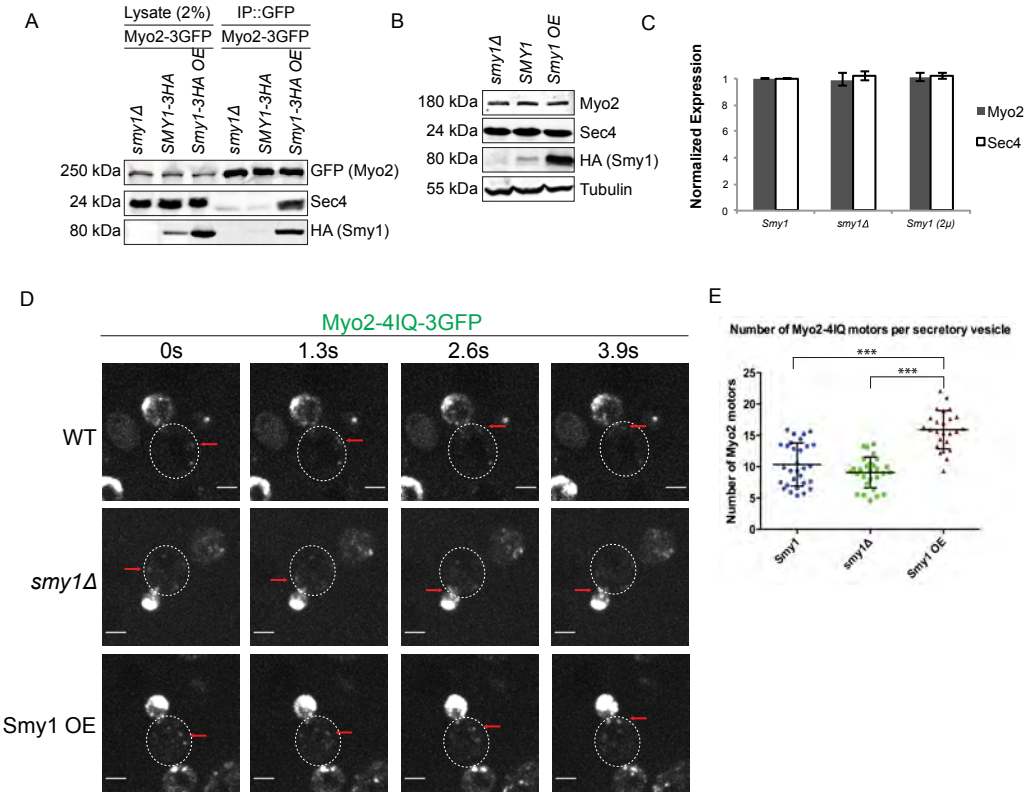

Figure 2.5. The association between Myo2 and Sec4, and with secretory vesicles, is enhanced by full length Smy1.
(A) Coimmunoprecipitation of Myo2-3GFP in different Smy1 backgrounds (*smy1Δ, SMY1-3HA, SMY1-3HA* over-expression). Myo2-3GFP was immunoprecipitated, resolved by gel electrophoresis and immunoblotted for GFP (Myo2), Sec4 and HA (Smy1).
(B) and (C) Expression level of Myo2 and Sec4 in different Smy1 backgrounds. 20μg of total protein lysate was loaded into each lane and immunblotted for Myo2, Sec4, HA (Smy1) and tubulin. Mean values are from three independent western blots and error bars indicate SD.
(D) and (E) Number of Myo2-4IQ-3GFP motors per moving secretory vesicle respectively. Data from puncta captured in three consecutive time-lapse frames were analyzed. n = 50. Dotted white circle shows the mother cell. Three asterisks indicates P value <0.0001.

Figure 2.5 (Continued)

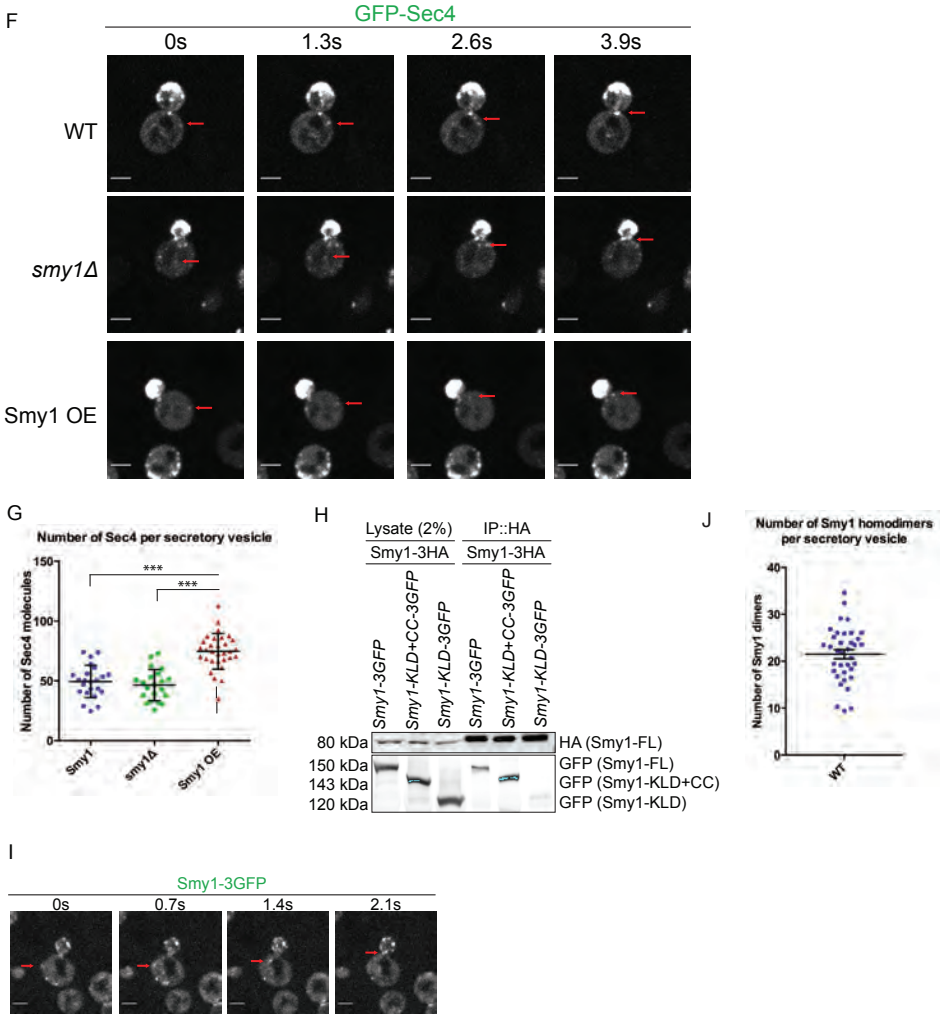

Figure 2.5 (continued). The association between Myo2 and Sec4, and with secretory vesicles, is enhanced by full length Smy1.
(F) and (G) Number of GFP-Sec4 per moving secretory vesicle respectively. Data from puncta captured in three consecutive time-lapse frames were analyzed. n = 50. Three asterisks indicates P value <0.0001.
(H) Coimmunoprecipitation of full length Smy1 tagged with 3HA from different Smy1 constructs with or without coiled-coil domain tagged with 3GFP.
(I) Smy1-3GFP puncta (arrows) on moving vesicle in wild-type.
(J) Quantification of number of Smy1 homodimers per moving secretory vesicle. Data from puncta captured in three consecutive time-lapse frames were analyzed. n = 50.

Thus, Smy1 can oligomerize through its CC domain, most likely existing as a homodimer in vivo. Quantitating the fluorescence in cells expressing Smy1-3GFP revealed that about 22 Smy1 homodimers (22 ± 6 (n=46)) are estimated to be present on each transporting secretory vesicle (Figure 2.5, I and J). Given the possibility of a systematic difference in the fluorescence of GFP tagged to different proteins, the best we can conclude is that Smy1 and Myo2 are both in the range of 10-20 molecules per secretory vesicle, but the possibility on an excess of Smy1 over Myo2 remains an open question.

We also wished to estimate the number of Sec4 and Myo2 molecules in our conditional *myo2-41 smy1-15* mutant. We therefore tagged endogenous *SEC4* with GFP, and the amount of GFP-Sec4 per moving secretory vesicle in the single and double mutants at both 25° and after a 5 minute shift to the restrictive temperature. None of the single or double mutants at either temperature had a significantly different number of copies of GFP-Sec4. (Figure 2.6 A). As explained above, to count the number of Myo2 motors, we needed to reduce the number of IQ repeats in the *myo2-41* allele from the wild type 6IQ to 4IQ, to generate *myo2-4IQ-41*. Surprisingly, when we did this, the temperature sensitivity of *myo2-14 smy1-15* was eliminated, whether or not the *myo2-4IQ-41* was tagged or not (Figure 2.6 B). This allowed us to estimate the number of Myo2 dimers in the single and double mutants at the two temperatures. Consistent with robust growth, the number of Myo2 dimers was not significantly changed in these mutants (Figure 2.6 C). These unexpected results may provide additional insights into the function of Smy1, which we offer in the Discussion.

Figure 2.6

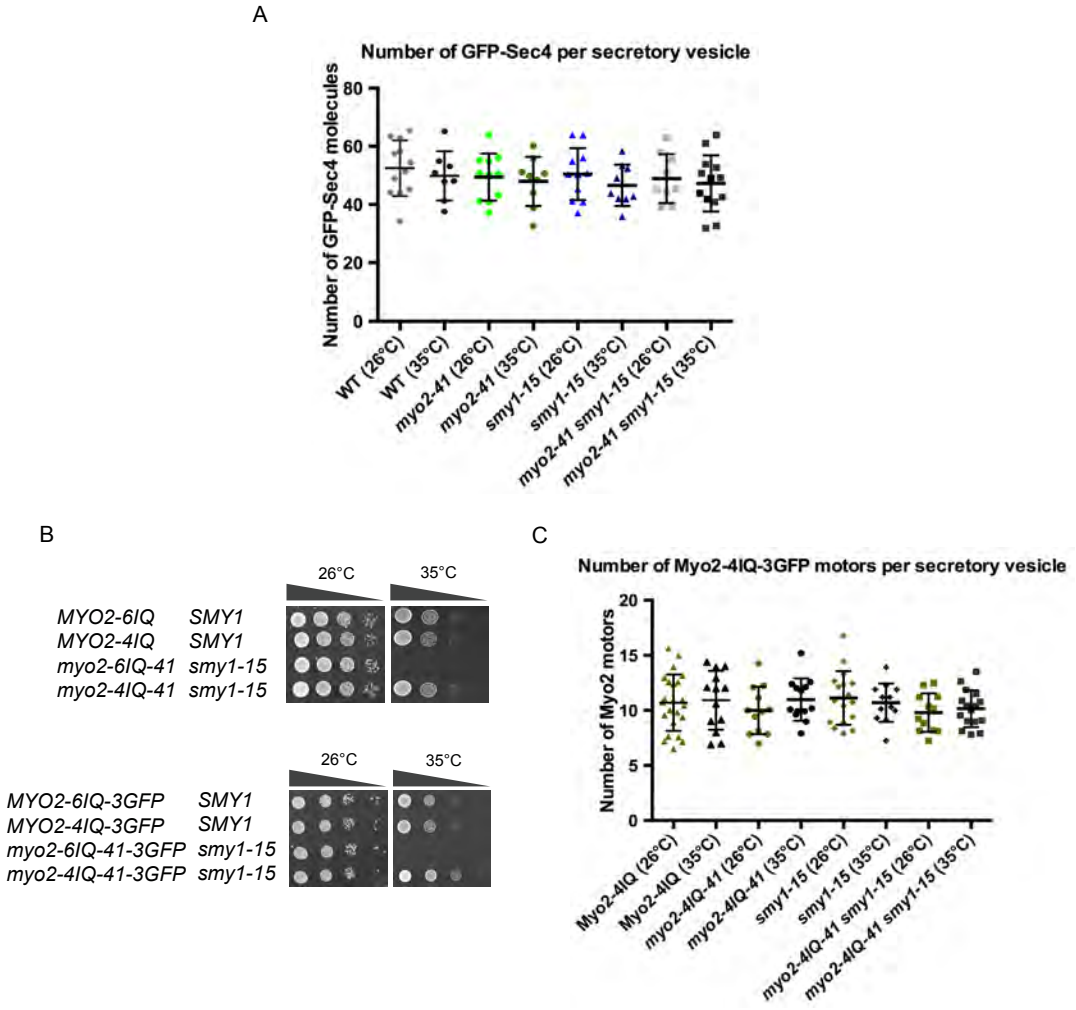

Figure 2.6. Number of Sec4 and Myo2-4IQ-3GFP motors per secretory vesicle in myo2 smy1 mutant.
(A) Number of GFP-Sec4 per secretory vesicle in different strains at both 26˚C and after shifting to 35˚C for 5 min. Error bars indicate SD.
(B) Growth assay of the indicated strains in which Myo2 has either 6IQ or 4IQ motifs.
(C) Number of Myo2-4IQ-3GFP motors per secretory vesicle in different strains at both 26˚C and after shifting to 35˚C for 15 min. Error bars indicate SD.

The tail domain of Smy1 is critical for its polarization, and the coiled-coil and head domains are essential for its function.

To dissect the contribution of the different domains in Smy1, we expressed several Smy1 constructs tagged with GFP behind the endogenous promoter in *smy1Δ* cells (Figure 2.7 A). Of these, only full length and a construct containing the coiled-coil and myosin-binding domain (Smy1-CC-MBD-3GFP) were polarized in otherwise wild type strains (Figure 2.7 B). Further, whereas *SMY1* overexpression can suppress the temperature-sensitivity of *myo2-12, -13, -16* and *-66* (Schott et al., 1999), constructs overexpressing either a *SMY1* construct lacking the Myo2-binding domain (KLD+CC) or lacking the head domain (CC-MBD) cannot (Figure 2.7 C). Therefore, the Smy1 coiled-coil and myosin-binding domains are necessary for localization, and the full-length protein is required for its function. Consistent with this, overexpression of full-length *SMY1* enhanced the association of Sec4 with immunoprecipitated Myo2-3GFP, whereas over-expression of Smy1 lacking the head domain does not and was not recovered in the immunoprecipitates (Figure 2.7 D). Thus, the head domain of Smy1 is critical for its function enhancing the association between Myo2 and Sec4. In support of this conclusion, overexpression of either full-length *smy1-12* or *smy-15*, that carry missense point mutations in the head domain, were unable to suppress any of these conditional *myo2* alleles (Figure 2.7 C).

Smy1 function with Myo2 is restricted to the transport of secretory vesicles

Myo2 is involved in the segregation of essentially all organelles during the cell cycle (Bretscher, 2003). One of these, mitochondria, also involves an interaction with a Rab protein Ypt11 (Itoh et al., 2002). Active segregation of mitochondria requires an association of Myo2 with either Mmr1 or Ypt11, and in the absence of this segregation, yeast is inviable (Chernyakov et al., 2013; Itoh et al., 2004). Mutations that reduce Ypt11 binding to the Rab-binding site of the Myo2 tail render *MMR1* essential (Chernyakov et al., 2013).

Figure 2.7

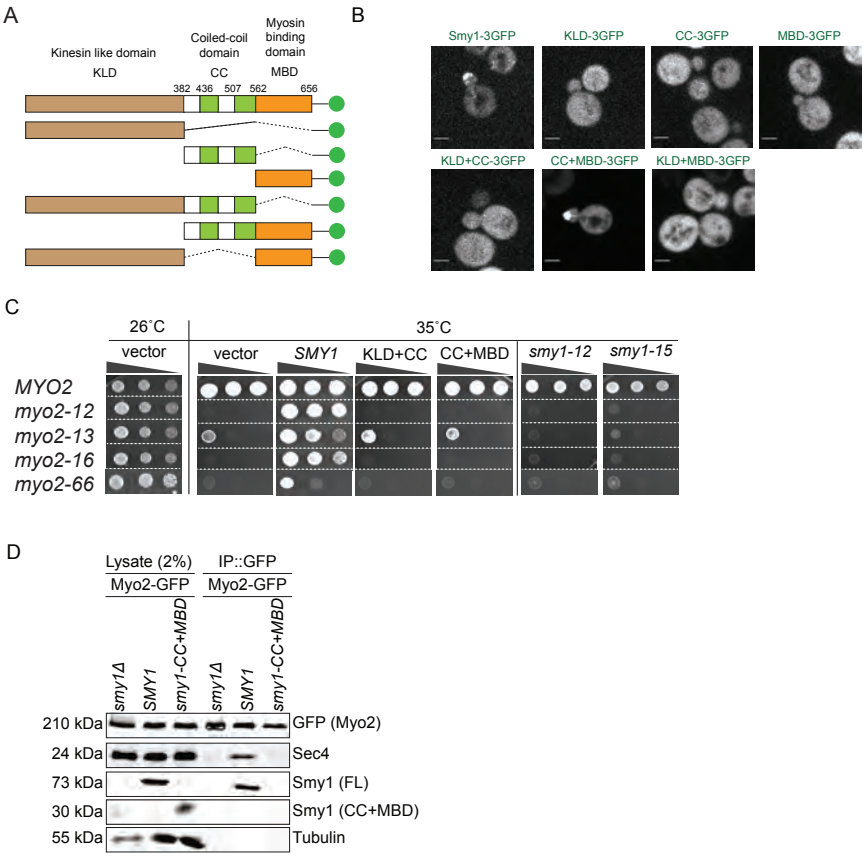

Figure 2.7. The tail domain of Smy1 is critical for its polarization and the head domain of Smy1 is essential for its functions.
(A) Smy1 constructs generated, all with C-terminal 3xGFP tags. KLD, kinesin-like head domain; CC, coiled-coil domain; and MBD, myosin-binding domain.
(B) Localization of the constructs in smy1Δ cells. Scale bars: 2μm.
(C) Ability of full length Smy1 (FL), KLD-CC domains, or the CC-MBD domains to suppress the indicated myo2 conditional mutants. The constructs were overexpressed from a 2μ plasmid. Overexpression of wild-type SMY1, but not smy1-12 or smy1-15 can suppress the myo2 conditional mutations.
(D) GFP immunoprecipites from Myo2-GFP cells over-expressing Smy1 or Smy1-CC-MBD blotted for GFP (Myo2), Sec4, Smy1 and tubulin.

Figure 2.8

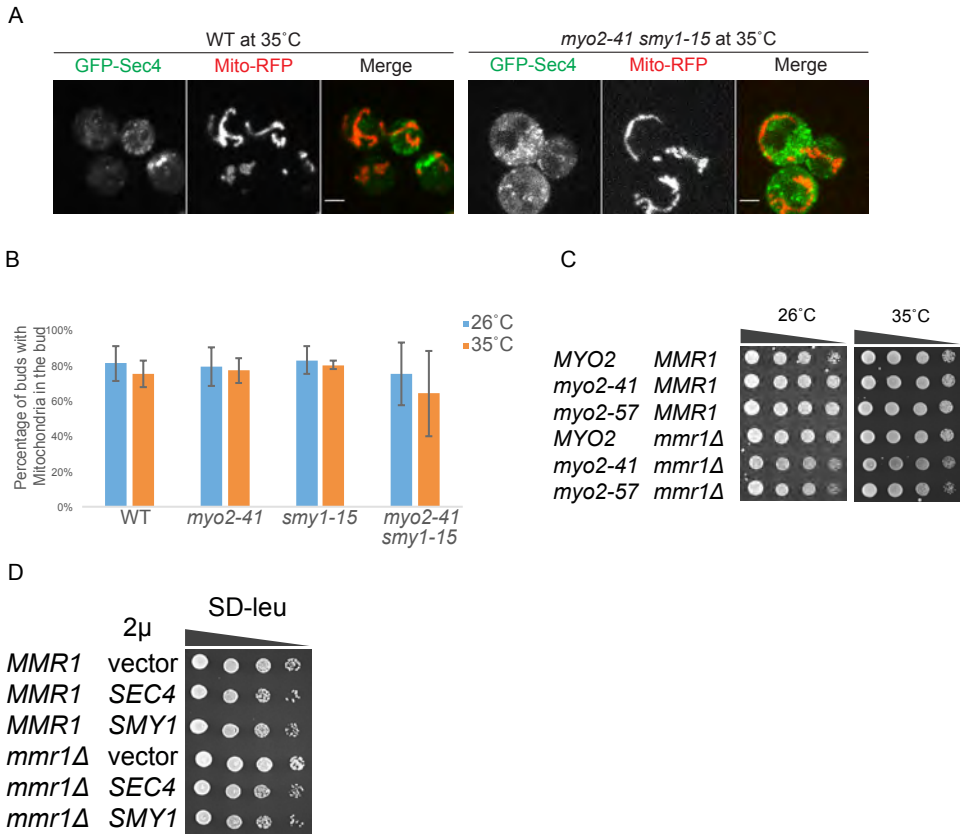

Figure 2.8. Smy1 function with Myo2 is restricted to the transport of secretory vesicles.
(A) Wildtype and *myo2-41 smy1-15* cells expressing GFP-Sec4 and the mitochondrial marker Mito-RFP after shifting to 35° for 1hr. Scale bars: 2μm.
(B) Percentage of cells with mitochondria in the buds at 26° or after shifting cells to 35° for 1hr. Mean values from three independent experiments (n=50) and error bars indicate SD.
(C) Affect of *mmr1Δ* on the growth of *myo2-41* and *myo2-57* for 2 days at 26˚C and 35˚C.
(D) Growth of cells overexpressing *SEC4* or *SMY1* in wild type and *mmr1*Δ cells.

Figure 2.8 (Continued)

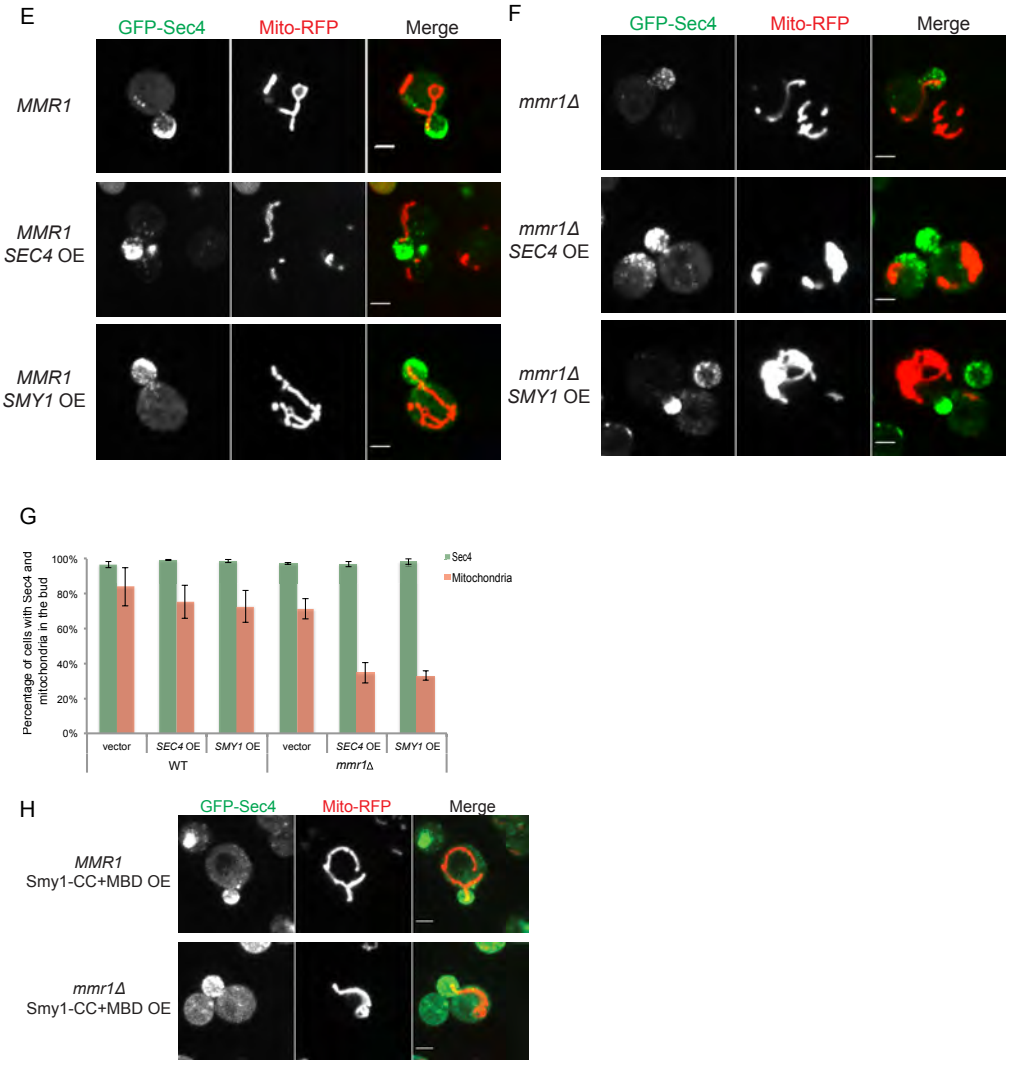

Figure 2.8 (continued). Smy1 function with Myo2 is restricted to the transport of secretory vesicles.
(E) and (F) Overexpression of SEC4 or SMY1 in wild type and *mmr1Δ* cells expressing GFP-Sec4 and Mito-RFP. Scale bars: 2μm. (G) Percentage of small budded cells (≤ 2μm) with polarized vesicles (GFP-Sec4) and mitochondria (Mito-RFP) in the bud upon over-expression of SEC4 or SMY1. Mean values from three independent experiments (n=100 each) and error bars indicate SD. (H) Mitochondrial inheritance in cells over-expressing Smy1-CC+MBD in wild type and *mmr1Δ* cells. Scale bars: 2μm.

We examined whether *myo2-41 smy1-15* might have a defect in mitochondrial distribution. Whereas GFP-Sec4 polarization is strongly affected in *myo2-41 smy1-15* cells at 35°C, there is no significant defect in mitochondrial inheritance, suggesting that Smy1 function may be specific to coupling secretory vesicles with Myo2 motors (Figure 2.8, A and B). Further, the *myo2-41* and *myo2-57* mutations that renders *SMY1* essential, have no growth defect at any temperature when combined with *mmr1*Δ, which makes mitochondrial inheritance dependent on the Myo2-Ypt11 interaction (Figure 2.8 C).

To explore in a different manner whether Smy1 can enhance the association of Rab proteins other than Sec4 with Myo2, we looked in more detail at mitochondrial inheritance. In *mmr1*Δ cells, mitochondrial inheritance is dependent on Ypt11, whose binding site overlaps with Sec4 on domain II of Myo2 (Eves et al., 2012). If Smy1 enhances the binding of all Rab proteins to the Myo2 tail, its over-expression might enhance mitochondrial inheritance. However, if it is specific for Sec4, *SMY1* overexpression might compromise the availability of the Myo2 tail to bind Ypt11. To test this idea, we initially examined whether Sec4 overexpression compromised mitochondrial inheritance in *MMR1* and *mmr1*Δ cells. Although the cells remain viable (Figure 2.8 D), there is a clear defect in mitochondrial inheritance in *mmr1*Δ cells with most of the mitochondria being retained in the mother cell (Figure 2.8, E, F and G). Similarly, when *SMY1* is overexpressed in *mmr1*Δ cells, there is a defect in mitochondrial inheritance (Figure 2.8, E, F and G), showing that Smy1 functions with Sec4 and not with Ypt11. This effect is only seen when full-length *SMY1* is overexpressed, as no defect is seen when Smy1-CC-MBD is overexpressed, further indicating that the Smy1 head domain is necessary for its function (Figure 2.8H). Thus our data imply that Smy1's role is specific to secretory vesicles.

Discussion

The mechanism by which molecular motors are activated and bind and transport specific cargos is critical for understanding the functional organization of cells. The myosin-V class of motors is found in all fungi and animal cells, as well as plants where they are called myosin-X1 motors (Hammer and Sellers, 2012). Myosin-Vs are well known to bind Rab proteins - mammalian myosin-Vs have been shown to bind Rabs 8, 10 and 11 directly, and Rab27a indirectly through melanophilin (Hammer and Sellers, 2012). In yeast, Myo2 binds four of the 11 Rab proteins: Ypt31/32 (Lipatova et al., 2008), Sec4 (Jin et al., 2011; Santiago-Tirado et al., 2011) and Ypt11 (Chernyakov et al., 2013; Eves et al., 2012; Itoh et al., 2002).

Since its identification more than 20 years ago as an over-expression suppressor of the conditional *myo2-66* mutation, the specific function of Smy1 has been mysterious. The early genetic data discussed in the introduction made a strong case that it functions with Myo2 and is involved in some aspect of the late secretory pathway. Here we have generated *myo2^{sens}* mutations that confer no obvious phenotype except to render *SMY1* essential, thereby allowing for the subsequent isolation of conditional mutations in *SMY1*. Analysis of the phenotype of *myo2^{sens} smy1* conditional mutants reveals a clear defect in the transport of post-Golgi secretory vesicles, very similar to the phenotype of conditional *myo2* mutations that affect this function. This is a clear indication that Smy1's function is to cooperate with Myo2 in secretory vesicle transport. Additional support for this conclusion - and the specificity of this function - is discussed below.

The reported two-hybrid interaction between the tail of Myo2 and the tail of Smy1 was not readily reproduced in vitro or by co-immunoprecipitation, so naturally the validity of the two-hybrid interaction was questioned (Beningo et al., 2000; Hodges et al., 2009). Here we show that the polarized colocalization of Smy1 with Myo2 is lost when either a *myo2* mutant defective in binding Smy1 is examined, or when Smy1 lacking the Myo2 binding domain (MBD) is expressed. Further, the region of Smy1 necessary for the two-hybrid interaction is also

necessary for its ability to suppress conditional *myo2* mutations. In cells where Smy1 is over-expressed, Smy1 is recovered in immunoprecipitates of endogenous Myo2. These results make a compelling case for the relevance of the original Myo2-Smy1 two-hybrid interaction (Lillie and Brown, 1998).

We have also delineated functions for the other two domains of Smy1, the coiled-coil region and the kinesin-related motor domain. The coiled-coil region is required, with the Myo2-binding region, for the polarized distribution of Smy1. This is almost certainly because the coiled-coil region is necessary for the dimerization, or oligomerization, of the protein. One intriguing possibility is that the binding of just one Myo2-binding region to Myo2 is not of sufficient affinity to localize the protein, whereas the combination of two low affinity sites may be sufficient. The head domain is not polarized on its own, or in constructs together with the coiled-coil domain, thus revealing that the Myo2-binding region is necessary for Smy1's polarized distribution. Although just the a construct lacking the head domain of Smy1 is polarized, the full-length protein (KLD-CC-MBD) is necessary to suppress the conditional *myo2* mutations, and to provide the essential function in our newly generated *myo2*^{sens} alleles. Therefore the kinesin-like head is a functionally important domain of Smy1.

What is the precise function of Smy1? In otherwise wild-type cells, we have found that *SMY1* over-expression enhances the association of Sec4 with Myo2 as assessed by coimmunoprecipitation, and also enhances the number of Sec4 receptors and Myo2 motors on secretory vesicles. One simple possibility that we favor and is consistent with our data is that Myo2/Sec4-GTP/Smy1 form a ternary complex in which Smy1 enhances the association between Myo2 and Sec4. The finding that there are sufficient Smy1 molecules, and an excess of Sec4 receptors, to engage all the Myo2 motors on transporting secretory vesicles is consistent with this model. So far, our attempts to reconstitute a Myo2/ Sec4 /Smy1 complex on lipid vesicles has not been successful - the conditions may not be correct, such as a specific lipid or curvature requirement, or another protein might be required. If another factor functions with Smy1 in this process, and this function is essential, deletion of the gene for the factor should

be synthetically lethal with *smy1*Δ. We therefore explored the literature and data bases for genetic interactions that may support this possibility. As mentioned above, *smy1*Δ is synthetically lethal with m*yo2-66*, *sec4-8* and *sec2-41* (Lillie and Brown, 1998). The SGD data base reports that *smy1*Δ is synthetically lethal with *bem1*Δ, *bem2*Δ, *bni1*Δ, and *cla4*Δ, each of which affects the integrity of actin cables, the substrate on which Myo2 transports secretory vesicles. No obvious candidates functioning with Smy1 are found among the other reported genetic or biochemical interactions. Thus, we believe that Smy1 functions to make the interaction between Myo2 and Sec4 more robust, perhaps using a coincidence detection mechanism to enhance specificity.

We were initially surprised to find that shortening of the *myo2-41* neck domain from 6IQ motifs to 4IQ fully suppressed the temperature sensitive growth phenotype of the *myo2-41 smy1-15* mutant. However, this result further clarifies the role for the cooperation between Smy1 and Sec4 in binding Myo2. We have shown that Myo2 is activated by binding to secretory cargo (Donovan and Bretscher, 2012). We have also shown that wild type Myo2 undergoes a head-to-tail interaction that regulates the activity of Myo2. Moreover, the *MYO2-4IQ* allele, while not affecting the overall growth rate, partially activates the motors resulting in a higher percentage of active motors (Donovan and Bretscher, 2015). The finding that partial activation of Myo2 can overcome the temperature sensitivity, suggests that the problem in the *myo2-14 smy1-15* strain is in motor activation of Myo2. The *myo2-41* mutation reduces the affinity for Sec4, which presumably impairs Sec4's ability to activate Myo2 and therefore makes Myo2 activation dependent on Smy1. This strongly suggests that Smy1 cooperates with Sec4 in the activation step of Myo2 for transport of secretory vesicles. Remarkably, in the Myo2-4IQ background, the number of motors on secretory vesicles is independent of the *myo2-41* or *smy1-15* mutations, possibly suggesting that the cell has a robust mechanism to regulate motor number on secretory vesicles.

What is the biological function of Smy1's kinesin-like head domain? Essentially all the mutations we generated to make the conditional *smy1* alleles were found to lie in the head,

underscoring the importance of this region for the function of Smy1. This is surprising, as one would expect the mutations to lie in the Myo2-binding region. However, it is possible that mutations in the Myo2-binding region are too severe to generate a conditional phenotype, whereas subtle perturbations in the Smy1 head may be more easily tolerated. In support of this, there are no obvious mutational hotspots in the head, suggesting that a variety of small perturbations may be able to generate a conditional phenotype. Whatever the reason, it emphasizes that the head is functionally important. One possible function it might have is to bind Sec4, but we have not been able to detect a two-hybrid interaction between Sec4 and Smy1's head domain. Another possibility is that Smy1's head binds to another component present on secretory vesicles, thereby enhancing the association of Myo2 with them, and possibly indirectly enhancing the number of Sec4 receptor molecules.

The cooperation between Sec4 and Smy1 in the Myo2-dependent transport of secretory vesicles is reminiscent of the involvement of the mitochondrial receptors Mmr1 and the Rab Ypt11 in the segregation of mitochondria, another essential function of Myo2 (Chernyakov et al., 2013). This similarity is underscored by the finding that Sec4 and Ypt11 bind to the same Rab-binding site on the Myo2 tail (Eves et al., 2012), and that over-expression of Sec4 negatively impacts mitochondrial inheritance in an *mmr1*Δ strain. Moreover, in both cases the receptors Mmr1 and Ypt11, and Sec4 and Smy1, bind directly to Myo2. A significant difference is that Mmr1 or Ypt11 can each provide the essential bridge to Myo2 for mitochondrial inheritance, whereas Smy1 cannot provide the essential secretory vesicle function as loss of Sec4 cannot be bypassed by Smy1 over-expression. This may be because Sec4 has the additional essential function of binding the exocyst for vesicle tethering. So far there are no *sec4* separation of function alleles that affect just transport and not tethering, which could be used to address whether Smy1 alone is sufficient for coupling Myo2 to secretory vesicles.

Our genetic data strongly imply that Smy1's role is specific to secretory vesicles. First, over-expression of Smy1, where the association between Sec4 and Myo2 is enhanced, compromises the Ypt11-Myo2 interaction necessary for mitochondrial inheritance in *mmr1*Δ cells. Moreover,

our *myo2*^{sens} mutations that render *SMY1* essential and compromise the interaction of Sec4 with the Myo2 tail, have no effect on mitochondrial inheritance even in an *mmr1*Δ background.

In summary, we have found that an important function of Smy1 is to cooperate with Myo2 and Sec4 in the transport of secretory vesicles for polarized growth. It is not clear why a kinesin-related protein should perform this function. It is possible that it derives from an evolutionary relic reflecting a time when secretory vesicles were first transported by a kinesin on microtubules and then by a myosin-V on actin filaments, making their association and functional interplay meaningful. The report of a direct interaction between mammalian kinesin and myosin-Va (Huang et al., 1999) supports such a possibility.

Table 3, Yeast strains used in this study

Strain	Genotype	Parent
BY4741	*MATa his3Δ1 leu2Δ0 ura3Δ0 met15Δ0*	
BY4742	*MATalpha his3Δ1 leu2Δ0 ura3Δ0 lys2Δ0*	
ABY4035	*smy1Δ::KanR his3Δ1 leu2Δ0 ura3Δ0 met15Δ0*	BY4741
ABY3313	*MATa his3Δ1 leu2Δ0 ura3Δ0 met15Δ0 trp1Δ::KanR*	BY4741
ABY4007	*MYO2-3GFP::URA3 trp1Δ::KanR*	ABY3313
ABY4009	*MYO2-3GFP::URA3 smy1Δ::KanR*	ABY4035
ABY4143	*GFP-Sec4::URA3 trp1Δ::KanR*	ABY3313
ABY4144	*GFP-Sec4::URA3 smy1Δ::KanR*	ABY4035
ABY2408	*MATa MYO2-4IQ::HIS3*	
ABY3189	*MATa MYO2-4IQ-3GFP::URA3 pRS415-RFP-Snc2*	ABY2408
ABY3122	*MATa CSE4-3GFP::TRP1*	YWL980
ABY4129	*MATa his3Δ1 leu2Δ0 ura3Δ0 trp1Δ::KanR SMY1-3GFP::URA3*	ABY3313
ABY3315	*MATa myo2-47::HIS3 leu2Δ0 ura3Δ0 met15Δ0 trp1Δ::KanR*	BY4741
ABY3316	*MATa myo2-57::HIS3 leu2Δ0 ura3Δ0 met15Δ0 trp1Δ::KanR*	BY4741
ABY3317	*MATa myo2-51::HIS3 leu2Δ0 ura3Δ0 met15Δ0 trp1Δ::KanR*	BY4741
ABY3318	*MATa myo2-43::HIS3 leu2Δ0 ura3Δ0 met15Δ0 trp1Δ::KanR*	BY4741
ABY3319	*MATa myo2-41::HIS3 leu2Δ0 ura3Δ0 met15Δ0 trp1Δ::KanR*	BY4741
ABY4151	*MATa myo2-41-3GFP::URA3 his3Δ1 leu2Δ0 ura3Δ0 met15Δ0*	ABY3319
ABY3320	*MATa myo2-41::HIS3 smy1-15::TRP1 trp1Δ::KanR*	ABY3319
ABY4171	*MATa myo2-41-3GFP::URA3 smy1-15-3mCherry::LEU2*	ABY3320
ABY4158	*MATa myo2-41::HIS3 GFP-Sec4::URA3*	ABY3319
ABY4182	*MATa smy1-15::TRP1 his3Δ1 leu2Δ0 ura3Δ0 trp1Δ::KanR*	ABY4741
ABY4181	*MATa smy1-12::TRP1 his3Δ1 leu2Δ0 ura3Δ0 trp1Δ::KanR*	ABY4741
ABY4167	*MATa MYO2-3GFP::URA3 smy1-15::TRP1*	ABY4182
ABY4010	*MATa MYO2-3GFP::URA3 smy1-12::TRP1*	ABY4181
ABY4152	*MATa myo2-57-3GFP::URA3 his3Δ1 leu2Δ0 ura3Δ0 met15Δ0*	ABY3316
ABY3351	*MATa myo2-57::HIS3 smy1-12::TRP1 trp1Δ::KanR*	ABY3316
ABY4179	*MATa myo2-57-3GFP::URA3 smy1-12-3mCherry::LEU2*	ABY3351
ABY4098	*MATa myo2-57::HIS3 GFP-Sec4::URA3*	ABY3316
ABY4048	*smy1Δ::KanR pRS316-SMY1-3GFP*	ABY4035
ABY4049	*smy1Δ::KanR pRS316-SMY1-KLD-3GFP*	ABY4035
ABY4050	*smy1Δ::KanR pRS316-SMY1-CC-3GFP*	ABY4035
ABY4051	*smy1Δ::KanR pRS316-SMY1-MBD-3GFP*	ABY4035
ABY4052	*smy1Δ::KanR pRS316-SMY1-KLD+CC-3GFP*	ABY4035
ABY4053	*smy1Δ::KanR pRS316-SMY1-CC+MBD-3GFP*	ABY4035
ABY4054	*smy1Δ::KanR pRS316-SMY1-KLD+MBD-3GFP*	ABY4035
ABY2766	MATa, *trp1-901, leu2-3, 112, ura3-52, his3-200, gal4Δ, gal80Δ*	AH109a
ABY3319	*MATa myo2-41::HIS3 his3Δ1 leu2Δ0 ura3Δ0 met15Δ0 trp1Δ::KanR*	ABY3313
ABY3318	*MATa myo2-43::HIS3 his3Δ1 leu2Δ0 ura3Δ0 met15Δ0 trp1Δ::KanR*	ABY3313

ABY3317	*MATa myo2-51::HIS3 his3Δ1 leu2Δ0 ura3Δ0 met15Δ0 trp1Δ::KanR*	ABY3313
ABY3316	*MATa myo2-57::HIS3 his3Δ1 leu2Δ0 ura3Δ0 met15Δ0 trp1Δ::KanR*	ABY3313
ABY4300	*MATa MYO2-4IQ::HIS3*	BY4741
ABY4313	*MATa MYO2-4IQ::HIS3 smy1-15::TRP1*	ABY4300
ABY4314	*MATa MYO2-4IQ-41::HIS3*	BY4741
ABY4315	*MATa MYO2-4IQ-41::HIS3 smy1-15::TRP1*	ABY4314
ABY4304	*MATa MYO2-4IQ-3GFP::URA3*	BY4741
ABY4305	*MATa MYO2-4IQ-3GFP::URA3 smy1-15::TRP1*	ABY4304
ABY4316	*MATa MYO2-4IQ-41-3GFP::URA3*	BY4741
ABY4306	*MATa MYO2-4IQ-41-3GFP::URA3 smy1-15::TRP1*	ABY4316

Table 4, Plasmids used in this study

Name	Insert	Backbone	Marker
3471	GFP-Sec4	pRS306	URA3
2589	Sec4ΔCC (prenylation site deleted)	pBridge	TRP1
LCB109	SMY1	pRS316	URA3
LCB13	SMY1 KLD-3GFP (aa1-382)	pRS316	URA3
LCB14	SMY1 CC-3GFP (aa-436-562)	pRS316	URA3
LCB15	SMY1 MBD-3GFP (aa562-657)	pRS316	URA3
LCB16	SMY1 KLD+CC-3GFP (aa1-562)	pRS316	URA3
LCB17	SMY1 CC+MBD-3GFP (aa436-656)	pRS316	URA3
LCB18	SMY1 KLD+MBD-3GFP	pRS316	URA3
LCB45	Smy1 CC+MBD (aa436-656)	pGBKT7	TRP1
2579	myo2cctail-12	pGADT7	LEU2
LCB54	myo2cctail-41	pGADT7	LEU2
LCB70	myo2cctail-57	pGADT7	LEU2
LCB102	smy1-12	YEp351	LEU2
LCB104	smy1-15	YEp351	LEU2
LCB98	Smy1-K+C	YEp351	LEU2
LCB99	Smy1-C+M	YEp351	LEU2
LCB43	Sec4	YEp351	LEU2
LCB106	mito-RFPff	313	HIS3
LCB3	Myo2cctail-3GFP	306	URA3
1643	Myo2-4IQ	303	HIS3

References

Beningo, K.A., S.H. Lillie, and S.S. Brown. 2000. The yeast kinesin-related protein Smy1p exerts its effects on the class V myosin Myo2p via a physical interaction. *Molecular biology of the cell*. 11:691-702.

Bretscher, A. 2003. Polarized growth and organelle segregation in yeast: the tracks, motors, and receptors. *J Cell Biol*. 160:811-816.

Cadwell, R.C., and G.F. Joyce. 1992. Randomization of genes by PCR mutagenesis. *PCR Methods Appl*. 2:28-33.

Chernyakov, I., F. Santiago-Tirado, and A. Bretscher. 2013. Active segregation of yeast mitochondria by Myo2 is essential and mediated by Mmr1 and Ypt11. *Curr Biol*. 23:1818-1824.

Chesarone-Cataldo, M., C. Guérin, J.H. Yu, R. Wedlich-Soldner, L. Blanchoin, and B.L. Goode. 2011. The myosin passenger protein Smy1 controls actin cable structure and dynamics by acting as a formin damper. *Developmental cell*. 21:217-230.

Donovan, K.W., and A. Bretscher. 2012. Myosin-V is activated by binding secretory cargo and released in coordination with Rab/exocyst function. *Dev Cell*. 23:769-781.

Donovan, K.W., and A. Bretscher. 2015. Head-to-tail regulation is critical for the in vivo function of myosin V. *J Cell Biol*. 209:359-365.

Eskin, J.A., A. Rankova, A.B. Johnston, S.L. Alioto, and B.L. Goode. 2016. Common formin-regulating sequences in Smy1 and Bud14 are required for the control of actin cable assembly in vivo. *Mol Biol Cell*. 27:828-837.

Eves, P.T., Y. Jin, M. Brunner, and L.S. Weisman. 2012. Overlap of cargo binding sites on myosin V coordinates the inheritance of diverse cargoes. *The Journal of cell biology*. 198:69-85.

Gietz, R.D., and R.A. Woods. 2002. Transformation of yeast by lithium acetate/single-stranded carrier DNA/polyethylene glycol method. *Methods Enzymol*. 350:87-96.

Hammer, J.A., 3rd, and J.R. Sellers. 2012. Walking to work: roles for class V myosins as cargo transporters. *Nature reviews. Molecular cell biology*. 13:13-26.

Hodges, A.R., C.S. Bookwalter, E.B. Krementsova, and K.M. Trybus. 2009. A nonprocessive class V myosin drives cargo processively when a kinesin- related protein is a passenger. *Current biology : CB*. 19:2121-2125.

Huang, J.D., S.T. Brady, B.W. Richards, D. Stenolen, J.H. Resau, N.G. Copeland, and N.A. Jenkins. 1999. Direct interaction of microtubule- and actin-based transport motors. *Nature*. 397:267-270.

Itoh, T., A. Toh-E, and Y. Matsui. 2004. Mmr1p is a mitochondrial factor for Myo2p-dependent inheritance of mitochondria in the budding yeast. *The EMBO journal*. 23:2520-2530.

Itoh, T., A. Watabe, A. Toh-E, and Y. Matsui. 2002. Complex formation with Ypt11p, a rab-type small GTPase, is essential to facilitate the function of Myo2p, a class V myosin, in mitochondrial distribution in Saccharomyces cerevisiae. *Molecular and cellular biology*. 22:7744-7757.

Jin, Y., A. Sultana, P. Gandhi, E. Franklin, S. Hamamoto, A.R. Khan, M. Munson, R. Schekman, and L.S. Weisman. 2011. Myosin V transports secretory vesicles via a Rab GTPase cascade and interaction with the exocyst complex. *Dev Cell*. 21:1156-1170.

Lawrimore, J., K.S. Bloom, and E.D. Salmon. 2011. Point centromeres contain more than a single centromere-specific Cse4 (CENP-A) nucleosome. *J Cell Biol*. 195:573-582.

Lillie, S.H., and S.S. Brown. 1992. Suppression of a myosin defect by a kinesin-related gene. *Nature*. 356:358-361.

Lillie, S.H., and S.S. Brown. 1994. Immunofluorescence localization of the unconventional myosin, Myo2p, and the putative kinesin-related protein, Smy1p, to the same regions of polarized growth in Saccharomyces cerevisiae. *The Journal of cell biology*. 125:825-842.

Lillie, S.H., and S.S. Brown. 1998. Smy1p, a kinesin-related protein that does not require microtubules. *The Journal of cell biology*. 140:873-883.

Lipatova, Z., A.A. Tokarev, Y. Jin, J. Mulholland, L.S. Weisman, and N. Segev. 2008. Direct interaction between a myosin V motor and the Rab GTPases Ypt31/32 is required for polarized secretion. *Mol Biol Cell*. 19:4177-4187.

Longtine, M.S., A. McKenzie, 3rd, D.J. Demarini, N.G. Shah, A. Wach, A. Brachat, P. Philippsen, and J.R. Pringle. 1998. Additional modules for versatile and economical PCR-based gene deletion and modification in Saccharomyces cerevisiae. *Yeast*. 14:953-961.

Lwin, K.M., D. Li, and A. Bretscher. 2016. Kinesin-related Smy1 enhances the Rab-dependent association of myosin-V with secretory cargo. *Mol Biol Cell*. 27:2450-2462.

Santiago-Tirado, F.H., A. Legesse-Miller, D. Schott, and A. Bretscher. 2011. PI4P and Rab inputs collaborate in myosin-V-dependent transport of secretory compartments in yeast. *Developmental cell*. 20:47-59.

Schott, D., J. Ho, D. Pruyne, and A. Bretscher. 1999. The COOH-terminal domain of Myo2p, a yeast myosin V, has a direct role in secretory vesicle targeting. *The Journal of cell biology*. 147:791-808.

Schott, D.H., R.N. Collins, and A. Bretscher. 2002. Secretory vesicle transport velocity in living cells depends on the myosin-V lever arm length. *The Journal of cell biology*. 156:35-39.

Sherman, F. 1991. Getting started with yeast. *Methods Enzymol*. 194:3-21.

Chapter III

A Novel Rho GAP *GYM1* Mediates Myo2 Dependent Secretory Vesicle Transport by Downregulating the Rho3 Activity

Overview

Small molecular weight GTPase proteins such as members of the Ras, Rho and Rab families play central roles in regulating cell growth, polarity, morphogenesis, neural development, cytoskeletal dynamics, vesicle trafficking, and more. As discussed in Chapter I, the Rab GTPase Sec4 associates with Myo2 for secretory vesicle transport in budding yeast. Together with Sec4, Smy1 is involved in coupling secretory vesicles with the Myo2 tail. Conditional mutation of the *smy1* in mutant *myo2* background showed that temperature sensitive *myo2 smy1* mutants fail to couple secretory vesicle with the Myo2. By screening for overexpression suppressors of *myo2 smy1* mutants, we hoped to recover proteins potentially involved in Myo2 secretory vesicle transport. Interestingly we discovered an uncharacterized ORF that contains a Rho GAP domain in its C-terminus. We named the ORF, Gym1 (***G***ap with ***Y***east ***M***yo2). Gym1 colocalizes with Myo2 in the bud and its localization is dependent on Myo2 polarity. Consistent with this, Gym1 interacts with the Myo2 coiled-coil domain and it stimulates the hydrolysis of Rho3-GTP to Rho3-GDP. The catalytic activity is crucial in suppressing the *myo2 smy1*. Our finding provides the possibility that there is an interplay between Rho and Rab GTPases in the transport of secretory vesicles.

Materials and Methods

Yeast strains and transformation

Yeast strains and plasmids used in this study are listed in Table 5 and 6. Standard media and techniques for yeast growing and transformation were used and referred to Chapter II Methods (Sherman, 1991).

SGal-URA plate preparation

1L of agar media (SGal-URA) was prepared [6.7g YNP (Yeast Nitrogen Peptone), 1.3g SD-URA (Ura dropout in synthetic amino acids, 20g raffinose, 20g galactose and 20g agar) and autoclaved. Autoclaved media was allowed to become warm before pouring into petridish plates.

cDNA Library screening for *myo2 smy1* mutants

1ug of the GAL1-cDNA library (5ul of 200ng/ul cDNA library stock) was transformed into overnight culture (5ml) (OD_{600} = ~ 0.8) (Liu et al., 1992). After incubation at 42˚C for 45 minutes, the transformants were washed with dH_2O once, transferred to a 15ml falcon tube and resuspended in 5.1 ml of dH_2O. 100ul of resuspended transformants were spread onto each SGal-URA plate (50 plates x 0.1ml = 5ml) and incubated at 26˚C overnight to allow cDNA expression. The remaining 100ul of the transformants was spread on to one SD-URA plate and incubated at 26˚C for 5 days to serve as a control for the number of transformants. 50 Plates except the control plate were transferred to 35˚C the next day and incubated for 5 days. 80,000 transformants were screened against the *myo2-41 smy1-15* mutant, and 150,000 transformants against the *myo2-57 smy1-12* mutant. The cDNA plasmids were recovered from the transformants and sequenced to identify the gene.

Plasmid construction

The integrating plasmids pRS306 GFP-Sec4 (*URA3*) and pRS306 Myo2cctail-3GFP (*URA3*) used to tag Sec4 and Myo2 have been described (Donovan and Bretscher, 2012). To create pRS315 Gym1-RFP construct, the RFP fragment was initially cloned between BamHI and NotI and terminator ADH1 (tADH) was cloned between NotI and SacII in the pRS315 backbone. The fragment that contains the Gym1 endogenous promoter (~ 250bp) and Gym1 full length (2355bp without the stop codon) was cloned between the ApaI and XmaI in the pRS315 RFP-tADH vector. To create an integrating Gym1-RFP (i.e., pRS305 Gym1-RFP), two homologous regions were designed. In order to tag RFP at the C-terminus, the first cassette (Gym1-C-terminus+RFP) was cloned between HindIII and SacII in pRS305 vector. The forward primer

corresponding to genomic Gym1 sequence starting at near its C-terminus 5' ATTAAGCTTGCACAACTGCCACAGGAAAC 3' and the reverse primer corresponding to tADH 5' ATTCCGCGGAGGAAAGAGTTACTCAAGAA 3' were designed. Underlined nucleotides indicate respective restriction site and ATT was added to aid efficient cleavage. The cassette was amplified from the pRS315 Gym1-RFP-tADH construct. The second homologous region corresponding to Gym1 3'UTR, using the primers (5' ATTCTCGAGGATGTTCGTTAAAAGCTGCA 3') and (5' ATTAAGCTTCTATTAGAATCTGGGAAGTG 3') was cloned between XhoI and HindIII. The integrating Gym1-RFP was linearized by HindIII before transformation.

Microscopy

Micrographs were acquired on a CSU-X spinning disc confocal microscopy system (Intelligent Imaging Innovations) with a DMI 6000B microscope (Leica), 100x1.45 NA objective and a QuantEM EMCCD camera (Photometrics) or an HQII CCD camera (Photometrics) with 2x magnifying lens. All images shown are maximum projection of 10 confocal slices taken 0.28 μm apart, unless stated otherwise. Images were analyzed and processed with Slidebook 6.0 software (Intelligent Imaging Innovations). The images were further adjusted in Photoshop (Adobe) to give the clearest presentation of the results and assembled in Illustrator (Adobe). For live-cell imaging of yeast cells, cells were attached to a glass-bottomed dish coated with Concanavalin A (EY laboratories) and washed with respective cell medium. Imaging at high temperatures was performed in an environmental chamber (Okolab).

Yeast two-hybrid constructs and analysis

The coding sequence for Myo2cctail (2776-4725nt) was fused with the GAL4 DNA activation domain in pGADT7 vector between NdeI and BamHI. The full length Gym1 (1-785aa) was fused with GAL4 DNA activation domain in pGADT7 vector between XmaI and XhoI. Each of all Rho proteins (Rho1, Rho2, Rho3, Rho4, Rho5, Cdc42) were fused with GAL4 DNA binding domain in pGBKT7 vector between XmaI and PstI without their C-terminus CXC box to prevent prenylation. The AH109 strain co-transformed with both plasmids was selected in

media lacking leucine and tryptophan (SD-2DO: double dropout). Interaction was detected by growth on medium lacking leucine, tryptophan and histidine (SD-3DO: triple dropout) or (SD-3DO: triple dropout + 1mM 3AT to be more stringent in protein-protein interaction).

Purification of GST-Rho and SUMO-Gym1(GAP::495-785aa)

Full-length Rho proteins (Rho1, Rho2, Rho3, Rho4, Rho5, and Cdc42) were tagged with GST in their N-termini, using the pGEX-6p3 vectors. The GAP domain (495-725aa) of Gym1 was tagged with SUMO (Table 6). Constructs were expressed in Rosetta™ 2(DE3) pLysS competent cells separately. Cells were grown in terrific broth with antibiotics Ampicilin (100ug/ml) and chloramphenicol (34ug/ml) until A600=1.0. 1mM IPTG was added to induce protein expression overnight. Bacterially expressed SUMO-Gym1 was selected on a Ni^{2+} resin. GST-Rho proteins were isolated by glutathione beads and GST was later cleaved by 3Cpro.

Gym1 and Rho3 Antibody generation

Gym1 (495-725aa) tagged with SUMO and Rho3 with GST tag were expressed in Rosetta™ 2(DE3) pLysS competent cells separately. Bacterially expressed SUMO-Gym1 was selected on a Ni^{2+} resin, and the SUMO tag was cleaved with Ulp1. The SUMO-cleaved Gym1p was gel purified and sent to Pocono Rabbit Farm and Laboratory, PA for antibody production. Similarly, GST-Rho3 was isolated by glutathione beads and GST was later cleaved by 3Cpro. Gel purified Rho3 was sent for antibody production.

Immunoblotting

Overnight cultures were harvested and resuspended in disruption buffer (20mM Tris-CL, pH 7.9, 10mM $MgCl_2$, 1mM EDTA, 5% glycerol, 1mM dithiothreitol, 0.3M ammonium sulfate, 1mM PMSF, and 1x Sigma yeast protease inhibitor cocktail) with 0.1g acid-washed glass beads (Sigma-Aldrich, St. Louis, MO, USA). Vigorous vortexing was done at 4˚C for 3 times with 1 minute each and 1 minute in between resting on ice. The crude lysates were centrifuged at 17,000 g in a table-top centrifuge in a cold room (4˚C) for 10 minutes and supernatant was collected. For temperature sensitive strains, cells were grown at 26˚C overnight, and adjusted

to log phase OD_{600}=0.8 the next day. Cells were then shifted to 35˚C for 2 hours. Upon harvesting, cells were chilled on ice, washed twice with ice-cold water, frozen in dry ice and stored at -80°C. The concentrations of protein samples were measured using Bradford assay. The samples were resolved by SDS-PAGE, transferred to Immobilon-P membrane (Millipore), then blocked for 1 hour in 5% milk in PBS-T (0.1% Tween). Membranes were incubated with primary antibodies for 1 hour: mouse monoclonal anti-GFP antibody (Santa Cruz Biotechnology, Santa Cruz, CA, USA), or rabbit polyclonal antibodies against Myo2tail, Gym1 and Rho3 (generated in the lab). After washing, membranes were incubated with secondary antibodies: IRDye goat anti-mouse and donkey anti-rabbit antibodies. Membranes were analyzed using the Odyssey infrared imaging system (LI-COR Biosciences, Lincoln, NE, USA).

Coimmunoprecipitation

Total yeast protein extracts were prepared using the same protocols described above. 10µl of GFP-Trap® resin (ChromoTek) was used for 1mg of each cell lysate and agitated at 4˚C for 2 hours. Bound protein was eluted with 50µl hot (95°C) SDS-PAGE loading buffer. Eluted proteins were resolved on 7-15% split SDS gels.

Genetic interaction by Tetrad dissection

Genetic interaction between *gym1Δ* and temperature sensitive mutants (*myo2-66, myo2-12, sec2-41, sec4-8, sec6-4, sec9-4* and *sec15-1*) and non-essential genes (*mmr1Δ, smy1Δ* and *rgd1Δ*) was tested by dissecting tetrads after sporulation. Cells with opposite mating types were grown together overnight at 26˚C for mating. Mating efficiency was checked by shmoo projection and zygote formations the next day under the light microscope. Cells were washed with PBS and resuspended in sporulation media (1% yeast extract, 1% potassium acetate, and 0.05% glucose) and grown for 4-5 days. Tetrads formations were checked under light microscope. 25ul of zymolyase (1mg/ml) was added to 50ul of sporulated cells. Zymolyase treated cells were incubated at 37˚C for 5 minutes. Tetrads were dissected using MSM Singer instruments with 50um fiber needle.

GTPase activity assay

Malachite buffer (50mM HEPES, pH 7.5, 100mM KCL, 5mM EDTA, 10mM $MgCl_2$) was prepared for any adjustment of the protein volume. To prepare malachite reagent, one volume of 0.045% (w/v) Malachite Green oxalate, FW927.02 (Alfa Aezea #A16186) was added to two volumes of 4.2% (w/v) Ammonium Molybdate in 4M HCL and 0.01% (v/v) of Tween20 was added before use to prevent precipitation. For intrinsic GTPase activity assay, 10μM of Rho3 protein (GST cleaved) was treated with varying concentrations of GTP (10μM – 100μM) in nucleotide exchange buffer (50 mM Tris, pH 7.5, 100 mM KCl, 5mM DTT, 15 mM EDTA) in 100μl volume and incubated at 30˚C for 30min. $MgCl_2$ was added to a final concentration of 12.5mM to stop the reaction. 100μl of malachite reagent (1:1) was added. Released phosphate was detected by color change at absorbance 620nm, using 96-well plate reader. Minimum three duplicate experiments were done. The reaction time was calculated by phosphate released upon varying concentrations of GTP. The values of Km and Vmax were obtained by fitting the data in Michaelis-Menton equation (nonlinear regression curve fitting) in GraphPad Prism 6.0. (GraphPad software, Inc).

Stimulation of Rho GTPases activity by Gym1

GTPase activity of Rho3 in the presence of Gym1 was tested by malachite green assay. 10μM of Rho3 was nucleotide-exchanged with varying concentrations of GTP (10 – 100μM) and incubated at 30˚C for 30min. $MgCl_2$ was added to a final concentration of 12.5mM to stop the reaction. 3μM of SUMO-Gym1 (495-785aa) was added and incubated at 30˚C for 30min. Malachite reagent (1:1) was added and absorbance at 620nm was read at 96-well plate reader.

Table 5, Yeast strains used in this study

Strain	Genotype	Parent
BY4741	*MATa his3Δ1 leu2Δ0 ura3Δ0 met15Δ0*	
BY4742	*MATalpha his3Δ1 leu2Δ0 ura3Δ0 lys2Δ0*	
ABY4035	*smy1Δ::KanR his3Δ1 leu2Δ0 ura3Δ0 met15Δ0*	BY4741
ABY3313	*MATa his3Δ1 leu2Δ0 ura3Δ0 met15Δ0 trp1Δ::KanR*	BY4741
ABY4007	*MYO2-3GFP::URA3 trp1Δ::KanR*	ABY3313
ABY4009	*MYO2-3GFP::URA3 smy1Δ::KanR*	ABY4035
ABY4143	*GFP-Sec4::URA3 trp1Δ::KanR*	ABY3313
ABY4144	*GFP-Sec4::URA3 smy1Δ::KanR*	ABY4035
ABY3320	*MATa myo2-41::HIS3 smy1-15::TRP1 trp1Δ::KanR*	ABY3319
ABY3351	*MATa myo2-57::HIS3 smy1-12::TRP1 trp1Δ::KanR*	ABY3316
ABY2766	*MATa, trp1-901, leu2-3, 112, ura3-52, his3-200, gal4Δ, gal80Δ*	AH109a
ABY3451	*MATa his4-619 ura3-53 sec23-1 MYO2-3GFP::URA3*	RSY281
ABY824	*MATa his4-619 ura3-53 sec23-1*	RSY281
ABY2702	*MATa his3Δ1 leu2Δ0 ura3Δ0 met15Δ0 myo2-12::HIS3*	BY4741
ABY127	*MATa ura3-52 sec4-8*	NY405
ABY4230	*MYO2-3GFP::URA3 GYM1-RFPff::LEU2(CEN)*	BY4741
ABY4231	*GFP-SEC4::URA3 GYM1-RFPff::LEU2(CEN)*	BY4741
	gym1Δ::KanR his3Δ1 leu2Δ0 ura3Δ0 met15Δ0	BY4741(Δ consortium)
ABY4241	*gym1Δ::KanR MYO2-3GFP::URA3*	
ABY4242	*gym1Δ::KanR GFP-SEC4::URA3*	
ABY4279	*Myo2-12-3GFP::URA3 GYM1-RFPff::LEU2(CEN)*	ABY3423
ABY4281	*Sec23-1 MYO2-3GFP::URA3 GYM1-RFPff::LEU2(CEN)*	ABY3439

Table 6, Plasmids used in this study

Name	Insert	Backbone	Marker
3471	GFP-Sec4	pRS306	URA3
2589	Sec4ΔCC (prenylation site deleted)	pBridge	TRP1
LCB128	Rho1 (EcoRI-NotI)	pGEX-6p3	AMP
LCB129	Rho2 (EcoRI-NotI)	pGEX-6p3	AMP
LCB130	Rho3 (EcoRI-NotI)	pGEX-6p3	AMP
LCB131	Rho4 (EcoRI-NotI)	pGEX-6p3	AMP
LCB132	Rho5 (EcoRI-NotI)	pGEX-6p3	AMP
LCB133	Cdc42 (EcoRI-NotI)	pGEX-6p3	AMP
LCB135	Gym1	YEp352	URA3
LCB136	Gym1-GAP (490-785aa)	pE-SUMO	AMP
LCB137	Gym1-dead GAP (R546A) (490-785aa)	pE-SUMO	AMP
LCB127	Gym1-RFP	305	HIS3
LCB3	Myo2cctail-3GFP	306	URA3

Results

Identification of *myo2 smy1* suppressors

Previously we characterized the role of Smy1 in the association of Myo2 with secretory vesicles by studying the *myo2 smy1* mutants that were generated in our lab (Figure 3.1A) (Chapter 3). To further identify additional proteins potentially involved in Myo2 dependent vesicle transport, we screened for cDNAs whose overexpression would suppress the *myo2 smy1* mutants, using the cDNA library expressed under the *GAL1* promoter (Liu et al., 1992). To achieve full coverage of all budding yeast genes, we transformed 80,000 cDNAs and 150,000 cDNAs into *myo2-41 smy1-15* and *myo2-51 smy-12,* respectively. We identified a number of proteins, many of them involved in the secretory vesicle transport (Figure 3.1B).

Myo2-related cDNAs and Rab GTPases suppress *myo2 smy1* mutants

We hypothesized that identification of the *myo2 smy1* suppressors should reveal proteins potentially involved in the vesicle transport because the *myo2 smy1* mutants fail to transport secretory vesicles (Lwin et al., 2016). We confirmed that all our cDNAs suppressed *myo2-41 smy1-15* (Figure 3.2A). Characterization of all cDNA candidates supported our hypothesis. Calmodulin (*CMD1*), and Myosin Light Chain (*MLC1*) are involved in the regulation of myosin conformation (Brockerhoff et al., 1994; Terrak et al., 2005). Calmodulin Kinase (*CMK1*) also suppresses the *myo2-41 smy1-15*. The Smy1 and Rab GTPases such as Sec4, Ypt31/32 are involved in activating and coupling the Myo2 motors with secretory vesicles (Figure 3.2A) (Stevens and Davis, 1998; Wagner et al., 2002). Only a few cDNAs: *YHR182W*, *MLC1*, *SMY1*, and *YPT31* suppressed the *myo2-57 smy1-12,* presumably due to the presence of critical mutations (Y1415S together with other two alleles) in the Rab binding site (Figure 3.2A). Interestingly, we discovered a new hypothetical protein *YHR182W,* which we named as *GYM1* in this study. However, deletion of *GYM1* has no overt phenotype (Figure 3.2, C and D).

Figure 3.1. Identification of temperature sensitive *myo2 smy1* suppres-

A

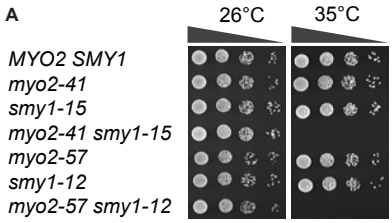

B

Overexpression suppression of *myo2-41 smy1-15*

Genes	Clones	Description
CMD1	*3/25*	Calmodulin; Ca++ binding protein that targets Nuf1p, Myo2p and calcineurin.
CMK1	*1/25*	Calmodulin-dependent protein kinase; may play a role in stress response.
MLC1	*3/25*	Light chain for Myo2p; stabilizes Myo2p by binding to the neck region.
SEC4	*2/25*	Rab family GTPase; essential for vesicle-mediated exocytic secretion and autophagy.
SMY1	*1/25*	Kinesin-like myosin passenger-protein; interacts with Myo2p.
SMI1	*6/25*	Aka KNR4; Protein involved in the regulation of cell wall synthesis.
YPT31	*8/25*	Rab family GTPase; mediates intra-Golgi traffic or the budding of post-Golgi vesicles.
YPT32	*1/25*	Rab family GTPase; mediates intra-Golgi traffic or the budding of post-Golgi vesicles.

Overexpression suppression of *myo2-57 smy1-12*

Genes	Clones	Description
MLC1	*1/8*	Light chain for Myo2p; stabilizes Myo2p by binding to the neck region.
YHR182W	*1/8*	Putative protein localizes to the cell periphery and cytoplasm, Rho GAP protein.
YPT31	*6/8*	Rab family GTPase; mediates intra-Golgi traffic or the budding of post-Golgi vesicles.

Figure 3.1. Identification of temperature sensitive *myo2 smy1* suppressors
(A) Growth of temperature sensitive strains: *myo2-41 smy1-15* and *myo2-57 smy1-12*. 10-fold serially diluted cells spotted on YPD plates and incubated at 26˚C and 35˚C for 2 days.
(B) A list of cDNA candidates from overexpression suppression screening of *myo2-41 smy1-12* (80,000 cDNAs coverage) and *myo2-57 smy1-12* (150,000 cDNAs coverage).

Figure 3.2. cDNA Candidates suppress *myo2 smy1*

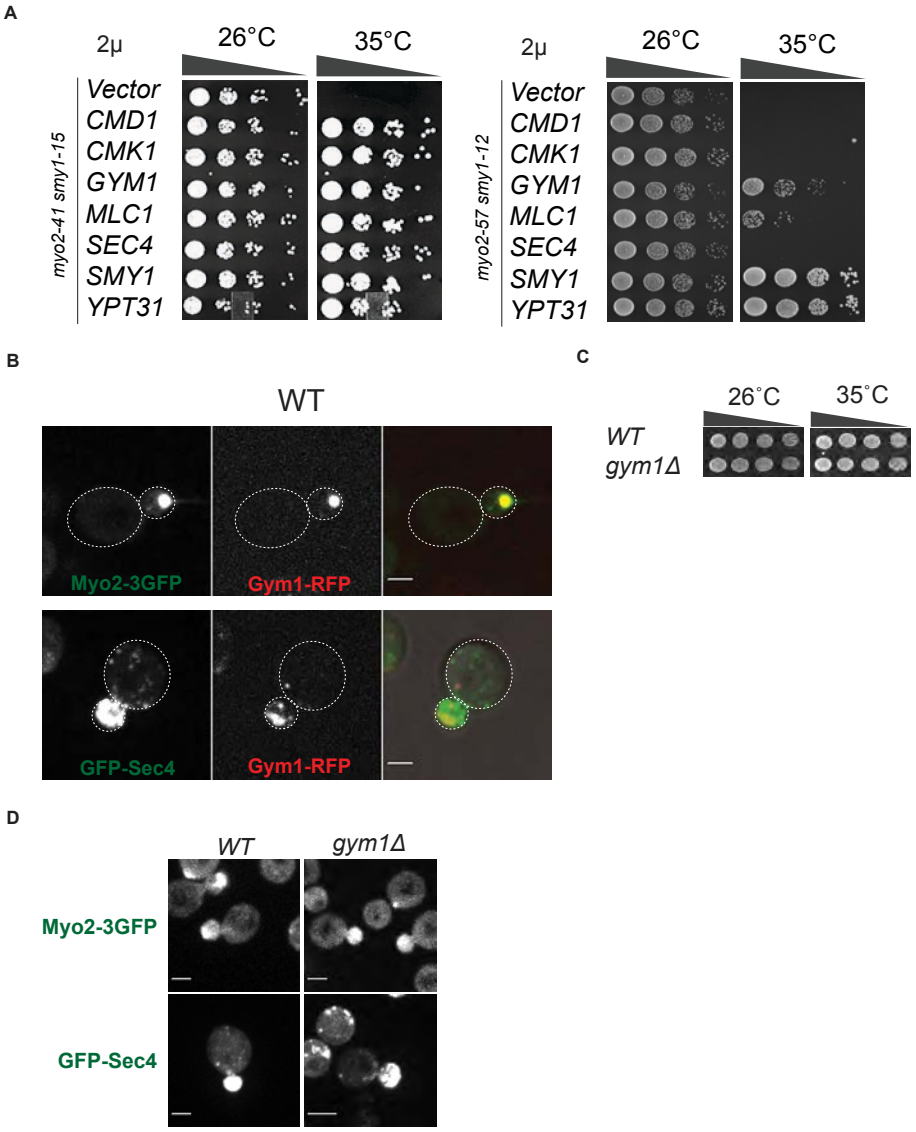

Figure 3.2. cDNA candidates suppress *myo2 smy1.*
(A) Overexpression of the cDNAs suppresses *myo2-41 smy1-15* and *myo2-57 smy1-12*.
(B) Gym1 localizes in the bud with Myo2 and secretory vesicle. Scale bars, 2μm.
(C) and (D) Deletion of Gym1 has no growth phenotype and Myo2 and Sec4 are still polarized in the bud. Scale bars, 2μm.

Gym1 is localized in the bud and its localization is dependent on Myo2 polarization

To localize Gym1, I tagged it with RFP. Gym1-RFP colocalized with the Myo2 motors (Myo2-3GFP) in the bud, together with the secretory vesicles marked by GFP-Sec4 (Figure 3.2B). Deletion of Gym1 had no effect on the polarity of Myo2 motors and secretory vesicles overall (Figure 3.2D). To test whether Gym1 localization is dependent on Myo2 or Sec4, I used *myo2-12* mutant, in which *myo2-12*-3GFP was still polarized and secretory vesicles (GFP-Sec4) failed to polarize at the restrictive temperature. In *myo2*-12, I found that Gym1 was still polarized at both permissive (26˚C) and restrictive (37˚C) temperatures (Figure 3.3, A, B and C), indicating that Gym1 polarity was not dependent on Sec4 or secretory vesicles. To further characterize if Gym1 localization was dependent on the Myo2 polarity, we used the conditional *sec23-1* mutant. In *sec23-1* when shifted to the restrictive temperature for 1 hour, Myo2 failed to polarize in the bud due to lack of secretory vesicle formation at the early secretory stage (Donovan and Bretscher, 2012). We observed that Myo2 and Gym1 failed to polarize in *sec23-1* at the restrictive temperature, which suggested that Myo2 polarity was required for the localization of Gym1 in the bud (Figure 3.3, D and E). These results suggest that Gym1 localization in the bud is dependent on the Myo2 polarity.

Gym1 interacts with the Myo2 coiled-coil domain and its full-length is required for its localization

Because Gym1 colocalized with the Myo2 motors and its localization was dependent on Myo2, we studied the interaction between Gym1 and Myo2. Yeast-two hybrid showed that Gym1 interacted with the Myo2 coiled-coil domain (Figure 3.4A). Immunoprecipitation of Myo2-FLAG pulled down the Gym1-3GFP, indicating that this interaction might account for their colocalization (Figure 3.4B). We also explored the possibility of Smy1 and Sec4 interaction with Gym1. Neither of these interacted with the Gym1 (Figure 3.4, C and D). Both active GTP-bound and inactive GDP-bound Sec4 ($Sec4^{Q74L}$ and $Sec4^{S34N}$) failed to interact with Gym1 (Figure 3.4D). We also further characterized which domain of Gym1 was localized in the bud.

Figure 3.3. Gym1p is localized in the bud and its localization is dependent on Myo2 polarity

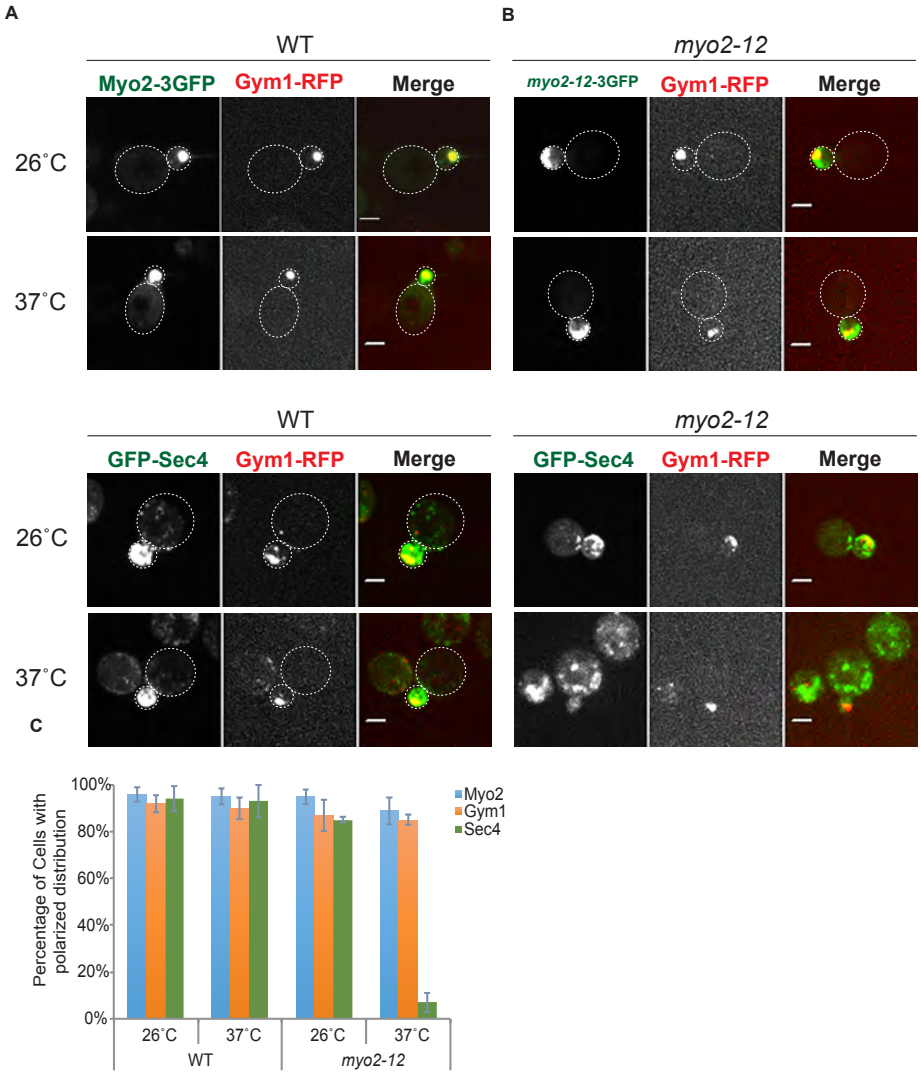

Figure 3.3. Gym1 is localized in the bud and its localization is dependent on Myo2 polarity.
(A) and (B) Localization of Myo2, Gym1 and Sec4 in the indicated strains at 26°C or after shifting to 37°C for 1hr. Scale bars, 2μm. (C) Quantification of small budded (≤ 2μm) cells with polarized Myo2, Gym1 and Sec4 at 26˚C and 37˚C. Mean values are from three independent experiments (n=50 each) and error bars indicate SD.

Figure 3.3. (Continued) Gym1p is localized in the bud and its localization is dependent on Myo2 polarity

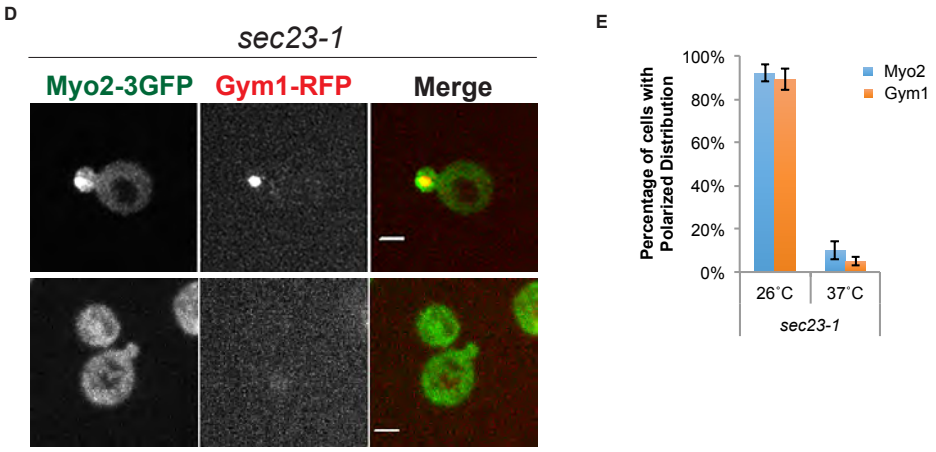

Figure 3.3. (continued) Gym1 is localized in the bud and its localization is dependent on Myo2 polarity.
(D) Localization of Myo2 and Gym1 in *sec23-1* at 26°C or after shifting to 37°C for 1hr. Scale bars, 2μm.
(E) Quantification of small budded (≤ 2μm) cells with polarized Myo2 and Gym1 at 26˚C and 37˚C. Mean values are from three independent experiments (n=50 each) and error bars indicate SD.

Figure 3.4. Gym1 interacts with Myo2 coiled-coil domain and its full length is required for localization in the bud.

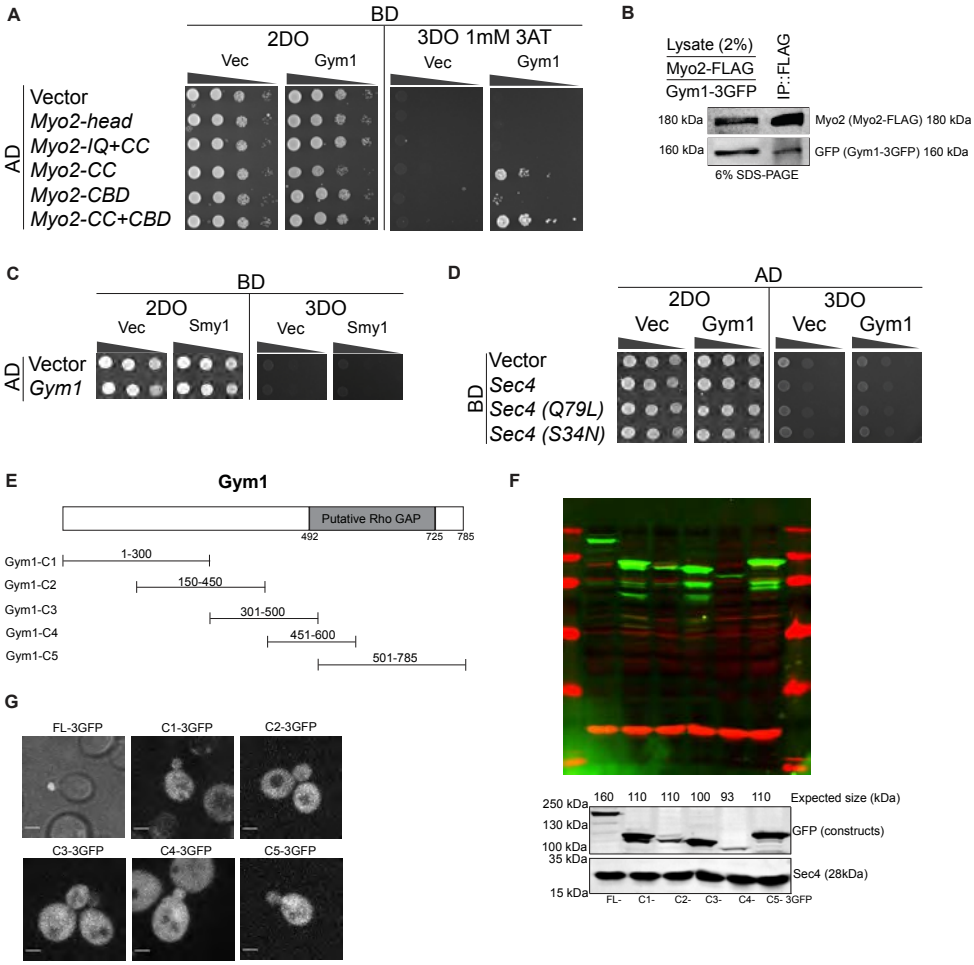

Figure 3.4. Gym1 interacts with Myo2 coiled-coil domain and its full length is required for localization in the bud.
(A) Yeast two-hybrid interactions between different domains of Myo2 fused to the activation domain (AD) and Gym1 fused to the binding domain (BD). 2DO = two amino acids (Leu2, Trp1) drop-out; 3DO = three amino acids (Leu2, Trp1, His3) drop-out. 3-AT = 3 amino 1,2,4 triazole agent to select more stringent interaction. Myo2-head (1-786aa); Myo2-IQ+CC (785-1086aa); Myo2-CC (926-1086aa); Myo2-CBD (1086-1574aa); Myo2-CC+CBD (926-1574aa)
(B) Coimmunoprecipitation of Myo2-FLAG in different Gym1-3GFP backgrounds (Myo2-FLAG; Gym1-3GFP; Myo2-FLAG Gym1-3GFP). Myo2-FLAG was immunoprecipitated, resolved by gel electrophoresis in 6% SDS-PAGE and immunoblotted for Myo2cctail Antibody (Myo2) and GFP (Gym1).
(C) and (D) Yeast two-hybrid interactions between Gym1 fused to the activation domain (AD) and Smy1 fused to the binding domain (BD) or Sec4Δ CC fused to the binding domain (BD). The C-terminal CXC motif of Sec4 was deleted to eliminate prenylation. Dominant active allele *Q74L* and dominant inactive *S34N* were introduced into pGBKT7-Sec4ΔCC. 2DO = two amino acids (Leu2, Trp1) drop-out; 3DO = three amino acids (Leu2, Trp1, His3) drop-out.
(E) Domain analysis of Gym1. Several constructs were tagged with 3GFP.
(F) Expression of several Gym1 constructs tagged with 3GFP. Sec4 was immunoblotted as a loading control.
(G) Domain analysis of Gym1. Scale bars, 2μm.

We created five constructs; each of which had about 200 to 300aa residues that were tagged with 3GFP, and their protein expressions were checked (Figure 3.4, E, F and G). Only full length Gym1 showed the polarity of Gym1, which indicated that none of the regions examined was sufficient for its localization (Figure 3.4 G).

Gym1 has a C-terminal Rho GAP domain and the critical arginine residue is necessary for its suppression activity

Gym1 has a putative Rho GTPase Activating Protein (GAP) domain in the C-terminal region of the protein. GAP proteins have highly conserved domains that facilitate the intrinsic GTPase hydrolytic activity of their respective GTPases such as Ras, Rho, and Rab proteins (Scheffzek et al., 1998). Rho GAP domains have a highly conserved arginine residue within the consensus motif. The arginine residue, which contacts the nucleotide-binding site, facilitates the hydrolysis of the bound GTP (Scheffzek et al., 1998). Budding yeast Rho GAPs have conserved GAP domains, characterized by motif 1 and motif 2 (Roumanie et al., 2001). To examine if Gym1 has Rho GAP activity, we aligned the Gym1 sequence with the budding yeast Rho GAPs: Bag7, Sac7, Rga1, Rga2, Bem2, Bem3, and Rgd1, using the clustalW2 alignment program. The arginine residue of Gym1 lies at the position 546 (Figure 3.5A). Mutation of the arginine to alanine lost the suppression activity of the Gym1 for *myo2 smy1* mutants (Figure 3.5, B and C). However, mutation of the lysine 519 to alanine (K519A) did not affect the Gym1 overexpression suppression activity, indicating that the arginine residue at the 546aa position was critical for Gym1 GAP activity. This finding suggests that Gym1 suppression on *myo2 smy1* mutants is dependent on its GAP activity.

Figure 3.5. Gym1 has Rho GAP domain and mutation of its critical arginine residue loses its suppression activity.

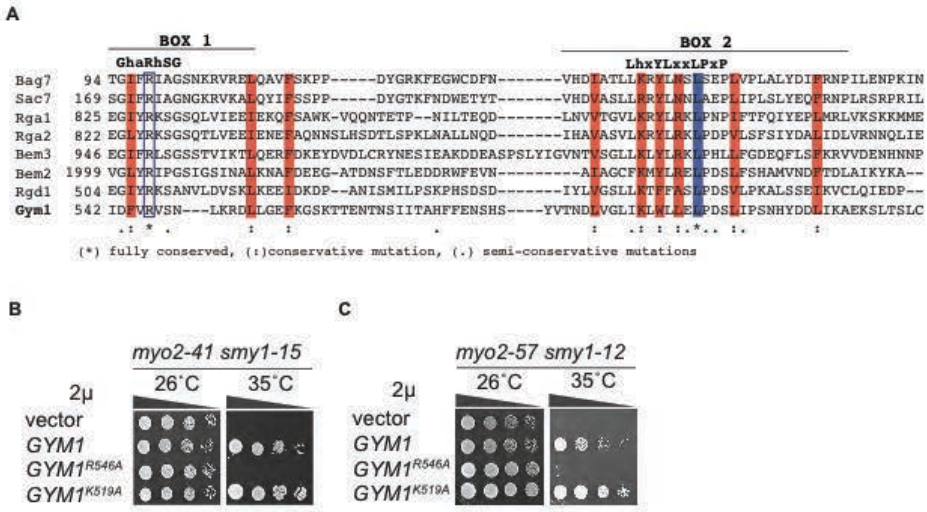

Figure 3.5. Gym1 has Rho GAP domain and mutation of its critical arginine residue loses its suppression activity.
(A) Alignment of Gym1 GAP domain with other Rho GAPs in budding yeast, using ClustalW2 program. Box1 indicates arginine finger motif. Box2 indicates 2nd motif with arginine or lysine residues crucial for stabilizing the arginine finger motif in Box1. a, aromatic; h, hydrophobic; x, any residue. (B) and (C) Gym1 dead mutant Gym1^{R546A} fail to suppress *myo2 smy1 ts* mutants.

Rho GAP, Gym1, stimulates the Rho3 GTPase activity

Rho proteins have intrinsic GTPase activity, which catalyzes the bound GTP into GDP, releasing inorganic phosphate (Pi). The hydrolytic activity, however, is slow in the absence of Rho GAPs (GTPase Activating Proteins). By facilitating GTP hydrolysis, Rho GAPs play an important role in down-regulating the activity of Rho proteins. Because Gym1 has a Rho GAP domain, we examined which Rho proteins interact with Gym1 in budding yeast. We tested all Rho proteins: Rho1, Rho2, Rho3, Rho4, Rho5, and Cdc42. By examining the yeast-two hybrid interaction, we found that Gym1 interacted with Rho3 (Figure 3.6A).

We also investigated the specificity of the Gym1 GAP activity biochemically. SUMO-Gym1 (GAP domain: 495-785aa) and GST-Rho proteins were expressed in bacteria and purified (Figure 3.6B). By using a colorimetric malachite green assay, which detects inorganic phosphate in the assay, we observed that Gym1 specifically stimulated the hydrolytic activity of Rho3 (Figure 3.6, C, D and E). Rho3 has an intrinsic K_m value at 123μM and Gym1 stimulates the GTPase activity of Rho3 by tenfold, which reduces the K_m value at 12 ± 1.9 μM (Figure 3.6F). We also showed that Gym1 dead mutant, R546A allele, failed to stimulate the Rho3 (Figure 3.6G). This finding showed that Gym1 GAP activity is specific to Rho3 and the activity is important in restoring Myo2 dependent vesicle transport in the *myo2-41 smy1-15* mutant.

Figure 3.6. Rho GAP Gym1 stimulates Rho3 GTPase activity.

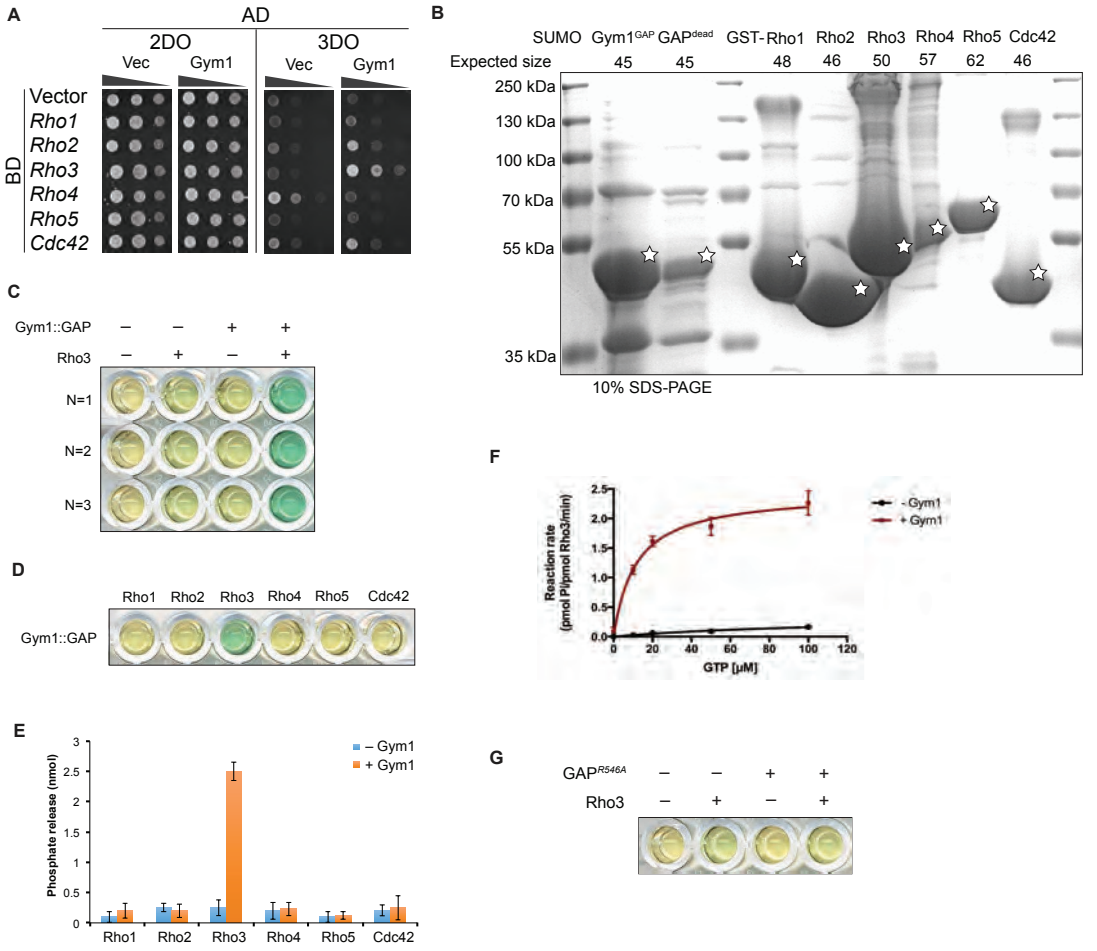

Figure 3.6. Rho GAP Gym1 stimulates Rho3 GTPase activity.
(A) Yeast two-hybrid interactions between all Rho GTPases fused to the binding domain (BD) and Gym1 fused to the activation domain (AD). The C-terminal CXC motifs of Rho proteins were deleted to eliminate prenylation. 2DO = two amino acids (Leu2, Trp1) drop-out; 3DO = three amino acids (Leu2, Trp1, His3) drop-out.
(B) Bacterial expression of SUMO-Gym1(GAP::495-785aa), SUMO-GYM1^{R546A}(GAP::495-785aa) and GST-Rho1/Rho2/Rho3/Rho4/Rho5/Cdc42.
(C) Colorimetric malachite green assay with or without SUMO-Gym1 (495-785aa) and Rho3. Green color indicates free phosphate released.
(D) Rho GTP hydrolysis specificity of Gym1 by colorimetric malachite green assay.
(E) Quantification of phosphate released (Pi) from three independent experiments. Error bars indicate SD.
(F) Kinetic analysis of Rho3 GTP hydrolysis by Gym1. GTP hydrolysis rates of Rho3 [10μM] were determined by monitoring the release of free phosphate using the malachite green assay. Values of V_{max} and K_m were determined by fitting the Michaelis-Menten equation using nonlinear regression algorithms in GraphPad Prism software.
(G) SUMO-Gym1^{R546A} fails to stimulate Rho3 GTPase activity observed by colorimetric malachite green assay.

Figure 3.7. Rho3 and Rho3 specific Gym1 are involved in Myo2 dependent secretory pathway.

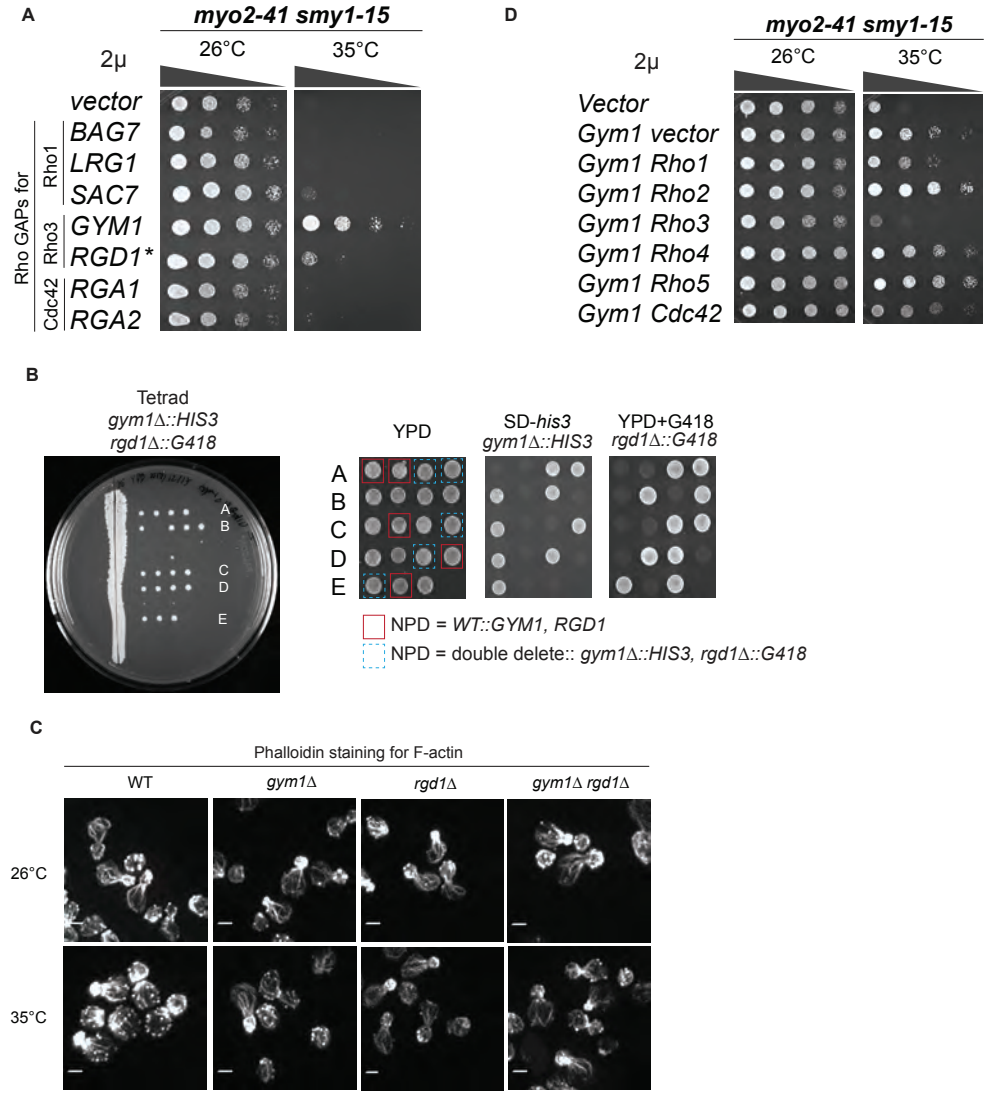

Figure 3.7. Rho3 and Rho3 specific Gym1 are involved in Myo2 dependent secretory pathway.
(A) Overexpression of Rho1, Rho3 and Cdc42 specific GAPs on *myo2-41 smy1-15*. *Rgd1 is GAPs for both Rho3 and Rho4.
(B) Gym1 and Rgd1 has no genetic interaction confirmed by tetrad analysis. YPD = Yeast Peptone Dextrose plate, NPD = non-parental ditype: WT or *gym1Δ rgd1Δ*.
(C) Phalloidin staining of F-actin in Rho3 GAP mutants: *gym1Δ, rgd1Δ* and double mutant *gym1Δ rgd1Δ*. Scale bar, 2µm.
(D) Genetic interaction tested by overexpressing Gym1 and Rho protein in *myo2-41 smy1-12 ts* mutant.

Gym1 is the only RhoGAP that suppresses *myo2 smy1* mutants

Yeast has a total of seven RhoGAP proteins: Bag7, Lrg1, Sac7, Rga1, Rga2, Rgd1 and now Gym1. Bag7, Lrg1 and Sac7 are Rho1 specific GAPs; Rga1 and Rga2 are Cdc42 specific GAPs (Smith et al., 2002), and Rgd1 is a GAP for both Rho3 and Rho4 (Doignon et al., 1999). We observed that Gym1, which is the only Rho3 specific GAP, suppressed the *myo2 smy1* mutants, indicating that Gym1 and Rho3 are specifically involved in the secretory vesicle transport (Figure 3.7A).

Because Rgd1 is a Rho3 GAP (Doignon et al., 1999), we examined if genetic interaction exists between Gym1 and Rgd1. Tetrad analysis showed that *gym1Δ* and *rgd1Δ* grow well as does *gym1Δ rgd1Δ* (Figure 3.7B), which suggested that Gym1 and Rgd1 could have different GAP activities, spatially and temporally, or another potential Rho3 GAP exists. We further explored the possibility of Rgd1 and Gym1 in the formation of actin filaments because Rho proteins are involved in actin organizations (Goode and Eck, 2007). Phalloidin staining of F-actin in *gym1Δ, rgd1Δ* and *gym1Δ rgd1Δ* showed no defect in formation of the actin filaments (Figure 3.7C).

We used an additional genetic approach to test the specificity of Gym1 for Rho3. The current data suggest that Gym1 overexpression suppresses the *myo2-41 smy1-15* mutant by deactivating Rho3-GTP. If this is correct, overexpressing both *GYM1* and *RHO3* in the mutant might abrogate the suppression. We therefore overexpressed each of the Rho proteins in *myo2-41 smy1-15* cells that also had Gym1 overexpressed. Only *RHO3* overexpression could reverse the suppression conferred by *GYM1,* further indicating a functional relationship between Gym1 and Rho3 (Figure 3.7D).

Discussion

Myosin motors are evolutionarily conserved proteins across eukaryotic species. Extensive studies on skeletal myosin have shed light on how myosin motors coordinate their step-wise movement on actin filaments (Vale, 2003). Similarly, budding yeast myosin-V, Myo2, also opened an interesting field of motors and cargos transport (Hammer and Sellers, 2012). Yeast myosin-V utilizes different receptors to recognize its specific cargos: Rab GTPase Sec4 for secretory vesicles (Jin et al., 2011); Mmr1 or Ypt11 for mitochondria (Chernyakov et al., 2013; Itoh et al., 2004); Inp2 for peroxisome (Fagarasanu et al., 2006) and Vac17/Vac8 for vacuole inheritance (Ishikawa et al., 2003). As organisms evolve, many proteins become redundant and yet provide the same function. For example, Smy1 is a non-essential protein. Deletion of Smy1 has no growth phenotype or effect on other proteins in the secretory vesicle transport (Lwin et al., 2016). Overexpression of Smy1, however, rescued *myo2* mutants such as *myo2-66* (Lillie and Brown, 1992), which was defective in secretory vesicle transport. This rescue phenotype supported the evolutionary role of the Smy1 in the secretory vesicle transport. We have previously shown that Smy1 enhances the Myo2 coupling with secretory vesicle receptor Rab GTPase Sec4 (Lwin et al., 2016). By using *myo2 smy1* mutants in our overexpression cDNA screening, we hypothesized that we would uncover new factors, potentially involved in the Myo2 dependent secretory vesicle transport. Most of the cDNA candidates that we identified support our hypothesis that as most of the suppressors are Myo2-related proteins such as Cmd1, Cmk1, Mlc1, and vesicle-related Rab GTPases such as Sec4 and Ypt31/32. Interestingly Smi1 is also a suppressor, which suggests that cell wall synthesis is somehow related to the Myo2 dependent secretory vesicle transport.

A hypothetical gene *YHR182W* (named *GYM1* in this study) also suppressed both of our mutants: *myo2-41 smy1-15* and *myo2-57 smy1-12*. We found that Gym1 was polarized in the bud and its polarity was dependent on Myo2. The fact that Gym1 polarity was lost in the *sec23-1* mutant indicated that Gym1 is somehow involved in the secretory vesicle transport. Yeast-two hybrid interaction between Gym1 and Myo2 further supported such a possibility. Analyzing the

Gym1 sequence returned a putative Rho GAP domain in the C-terminus (459-725aa). The N-terminus, which occupies about 300 amino acids residues, returned no known protein domain. Therefore, the functional importance of Gym1 N-terminal domain remains to be characterized.

All GAP proteins have a consensus motif that contains an arginine residue. The arginine residue facilitates the phosphodiester bond cleavage at the last phosphate (Pγ) from the bound GTP, releasing inorganic phosphate. Mutation of the Gym1 arginine residue at position 546 to alanine resulted in suppression failure, indicating that Gym1 GAP domain was functional and its GAP activity was crucial in suppression. Further characterization of Gym1 on all available Rho proteins in budding yeast led us to show that Gym1 is specific for Rho3. Because Gym1 is a Rho GAP, which suppresses conditional *myo2 smy1* mutants, we next investigated whether other Rho GAPs were also able to suppress the mutants. We observed that only Rho3 specific Gym1 suppressed the conditional mutants, suggesting that only Rho3 and Gym1 were possibly involved in the secretory vesicle transport. This opened the possibility of Rgd1, another Rho3 GAP, involvement in other functions rather than in membrane trafficking. Our examination of actin filaments formation in null mutants such as *rgd1Δ* and *gym1Δrgd1Δ* indicated that Gym1 and Rgd1 had no effect on actin organization. This could also suggest that another potential Rho3 GAP exists or Gym1 and Rgd1 have different GAP functions on Rho3, spatially and temporally.

In summary, our finding showed that Gym1 mediated the vesicle trafficking in a Myo2 dependent manner through Rho3 GTPase. It is also interesting to note that the majority of GTPases in vesicles trafficking are Rab GTPases (Hutagalung and Novick, 2011). Our data suggest that Rho3 is a negative regulator of the association of Myo2 with secretory vesicles. Because Myo2 also undergoes activation by a Rab protein and needs to recycle so as to transport cargo as necessary, it is possible that Rho3 is crucial in regulating the Myo2 recycling process. The question of how Rho3 regulates Myo2 recycling remains to be answered. The Rho-related protein TC10 in mammalian cells is also involved in transporting insulin induced GLUT4 transporter, CFTR receptor to the plasma membrane, and its GTP hydrolysis is

required for exocytic vesicle fusion (Cheng et al., 2005; Chiang et al., 2001; Inoue et al., 2003; Kawase et al., 2006). Therefore, our finding in budding yeast regarding the Rho GAP suggests a strong possibility that there is an interplay between Rho and Rab GTPases in vesicle trafficking and cargo transport.

References

Brockerhoff, S.E., R.C. Stevens, and T.N. Davis. 1994. The unconventional myosin, Myo2p, is a calmodulin target at sites of cell growth in Saccharomyces cerevisiae. *J Cell Biol*. 124:315-323.

Cheng, J., H. Wang, and W.B. Guggino. 2005. Regulation of cystic fibrosis transmembrane regulator trafficking and protein expression by a Rho family small GTPase TC10. *J Biol Chem*. 280:3731-3739.

Chernyakov, I., F. Santiago-Tirado, and A. Bretscher. 2013. Active segregation of yeast mitochondria by Myo2 is essential and mediated by Mmr1 and Ypt11. *Curr Biol*. 23:1818-1824.

Chiang, S.H., C.A. Baumann, M. Kanzaki, D.C. Thurmond, R.T. Watson, C.L. Neudauer, I.G. Macara, J.E. Pessin, and A.R. Saltiel. 2001. Insulin-stimulated GLUT4 translocation requires the CAP-dependent activation of TC10. *Nature*. 410:944-948.

Doignon, F., C. Weinachter, O. Roumanie, and M. Crouzet. 1999. The yeast Rgd1p is a GTPase activating protein of the Rho3 and rho4 proteins. *FEBS Lett*. 459:458-462.

Donovan, K.W., and A. Bretscher. 2012. Myosin-V is activated by binding secretory cargo and released in coordination with Rab/exocyst function. *Dev Cell*. 23:769-781.

Fagarasanu, A., M. Fagarasanu, G.A. Eitzen, J.D. Aitchison, and R.A. Rachubinski. 2006. The peroxisomal membrane protein Inp2p is the peroxisome-specific receptor for the myosin V motor Myo2p of Saccharomyces cerevisiae. *Developmental cell*. 10:587-600.

Goode, B.L., and M.J. Eck. 2007. Mechanism and function of formins in the control of actin assembly. *Annu Rev Biochem*. 76:593-627.

Hammer, J.A., 3rd, and J.R. Sellers. 2012. Walking to work: roles for class V myosins as cargo transporters. *Nature reviews. Molecular cell biology*. 13:13-26.

Hutagalung, A.H., and P.J. Novick. 2011. Role of Rab GTPases in membrane traffic and cell physiology. *Physiol Rev*. 91:119-149.

Inoue, M., L. Chang, J. Hwang, S.H. Chiang, and A.R. Saltiel. 2003. The exocyst complex is required for targeting of Glut4 to the plasma membrane by insulin. *Nature*. 422:629-633.

Ishikawa, K., N.L. Catlett, J.L. Novak, F. Tang, J.J. Nau, and L.S. Weisman. 2003. Identification of an organelle-specific myosin V receptor. *The Journal of cell biology*. 160:887-897.

Itoh, T., A. Toh-E, and Y. Matsui. 2004. Mmr1p is a mitochondrial factor for Myo2p-dependent inheritance of mitochondria in the budding yeast. *The EMBO journal*. 23:2520-2530.

Jin, Y., A. Sultana, P. Gandhi, E. Franklin, S. Hamamoto, A.R. Khan, M. Munson, R. Schekman, and L.S. Weisman. 2011. Myosin V transports secretory vesicles via a Rab GTPase cascade and interaction with the exocyst complex. *Dev Cell*. 21:1156-1170.

Kawase, K., T. Nakamura, A. Takaya, K. Aoki, K. Namikawa, H. Kiyama, S. Inagaki, H. Takemoto, A.R. Saltiel, and M. Matsuda. 2006. GTP hydrolysis by the Rho family GTPase TC10 promotes exocytic vesicle fusion. *Dev Cell*. 11:411-421.

Lillie, S.H., and S.S. Brown. 1992. Suppression of a myosin defect by a kinesin-related gene. *Nature*. 356:358-361.

Liu, H., J. Krizek, and A. Bretscher. 1992. Construction of a GAL1-regulated yeast cDNA expression library and its application to the identification of genes whose overexpression causes lethality in yeast. *Genetics*. 132:665-673.

Lwin, K.M., D. Li, and A. Bretscher. 2016. Kinesin-related Smy1 enhances the Rab-dependent association of myosin-V with secretory cargo. *Mol Biol Cell*. 27:2450-2462.

Roumanie, O., C. Weinachter, I. Larrieu, M. Crouzet, and F. Doignon. 2001. Functional characterization of the Bag7, Lrg1 and Rgd2 RhoGAP proteins from Saccharomyces cerevisiae. *FEBS Lett*. 506:149-156.

Scheffzek, K., M.R. Ahmadian, and A. Wittinghofer. 1998. GTPase-activating proteins: helping hands to complement an active site. *Trends Biochem Sci*. 23:257-262.

Sherman, F. 1991. Getting started with yeast. *Methods Enzymol*. 194:3-21.

Smith, G.R., S.A. Givan, P. Cullen, and G.F. Sprague, Jr. 2002. GTPase-activating proteins for Cdc42. *Eukaryot Cell*. 1:469-480.

Stevens, R.C., and T.N. Davis. 1998. Mlc1p is a light chain for the unconventional myosin Myo2p in Saccharomyces cerevisiae. *J Cell Biol*. 142:711-722.

Terrak, M., G. Rebowski, R.C. Lu, Z. Grabarek, and R. Dominguez. 2005. Structure of the light chain-binding domain of myosin V. *Proc Natl Acad Sci U S A*. 102:12718-12723.

Vale, R.D. 2003. Myosin V motor proteins: marching stepwise towards a mechanism. *J Cell Biol*. 163:445-450.

Wagner, W., P. Bielli, S. Wacha, and A. Ragnini-Wilson. 2002. Mlc1p promotes septum closure during cytokinesis via the IQ motifs of the vesicle motor Myo2p. *EMBO J*. 21:6397-6408.

Chapter IV

Summary and Future Directions

Ever since George Palade opened an era of research into protein secretion in the 1960s, many researchers devoted their scientific endeavors to understanding cellular mechanisms of protein secretion (Jamieson and Palade, 1967a; Jamieson and Palade, 1967b; Jamieson and Palade, 1968). It became apparent that several coordinated steps were involved in the secretory vesicle transport when Randy Schekman and Peter Novick showed their seminal work in vesicle secretion in budding yeast (Novick et al., 1981; Novick et al., 1980; Novick and Schekman, 1979). The Novick lab contributed much to the understanding of a ras-like protein, Sec4, which was later known as the master regulator of the late secretory pathway (Salminen and Novick, 1987; Walworth et al., 1989). Johnston et al., showed that myosin motor, Myo2 is essential in late secretory stage (Johnston et al., 1991). Connecting these two dots, the Bretscher lab showed that the tail domain of Myo2 was essential for transporting secretory vesicles, marked by Sec4 Rab GTPase (Schott et al., 1999). A clear understanding of receptors-mediated cargo transport became available when the Weisman lab crystallized the Myo2 tail domain and showed that several receptor-binding sites existed on the Myo2 tail (Eves et al., 2012; Pashkova et al., 2006). Myo2 motor behavior in vesicle transport also became clear after Donovan and Bretscher showed that the Myo2 motor underwent conformational changes upon vesicle binding and several steps were involved in both transporting and releasing the secretory vesicles at the plasma membrane (Donovan and Bretscher, 2012; Donovan and Bretscher, 2015a; Donovan and Bretscher, 2015b).

Within a span of 50 years, we became more knowledgeable about the secretory vesicle transport because more and more proteins were discovered and their functions were successfully characterized. Before I summarize our findings on Smy1 functions and subsequent discovery of Gym1, I would like to take a moment and mention here that research on Smy1 function since its discovery in 1992, has been very minimal with 10 published studies so far.

Four seminal papers from Lillie and Brown paved the way for Smy1 potential functions (Beningo et al., 2000; Lillie and Brown, 1992; Lillie and Brown, 1994; Lillie and Brown, 1998). The Trybus group found that Smy1 increased the processivity of Myo2 motors (Hodges et al., 2009). The Goode lab later claimed that Smy1 dampened the actin cable length (Chesarone-Cataldo et al., 2011). The two major functions of the Smy1, claimed by both Trybus and Goode labs, failed to explain why the overexpression of Smy1 suppressed the *myo2-66* mutant. The *myo2-66* mutant has a defect in the secretory vesicle transport, and it was the mutant in which Smy1 was discovered by overexpression suppression screening.

Based on several potential functions of Smy1, being a non-essential protein to begin with, much of our earlier effort was dedicated to creating conditional *smy1* mutants so that we could study the molecular function of the Smy1 in detail. To summarize Smy1 functions from Chapter II, I would like to highlight our finding that Smy1 stabilizes the interaction between Myo2 tail and vesicle receptor Sec4 Rab GTPase. Our finding answered why the overexpression of Smy1 was able to suppress temperature sensitive *myo2* mutants such as *myo2-66* (Lwin et al., 2016). Due to its stabilizing effect, overexpression of Smy1 increased the average number of Myo2 motors associated with a secretory vesicle by 1.5 fold. In addition, by forcing the two receptors Sec4 and Ypt11, to compete for the same binding site on Myo2 tail for secretory vesicle and mitochondria transport, respectively, we showed that Smy1 specifically enhanced the binding of Sec4, which brought more secretory vesicles and hindered the segregation of mitochondria into the bud. One of the striking features we found was that reduction of the Myo2 lever arm from 6IQ to 4IQ in our *myo2 smy1* mutants eliminated the temperature sensitivity of *myo2 smy1* which led us to explore the possibility of the importance of Myo2 head-to-tail interaction because shortening the lever arm would disrupt the head-to-tail interaction and it would probably leave the Myo2 in a constitutively active form.

Several labs have shown that myosin motors have two distinct conformations: (1) open or extended form, and (2) closed or folded forms. Most of the structural studies were done with changes in calcium or salt concentration, and electron micrograph imaging (Li et al.,

2004; Thirumurugan et al., 2006; Wang et al., 2004). How Myo2 structural changes have an impact on its molecular function is still unclear. Recently Donovan and Bretscher found that Myo2 head-to-tail interaction was critical for vesicle transport and losing such interaction was deleterious for cell growth (Donovan and Bretscher, 2015a). However, the mechanism that triggers the Myo2 to change its conformation still remains to be identified. Either the triggering mechanism begins from the head or tail or both domains simultaneously remains unanswered. From the Myo2 head domain and lever arm standpoints, several proteins, for e.g., calmodulin (Cmd1), myosin light chain (Mlc1), bind the lever arm. Rho3 GTPase binds the Myo2 coiled-coil domain and several receptors such as Sec4, Ypt31/32 Rab GTPases bind the Myo2 tail domain. Losing the recycling activity of the Myo2 motor due to its constitutively active conformation has deleterious effects on cell growth. Future research on such undertaking will be challenging because of the intricate nature of small molecules, necessity of powerful microscopes, and molecular techniques. However, investigation of such molecular mechanism will shed a light on our understanding of how the regulation of myosin motors is crucial for cell growth and subsequent cell survival.

With the knowledge of Myo2 conformational change kept in mind, I came upon a surprising turn of event when I was screening overexpressing suppressors on our *myo2 smy1* mutants, which I detailed in Chapter III. cDNA candidates from suppressors screening include Myo2-related proteins such as Cmd1, Mlc1, Cmk1 and vesicle-related proteins such as Sec4, Ypt31/32 and Smy1. A new ORF, *YHR182W*, was also found in our suppressors and it was named Gym1. To highlight the Gym1 function, I found that Gym1 was polarized in the bud, and its polarity was dependent on the Myo2 localization. The suppression activity of Gym1 on *myo2 smy1* mutants was dependent on the critical arginine R546 in its Rho GAP domain. I also showed that Gym1 stimulated Rho3 GTPase activity, and this activity was dependent on the arginine residue. Nicole *et al.*, in 1999 showed that Rho3 interacts with the Myo2 coiled-coil domain and is potentially involved in exocytosis (Robinson et al., 1999). Interestingly, we also found that Gym1 interacts with the Myo2 coiled-coil domain. We hypothesized that Gym1 down-regulates Rho3 activity that acts to inhibit secretory vesicle transport, thereby

suppressing the *myo2 smy1* mutants. To test our hypothesis, we overexpressed both Gym1 and Rho3. Overexpression of Rho3 reversed the Gym1 suppression, indicating that Gym1 indeed downregulates the Rho3 activity in the secretory pathway.

As of this writing, I found that Gym1 was involved in the secretory vesicle transport and it mediated the vesicle coupling with Myo2 by downregulating the Rho3 activity. How exactly Gym1 and Rho3, which bind at the Myo2 coiled-coil domain, exert their molecular function in the secretory vesicle transport is still unclear. One possible explanation is Rho3 together with Sec4 in their active form, i.e., prenylated and inserted into vesicle membrane, facilitate secretory vesicles coupling with the Myo2 in coiled-coil and tail domain, respectively. However this will cause Myo2 in folded form. In order for Myo2 to extend from the folded form, Gym1 stimulates the Rho3 GTPase activity, which releases the bound Rho3 from the Myo2 coiled-coil domain and facilitates the Myo2 to extend its tail and transport vesicle.

Regulation of the Myo2 conformation in the secretory vesicle transport became more convincing as half of all our suppressors were Myo2-related proteins such as Cmd1, Mlc1 and Cmk1. They all regulate Myo2 activity (Stevens and Davis, 1998). Another interesting area to explore is how these proteins mediate vesicles transport by changing the Myo2 conformation. Recently a few labs showed that myosin proteins underwent conformational change upon binding their respective proteins. Myo51 in fission yeast changed its conformation upon binding Rng8/9, which regulated its localization and function (Tang et al., 2016). MyoVa in mammalian cells also underwent a similar conformational change upon binding melanophilin (Mlph) (Zhang et al., 2016). As more structures are determined, we will come to understand regulation of many proteins from a structural perspective.

References

Beningo, K.A., S.H. Lillie, and S.S. Brown. 2000. The yeast kinesin-related protein Smy1p exerts its effects on the class V myosin Myo2p via a physical interaction. *Molecular biology of the cell*. 11:691-702.

Chesarone-Cataldo, M., C. Guérin, J.H. Yu, R. Wedlich-Soldner, L. Blanchoin, and B.L. Goode. 2011. The myosin passenger protein Smy1 controls actin cable structure and dynamics by acting as a formin damper. *Developmental cell*. 21:217-230.

Donovan, K.W., and A. Bretscher. 2012. Myosin-V is activated by binding secretory cargo and released in coordination with Rab/exocyst function. *Dev Cell*. 23:769-781.

Donovan, K.W., and A. Bretscher. 2015a. Head-to-tail regulation is critical for the in vivo function of myosin V. *J Cell Biol*. 209:359-365.

Donovan, K.W., and A. Bretscher. 2015b. Tracking individual secretory vesicles during exocytosis reveals an ordered and regulated process. *J Cell Biol*. 210:181-189.

Eves, P.T., Y. Jin, M. Brunner, and L.S. Weisman. 2012. Overlap of cargo binding sites on myosin V coordinates the inheritance of diverse cargoes. *The Journal of cell biology*. 198:69-85.

Hodges, A.R., C.S. Bookwalter, E.B. Krementsova, and K.M. Trybus. 2009. A nonprocessive class V myosin drives cargo processively when a kinesin- related protein is a passenger. *Current biology : CB*. 19:2121-2125.

Jamieson, J.D., and G.E. Palade. 1967a. Intracellular transport of secretory proteins in the pancreatic exocrine cell. I. Role of the peripheral elements of the Golgi complex. *J Cell Biol*. 34:577-596.

Jamieson, J.D., and G.E. Palade. 1967b. Intracellular transport of secretory proteins in the pancreatic exocrine cell. II. Transport to condensing vacuoles and zymogen granules. *J Cell Biol*. 34:597-615.

Jamieson, J.D., and G.E. Palade. 1968. Intracellular transport of secretory proteins in the pancreatic exocrine cell. 3. Dissociation of intracellular transport from protein synthesis. *J Cell Biol*. 39:580-588.

Johnston, G.C., J.A. Prendergast, and R.A. Singer. 1991. The Saccharomyces cerevisiae MYO2 gene encodes an essential myosin for vectorial transport of vesicles. *The Journal of cell biology*. 113:539-551.

Li, X.D., K. Mabuchi, R. Ikebe, and M. Ikebe. 2004. Ca2+-induced activation of ATPase activity of myosin Va is accompanied with a large conformational change. *Biochemical and biophysical research communications*. 315:538-545.

Lillie, S.H., and S.S. Brown. 1992. Suppression of a myosin defect by a kinesin-related gene. *Nature*. 356:358-361.

Lillie, S.H., and S.S. Brown. 1994. Immunofluorescence localization of the unconventional myosin, Myo2p, and the putative kinesin-related protein, Smy1p, to the same regions of polarized growth in Saccharomyces cerevisiae. *The Journal of cell biology*. 125:825-842.

Lillie, S.H., and S.S. Brown. 1998. Smy1p, a kinesin-related protein that does not require microtubules. *The Journal of cell biology*. 140:873-883.

Lwin, K.M., D. Li, and A. Bretscher. 2016. Kinesin-related Smy1 enhances the Rab-dependent association of myosin-V with secretory cargo. *Mol Biol Cell*. 27:2450-2462.

Novick, P., S. Ferro, and R. Schekman. 1981. Order of events in the yeast secretory pathway. *Cell*. 25:461-469.

Novick, P., C. Field, and R. Schekman. 1980. Identification of 23 complementation groups required for post-translational events in the yeast secretory pathway. *Cell*. 21:205-215.

Novick, P., and R. Schekman. 1979. Secretion and cell-surface growth are blocked in a temperature-sensitive mutant of Saccharomyces cerevisiae. *Proc Natl Acad Sci U S A*. 76:1858-1862.

Pashkova, N., Y. Jin, S. Ramaswamy, and L.S. Weisman. 2006. Structural basis for myosin V discrimination between distinct cargoes. *EMBO J*. 25:693-700.

Robinson, N.G., L. Guo, J. Imai, E.A. Toh, Y. Matsui, and F. Tamanoi. 1999. Rho3 of Saccharomyces cerevisiae, which regulates the actin cytoskeleton and exocytosis, is a GTPase which interacts with Myo2 and Exo70. *Mol Cell Biol*. 19:3580-3587.

Salminen, A., and P.J. Novick. 1987. A ras-like protein is required for a post-Golgi event in yeast secretion. *Cell*. 49:527-538.

Schott, D., J. Ho, D. Pruyne, and A. Bretscher. 1999. The COOH-terminal domain of Myo2p, a yeast myosin V, has a direct role in secretory vesicle targeting. *The Journal of cell biology*. 147:791-808.

Stevens, R.C., and T.N. Davis. 1998. Mlc1p is a light chain for the unconventional myosin Myo2p in Saccharomyces cerevisiae. *J Cell Biol*. 142:711-722.

Tang, Q., N. Billington, E.B. Krementsova, C.S. Bookwalter, M. Lord, and K.M. Trybus. 2016. A single-headed fission yeast myosin V transports actin in a tropomyosin-dependent manner. *J Cell Biol*. 214:167-179.

Thirumurugan, K., T. Sakamoto, J.A. Hammer, 3rd, J.R. Sellers, and P.J. Knight. 2006. The cargo-binding domain regulates structure and activity of myosin 5. *Nature*. 442:212-215.

Walworth, N.C., B. Goud, A.K. Kabcenell, and P.J. Novick. 1989. Mutational analysis of SEC4 suggests a cyclical mechanism for the regulation of vesicular traffic. *EMBO J*. 8:1685-1693.

Wang, F., K. Thirumurugan, W.F. Stafford, J.A. Hammer, 3rd, P.J. Knight, and J.R. Sellers. 2004. Regulated conformation of myosin V. *J Biol Chem*. 279:2333-2336.

Zhang, W.B., L.L. Yao, and X.D. Li. 2016. The Globular Tail Domain of Myosin-5a Functions as a Dimer in Regulating the Motor Activity. *J Biol Chem*. 291:13571-13579.

Appendix

Investigating the importance of Smy1 individual domains and Characterization of the Smy1 binding site on Myo2 tail

Overview

This chapter will describe some experiments that showed interesting results that could stand alone and become another interesting research area to explore. Some results were supportive of our hypothesis and yet we did not use in our published data because they warrant extra experiments to prove additional hypotheses. Some results led us to interesting findings. Among them, Smy1 binding site on Myo2 tail remains unanswered. Basically a number of receptor-binding sites on Myo2 tail have been mapped with yeast-two hybrid assay (Eves et al., 2012). I investigated the Smy1 binding site and the importance of its individual domains in secretory vesicle transport. I also followed up on Gym1 genetic interactions with all conditional mutants, which are involved in the secretory vesicle transport.

Materials and Methods

Yeast strains and transformation

Yeast strains and plasmids used in this study are listed in Table 3 and 4. Standard media and techniques for yeast growing and transformation were used (Sherman, 1991). Briefly, for transformation, 5ml of log phase OD_{600} = ~ 0.8 cells were harvested and resuspended in a mixture of 36µl of 1 M LiAc, 240 µl of 50% PEG 3350 (w/v), 50µl of salmon sperm DNA 10mg/mL, 1µg of DNA constructs, and volume-adjustable 29 μl H_2O (Gietz and Woods, 2002). Cells were incubated at 42˚C for 45 minutes and transformants were selected on selective synthetic dropout media plates. Gene deletion and chromosomal GFP tagging were performed by standard PCR-mediated techniques (Longtine et al., 1998). Plasmids from yeast were isolated using the plasmid isolation kit (YeaStar Genomic DNA kit).

Yeast two-hybrid constructs and analysis

The coding sequence for Myo2cctail (2776-4725nt) was fused with the DNA activation domain in pGADT7 vector between NdeI and BamHI. To create point mutation in Myo2cctail, 40 nucleotide long forward and reverse primers were designed with mutated nucleotides in the middle of the primers, and pGADT7-Myo2cctail was used as a template. The point mutation was verified after sequencing the miniprepped product from the bacteria transformants. The Smy1 myosin-binding domain (1308-1968nt) was fused with DNA binding domain in pGBKT7. The AH109 strain co-transformed with both plasmids was selected in media lacking leucine and tryptophan (SD-2DO: double dropout). Interaction was detected by growth on medium lacking leucine, tryptophan and histidine (SD-3DO: triple dropout).

Glucose depletion assay

The assay was discovered by postdoctoral associate Dr. Li Xu in Bretscher lab (Xu and Bretscher, 2014). Briefly, yeasts were attached to a glass-bottomed dish coated with Concanavalin A (EY laboratories) and washed with respective cell medium and replenished with media lacking glucose. Images were immediately taken since the Myo2 rigor state only lasts for 3-5 minutes.

Genetic interaction by Tetrad dissection

Genetic interactions between *gym1Δ* and temperature sensitive mutants (*myo2-66, sec2-41, sec4-8, sec6-4, sec9-4* and *sec15-1*) and non-essential genes (*mmr1Δ, smy1Δ* and *rgd1Δ*) were tested by dissecting tetrads after sporulation. Cells with opposite mating types were grown together overnight at 26˚C for mating. Mating efficiency was checked by shmoo projection and zygote formations the next day under the light microscope. Cells were washed with PBS and resuspended in sporulation media (1% yeast extract, 1% potassium acetate, and 0.05% glucose) and grown for 4-5 days. Tetrad formation was checked under the light microscope. 25µl of zymolyase (1mg/ml) was added to 50ul of sporulated cells. Zymolyase treated cells were incubated at 37˚C for 5 minutes. Tetrads were dissected using MSM Singer instruments with 50µm fiber needle.

Results and Discussion

Chimeric Smy1tail-Sec4 suppresses *myo2 ts* mutants.

I showed that Smy1 tail (MBD: Myosin Binding Domain) was required for binding the Myo2 tail and Smy1 head was involved in coupling secretory vesicles with the Myo2 in Chapter II. Smy1 has three distinct domains: (1) kinesin-like motor domain, (2) coiled-coil and (3) myosin binding domains. Interestingly, all of *smy1 ts* alleles recovered from our *myo2 smy1* mutants were clustered at the Smy1 head domain although we introduced random mutations in entire *SMY1* ORF (Figure 2.2 F). The fact that none of our conditional *smy1* mutations were localized in the Smy1 tail domain suggests that the tail domain (myosin binding domain) is indispensable for receiving any conditional mutations. Yeast-two hybrid showed that *myo2-12* failed to interact with the Sec4 although it still interacted with the Smy1 (Figure 4.1A). To test the function of individual domains of Smy1, my initial hypothesis was that the Smy1 head domain binds the secretory vesicle membrane through some receptor, and the tail domain solely functions as a myosin-binding domain. To test the idea, I created two chimeric proteins: (1) Smy1(head)+Sec4 and (2) Smy1(tail or MBD)+Sec4. The placement of Sec4 at the COOH terminus of both chimeric constructs was to make sure that Sec4 CAAX box could be properly prenylated (Figure 4.1B). I found that overexpression of Sec4 failed to suppress conditional *myo2* mutants while Smy1 overexpression can (Figure 4.1, C and D), further supporting our initial finding on yeast-two hybrid, in which *myo2-12* failed to interact with Sec4, but it still interacted with Smy1 (Figure 4.1A). Overexpression of the chimeric Smy1(head)+Sec4 failed to suppress *myo2-12*, presumably due to the lack of binding capacity from both proteins, i.e., Smy1(head) does not bind Myo2 and Sec4 in this case cannot bind *myo2-12*. However the chimeric Smy1(MBD)+Sec4 suppressed the *myo2-12* mutant, which supported the idea that Smy1 tail now presumably compensated for the loss of Sec4 binding to *myo2-12,* and conferred the full suppression from the Sec4.

Figure 4.1 Chimeric Smy1(MBD)+Sec4 suppresses temperature sensitivity of *myo2ts* mutants.

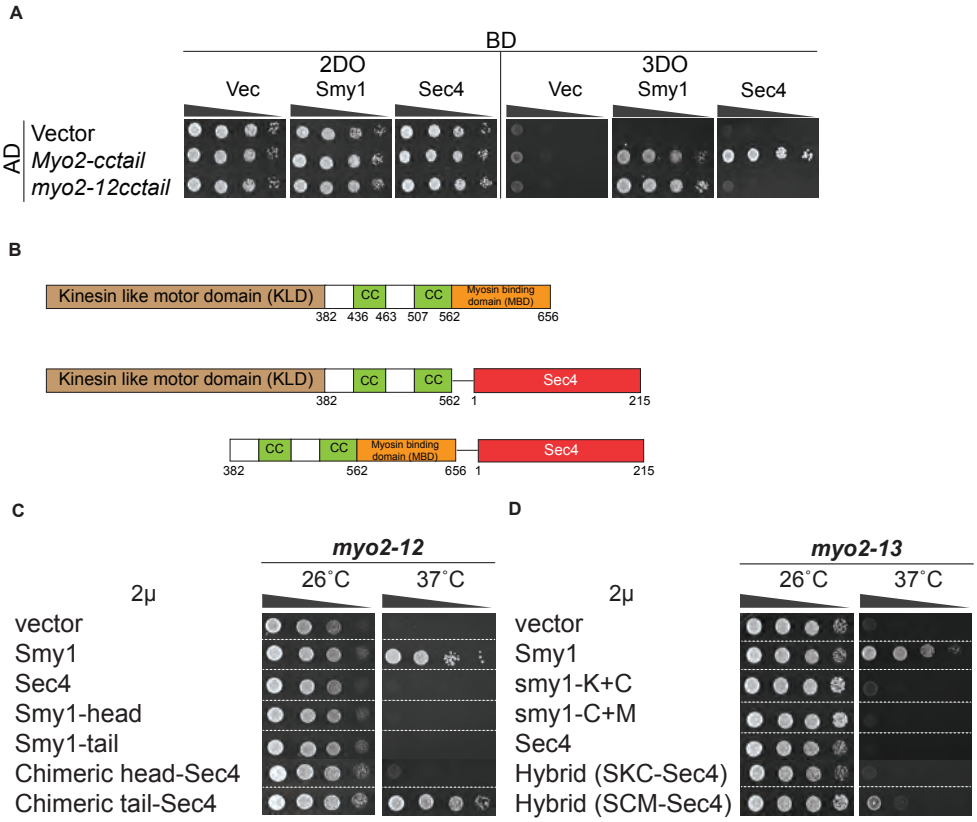

Figure 4.1 Chimeric Smy1(MBD)+Sec4 suppresses temperature sensitivity of *myo2ts* mutants.
(A) Yeast two-hybrid interactions between Myo2-cctail (926-1575aa) and *myo2-12*-cctail fused to the activation domain (AD) and Smy1 fused to the binding domain (BD) and Sec4 fused to the binding domain (BD). 2DO= 2 dropouts: leu and trp, 3DO = 3 dropouts: leu, trp, his.
(B) Chimeric constructs between Smy1 head domain (KLD+CC) and full length Sec4 or Smy1 tail domain (CC+MBD) fused to the full length Sec4.
(C) Overexpression suppression of individual Smy1, Sec4 constructs and chimeric constructs

Smy1 binding site on Myo2 cargo-binding domain

I investigated the Smy1 binding site on Myo2 tail because a number of receptor binding sites on Myo2 tail have been successfully identified for Sec4, Ypt31, Ypt11, Vac17, Mmr1 and Kar9 by yeast-two hybrid between the said receptors and point mutations on the Myo2 tail (Figure 4.2A) (Eves et al., 2012). In a similar fashion, I hoped to find the Smy1 binding site. The Weisman lab claimed that Smy1 binding site was yet to be identified. Fortunately, the Bretscher lab has a number of *myo2* mutants: *myo2-12, -13, -14, -16, -18* and *-20*. Interestingly earlier work in our lab showed that overexpression of Smy1 suppressed all aforementioned *myo2* mutants except *myo2-14* (Schott et al., 1999). A previous graduate student, Donghao Li, also showed that *myo2-14* failed to interact with Smy1 (unpublished data). The mutant is temperature sensitive and fails to transport mitochondria without affecting secretory vesicle transport (Chernyakov et al., 2013). The *myo2-14* allele has 3 mutations: Y1451D, G1461V and L1536amber (Figure 4.2B). The non-sense mutation truncates the last 38 amino acids in sub-domain II completely. Thus the last 38 residues may be important for Myo2 to bind Smy1.

To characterize the binding site, I created a serial truncation of Myo2 tail with 5 amino acids truncated each time, i.e., Myo2 tail (-5aa), Myo2 tail (-10aa), so on until the Myo2 tail (-40aa), making a total of 8 Myo2 tail variants (Figure 4.2C). Smy1 strongly interacted with the Myo2 tail until the last 15 residues were truncated (Figure 4.2D). I thought this probably suggested that the Smy1 binding site was between residues 10 and 15. I created site-directed mutagenesis on residues in-between (1559, 1560, 1563, 1567, 1569, 1570aa) on full length Myo2 tail accordingly. Interestingly, I found no loss in Smy1 interaction but those point-mutants failed to interact with Sec4 Rab GTPase whose binding site is in domain II (Figure 4.2E). This suggested that Smy1 binding site on Myo2 was still elusive and the fact that Smy1 fails to interact with Myo2 (-15aa) was not due to its loss of binding site, rather presumably due to some conformational change upon loss of its last residues.

Figure 4.2 Smy1 binding site on Myo2 cargo binding domain

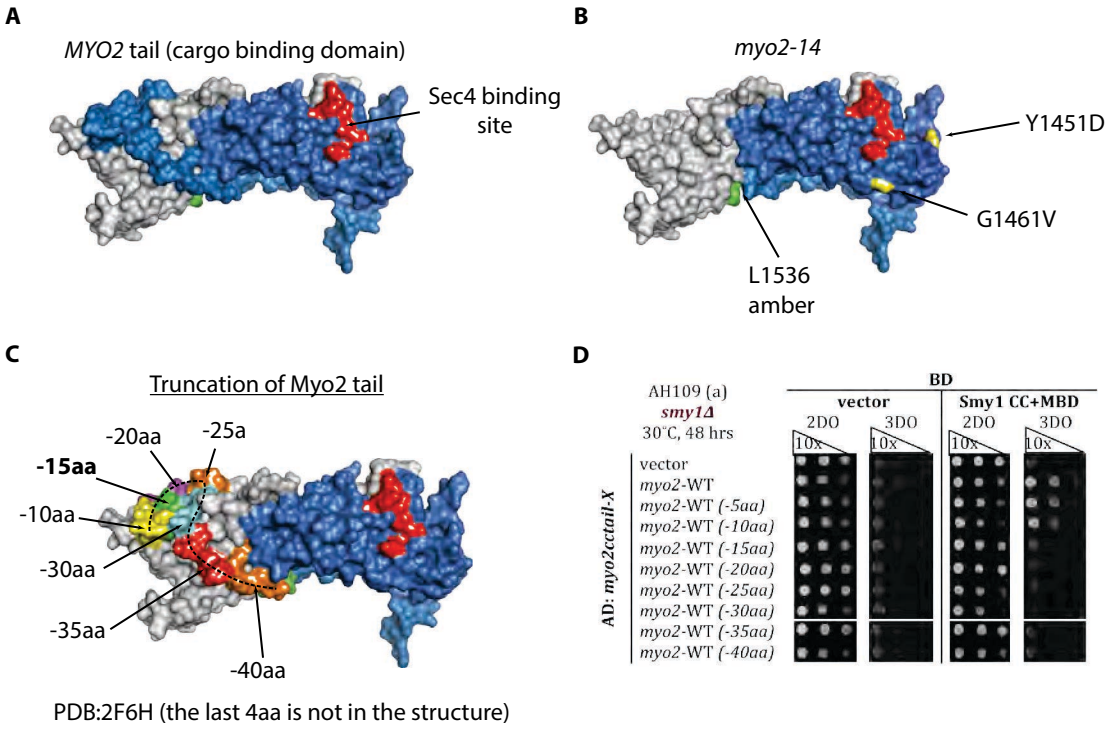

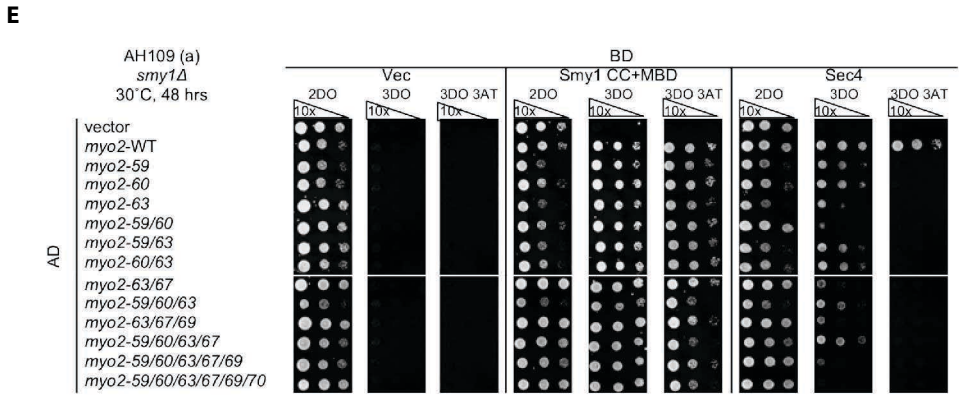

Figure 4.2. Smy1 binding site on Myo2 tail.
(A) Structure of wild-type Myo2 tail. Sub-domain I is in gray (1152–1309aa) and sub-domain II and linker is in blue (1310–1574aa). The mapped Sec4 Rab binding site (Eves et al., 2012) is shown in red.
(B) Mutations of *myo2-14* shown in Myo2 tail.
(C) Illustration of serial truncations on the last 40 amino acids of Myo2 tail. The geography of the last 40 amino acids was shown in dotted black lines.
(D) Yeast two-hybrid interactions between truncated Myo2-cctails (926-1575aa) and Smy1.
(E) Yeast two-hybrid interactions between Myo2 tail (full length tail with point mutations) and Smy1 and Sec4. The mutant *myo2-59* indicates that the point mutation is made at 15**59**aa; the mutant *myo2-59/60/63* indicates that triple point mutations were made at 15**59**, 15**60**, 15**63**aa positions on Myo2 tail.

Glucose depletion and Smy1 effect on secretory vesicle in Myo2 rigor state

Since Smy1 increases the Myo2 coupling with secretory vesicles by Sec4 Rab GTPase, I was keen on taking advantage of the Myo2 rigor phenotype in glucose depletion, the phenotype of which was observed in our lab by postdoctoral associate Dr. Li Xu. Our yeast microscopic experiments were done in media suitable for yeast growth. Li observed that Myo2 motors, upon nutrient depletion in yeast media, underwent rigor state on actin filaments, presumably to preserve energy in the cell to counteract the external nutrient depleted condition. Secretory vesicles, marked by GFP-Sec4 were immediately decoupled from the Myo2 tail and became cytoplasmic upon glucose depletion (Xu and Bretscher, 2014). Taking advantage of such phenotype, I looked at Myo2 and Sec4 phenotype upon glucose depletion in overexpressed Smy1 condition.

Interestingly, I found that secretory vesicles stayed together with the Myo2 in Smy1 overexpressed condition, indicating that Smy1 indeed stabilized the interaction between Myo2 and Sec4 (Figure 4.3A). Co-imaging the Myo2-3mCherry and GFP-Sec4 showed that Myo2 and secretory vesicles were seen along the supposedly actin filaments for about 2 minutes compared to wild-type cell (Figure 4.3B). This result supported our hypothesis that Smy1 stabilized the Myo2 coupling with secretory vesicles. However, the result was not published due to its technical novelty and being a separate research area of Myo2 rigor condition.

Figure 4.3 Myo2 and Sec4 stays together after glucose depletion in overexpressed Smy1 condition.

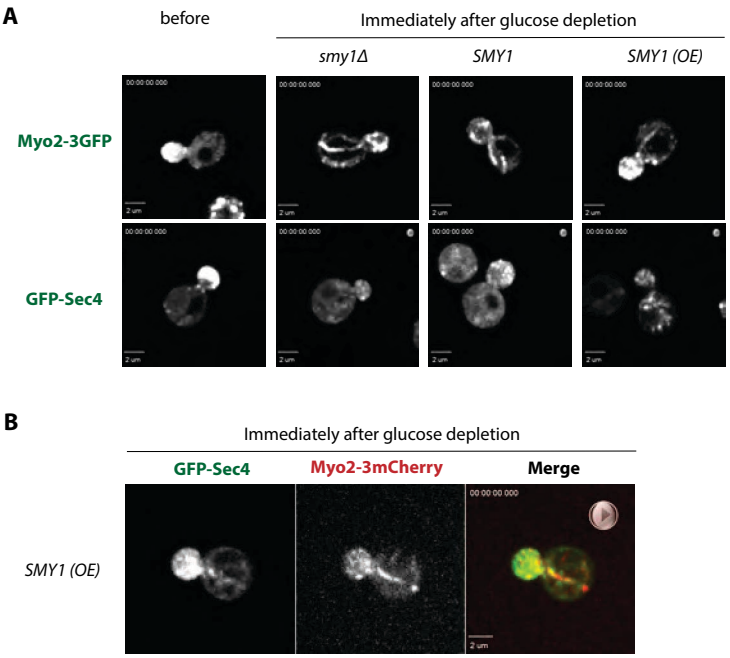

Figure 4.3 Myo2 and Sec4 stays together after glucose depletion in overexpressed Smy1 condition.
(A) Myo2-3GFP and GFP-Sec4 phenotypes after glucose depletion on different smy1 backgrounds.
(B) Co-imaging of Myo2 and Sec4 on overexpressed Smy1 condition.

Gym1 minimally suppresses *sec4-8*

As previously described in Chapter III, a novel Rho GAP Gym1 was involved in the secretory vesicle transport. By stimulating the Rho3 GTPase catalytic activity, Gym1 was able to suppress *myo2 smy1* mutants. To characterize which steps of the secretory pathway Gym1 was involved, I sought to take advantage of all the conditional mutants available in our lab, i.e., *sec23-1* – the mutant defective in the early secretory stage, and *sec15-1* – the mutant defective in the late secretory vesicle fusion at the plasma membrane. Overexpression of the Gym1 minimally suppressed the *sec4-8* (Figure 4.4A). "Minimally" suggests that when I repeated the overexpression suppression of Gym1 on *sec4-8,* I found that the suppression of Gym1 was minimal compared to control vector. The original strain we received from the Peter Novick lab (ID:ABY127 or NY405) was very sick at 32˚C. Overexpression of Gym1 suppresses *sec4-8* (NY) minimally (Figure 4.4B). Similarly, when I created *sec4-8* in BY background, I found the temperature sensitivity of *sec4-8* allele alleviated and it only became sick at 35˚C. Overexpression of Gym1 suppressed *sec4-8* (BY) minimally (Figure 4.4B). Whether or not Gym1 required additional suppressors to fully suppress the *sec4-8* would be interesting. I also tested the genetic interaction between *gym1Δ* and all conditional mutants such as *myo2-66, sec2-41,* and *sec4-8* to characterize any genetic interplay in the secretory pathway (Figure 4.4C). Unfortunately I did not find any synthetic lethality between *gym1Δ* and all mutants because all double mutants or double nulls are viable.

Figure 4.4 Gym1 minimally suppresses sec4-8

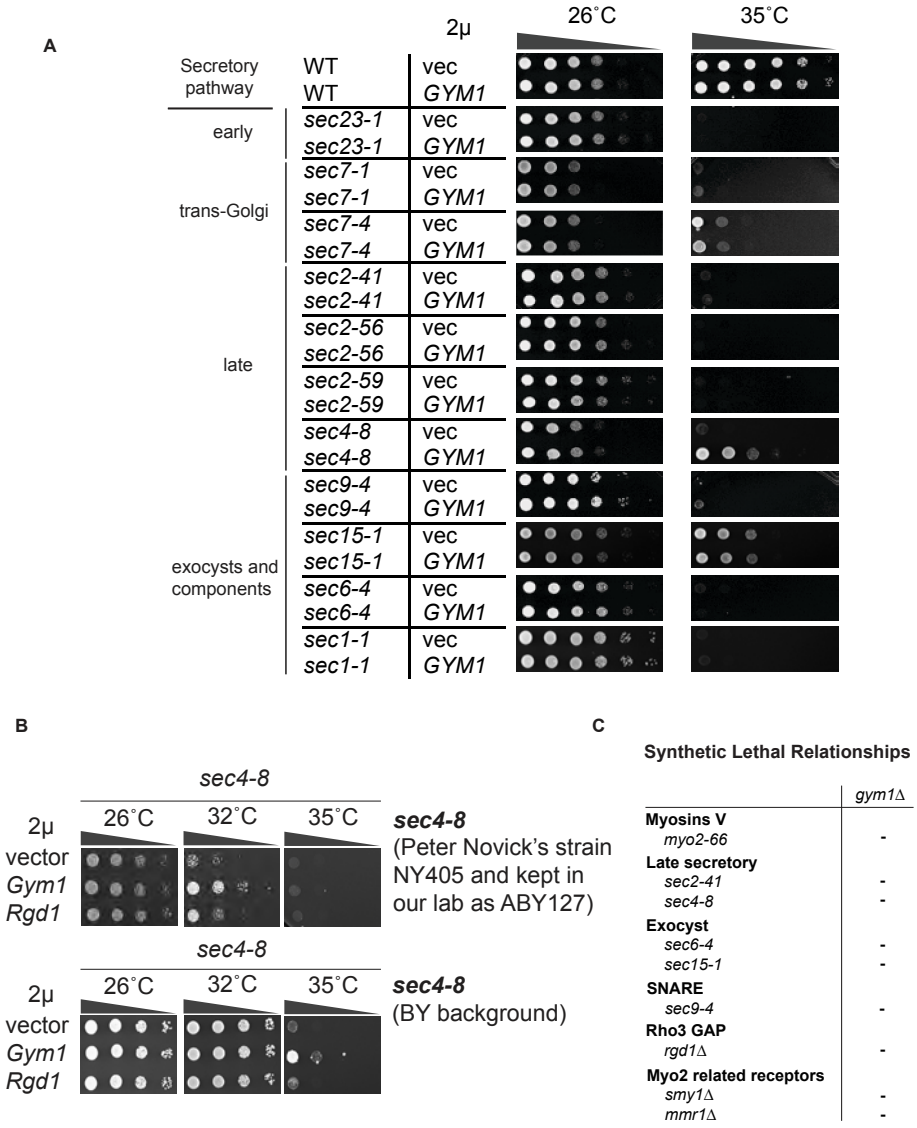

Figure 4.4 Gym1 minimally suppresses sec4-8.
(A) Overexpression suppression of Gym1 on several conditional mutants in secretory pathway (*sec7-1* and *sec7-4* were kindly received from Fromme lab.)
(B) Gym1 suppression on *sec4-8* in two different backgrounds: one is originally from Peter Novick's lab, and the other one is created in BY background.
(C) Genetic interaction between several conditional mutants, null mutants and *gym1*Δ done by tetrads analysis. "-" indicates there is no genetic interaction, i.e., all double mutants are viable,

References

Chernyakov, I., F. Santiago-Tirado, and A. Bretscher. 2013. Active segregation of yeast mitochondria by Myo2 is essential and mediated by Mmr1 and Ypt11. *Curr Biol*. 23:1818-1824.

Eves, P.T., Y. Jin, M. Brunner, and L.S. Weisman. 2012. Overlap of cargo binding sites on myosin V coordinates the inheritance of diverse cargoes. *The Journal of cell biology*. 198:69-85.

Gietz, R.D., and R.A. Woods. 2002. Transformation of yeast by lithium acetate/single-stranded carrier DNA/polyethylene glycol method. *Methods Enzymol*. 350:87-96.

Longtine, M.S., A. McKenzie, 3rd, D.J. Demarini, N.G. Shah, A. Wach, A. Brachat, P. Philippsen, and J.R. Pringle. 1998. Additional modules for versatile and economical PCR-based gene deletion and modification in Saccharomyces cerevisiae. *Yeast*. 14:953-961.

Schott, D., J. Ho, D. Pruyne, and A. Bretscher. 1999. The COOH-terminal domain of Myo2p, a yeast myosin V, has a direct role in secretory vesicle targeting. *The Journal of cell biology*. 147:791-808.

Sherman, F. 1991. Getting started with yeast. *Methods Enzymol*. 194:3-21.

Xu, L., and A. Bretscher. 2014. Rapid glucose depletion immobilizes active myosin V on stabilized actin cables. *Curr Biol*. 24:2471-2479.